AD_____

Award Number: W81XWH-10-1-0626

TITLE: Placental Vascular Tree as Biomarker of Autism/ASD Risk

PRINCIPAL INVESTIGATOR: Carolyn M. Salafia, M.D., M.S.

CONTRACTING ORGANIZATION: Research Foundation for Mental Hygiene, Inc.
Staten Island, NY 10314-6356

REPORT DATE: September 2013

TYPE OF REPORT: Final

PREPARED FOR: U.S. Army Medical Research and Materiel Command
Fort Detrick, Maryland 21702-5012

REPORT DOCUMENTATION PAGE

Form Approved
OMB No. 0704-0188

1. REPORT DATE	**2. REPORT TYPE**	**3. DATES COVERED**
September 2013	Final	15 August 2010 – 14 August 2013

4. TITLE AND SUBTITLE

Placental Vascular Tree as Biomarker of Autism/ASD Risk

5a. CONTRACT NUMBER

5b. GRANT NUMBER
W81XWH-10-1-0626

5c. PROGRAM ELEMENT NUMBER

6. AUTHOR(S)

Carolyn M. Salafia, M.D., M.S.
Dawn P Misra, Ph.D.; Michael Yampolsky, Ph.D.; Theresa Girardi, Ph.D.

E-Mail: carolyn.salafia@gmail.com

5d. PROJECT NUMBER

5e. TASK NUMBER

5f. WORK UNIT NUMBER

7. PERFORMING ORGANIZATION NAME(S) AND ADDRESS(ES)

Research Foundation for Mental Hygiene, Inc.
Staten Island, NY 10314-6356

8. PERFORMING ORGANIZATION REPORT NUMBER

9. SPONSORING / MONITORING AGENCY NAME(S) AND ADDRESS(ES)
U.S. Army Medical Research and Materiel Command
Fort Detrick, Maryland 21702-5012

10. SPONSOR/MONITOR'S ACRONYM(S)

11. SPONSOR/MONITOR'S REPORT NUMBER(S)

12. DISTRIBUTION / AVAILABILITY STATEMENT
Approved for Public Release; Distribution Unlimited

13. SUPPLEMENTARY NOTES

14. ABSTRACT
Autism Spectrum Disorder (ASD) encompasses a range of complex developmental disorders characterized by variable challenges to social, emotional and communication abilities. Given evidence that angiogenesis drives neurogenesis, we have measured the placenta, a fetal organ commonly discarded at birth as medical waste, in the Avon Longitudinal Study of Parents and Children (ALSPAC). Placental chorionic surface shape and cord insertion centrality are less variable in ALSPAC ASD cases compared to controls, These shape features also differ by specific ASD phenotypes. We have demonstrated significant alterations in branching, and in linear extension/outgrowth of placental chorionic surface vessels in ALSPAC ASD cases compared to controls, and found these effects to be greater in arterial as compared to venous networks. The above two results have been replicated in comparisons of a high ASD risk (Early Autism Risk Longitudinal Investigation, EARLI and a low ASD cohort of the National Children's Study (NCS). Finally, we have found that the placental chorionic plate surface vessels have a different "relationship" to the subjacent placental villous tree, with reduced maximal thickness (a proxy for villous arborization) and reduced variability for surface vessels of similar calibers in ALSPAC ASD cases compared to controls. The placenta in ASD (ALSPAC), and in high ASD risk children (EARLI), is measurably different from controls without identified eurodevelopmental handicap (ALSPAC) or low risk contemporary cohorts (NCS) controls. The findings all point to a placenta with branching growth that is more constrained and less flexible in ASD than those of controls or low risk newborns.

15. SUBJECT TERMS
None provided.

16. SECURITY CLASSIFICATION OF:			**17. LIMITATION OF ABSTRACT**	**18. NUMBER OF PAGES**	**19a. NAME OF RESPONSIBLE PERSON**
a. REPORT	**b. ABSTRACT**	**c. THIS PAGE**			USAMRMC
U	U	U	UU	83	**19b. TELEPHONE NUMBER** *(include area code)*

Final Report

Table of Contents

Page

FINAL REPORT
Characterization of the Placental Vascular Tree as a Biomarker of Autism/ASD risk.
Carolyn M. Salafia, M.D., M.S, (PI)
Award: W81XWH-10-0626

1. INTRODUCTION

The overall aim of this multidisciplinary project was to determine the correlation between patterns of branching growth at all levels of the vascular tree in placentas with diagnoses of autism spectrum disorder (ASD), as compared to two sets of population derived controls, one with diagnoses of special education needs (SEN) and a second with "normal" neurodevelopmental outcomes. We also sought to establish grounds for the development of a risk assessment tool built on measures of placental shape and structure that can be performed on all infants at birth to improve identification of children who are at increased risk of ASD for early screening and diagnosis. In this project we measured the branching of larger blood vessels on the surface of the placenta (2D), the placental shape (that contains the placental vascular fractal), and the branching structure of the fine vessels of the thickness of the placenta (3D). Our intent also was to analyze the maternal medical and gestational factors that may have led to differences observed between the ASD group, a group of children with other special educational needs and healthy control children. We also present comparable analyses of the placentas of the Early Autism Risk Longitudinal Investigation (EARLI), a cohort of newborns in families with an older sibling diagnosed with ASD and thus at high risk for development of ASD, and the National Children's Study (NCS) a low ASD risk population based cohort.

2. KEY WORDS

Autism, prenatal origins, branching morphogenesis, placenta, placental shape, placental vasculature

3. OVERALL PROJECT SUMMARY

The placental examination and dissection, and the subprojects were drawn from a nested case control study of the placental archive of the Avon Longitudinal Study of Parents and Children (ALSPAC). The proposed case group included 56 children in the cohort with archived placentas who have been diagnosed with ASD. Two control groups of children were available from the same cohort, one group with special education needs but not a diagnosis of ASD, and one group with no diagnoses related to neurodevelopmental pathology, at a 3:1 ratio to cases.

Based on our analyses, we conclude that:

1. The chorionic surface vasculature in most cases of ASD differs from that of controls. The differences in the placental chorionic surface networks are most striking in the arterial networks, with similar but generally smaller effects seen in the venous networks. These differences consist of a total reduction in the number of branch generations although not in a change in the number of vessels originating off the umbilical cord, a reduction of almost 42.5% in vascular branch points, total vascular surface length and failed extension of the chorionic vessels over the full surface of the placenta chorionic plate (measured by an increased distance of vessels from the perimeter), and altered angles of vascular branching. (**Table 1**). These reductions are common to ASD males and ASD females. (**Table 2**)

2. There is a striking bimodal distribution of chorionic surface vascular parameters within ALSPAC ASD cases, with the majority showing a ~40% reduction of chorionic surface branch points compared to controls but 6 cases with markedly increased placental chorionic surface branching, greater than one standard deviation above the mean for normal controls. (**Figure 1**) The two groups of ALSPAC ASD cases cannot be distinguished by gender, or gestational age or extremes of birth weight or placental weight. We speculate, since pertinent data are not available from ALSPAC, that this reflects heterogeneity within the ASD population as it was determined in the early-mid 1990's, and that these ASD "outliers" with marked surface hypervascularity are cases of ASD diagnosed in genetic syndromes that currently are excluded from the spectrum of ASD (e.g., Fragile X, Rett's syndrome,

etc). These cases have been excluded from all analyses (including (1), above). We propose this because in the ALSPAC cohort, the ASD sparse-vascularized group shares essentially the identical mean and SD of placental chorionic surface branch points with the high ASD risk EARLI (Early Autism Longitudinal Investigation) cohort of newborns in families with an older child who has an ASD diagnosis (**Table 3**), while the ALSPAC controls and the low ASD risk National Children's Study have essentially identical chorionic vascular parameters. **Figure 2a-c** presents the original photograph from which placental chorionic surface vascular networks are traced with the completed tracing, extracted, on the right, as arterial and venous networks. **Figures 3a-c** include representative chorionic surface vascular networks of NCS placentas, and EARLI placentas both with arterial branchpoints at the mean and 1 SD above the mean.

3. No gender dimorphism of vascular network structure is appreciated in ALSPAC ASD cases or neurodevelopmentally normal controls in EARLI as a whole or stratified by gender. (**Tables 2-3**)

4. There is a statistically significant difference in ALSPAC ASD placental chorionic surface shape, with **reduced** maximum radius, and **reduced** standard deviation of the radius of the chorionic surface shape, compared to placentas of neurodevelopmentally normal control children. (**Table 4**) This contrasts with last year's report (see discussion, following).

5. There is a statistically significant **reduced** eccentricity of the umbilical cord insertion, as compared to placentas of neurodevelopmentally normal control children. (**Table 5**) This contrasts with last year's report (see discussion, following).

6. After stratification by gender, these findings are also generally preserved, although significance is attenuated among females with ASD due to the extremely small sample size for females. (**Tables 4-5**)

7. Differences in these measures carry over into the range of the ASD phenotypes, with significant differences in placental shape features when stratifying on either social understanding phenotype or on "repetitive stereotyped behaviour" phenotype. (**Tables 6-7**)

8. There are no statistically significant differences in the slice dimensions of ALSPAC ASD placentas as compared to the control group although the limited sample size in ALSPAC may restrict inference. (**Table 8**) However, EARLI placentas have significantly different slice dimensions when compared to a large birth cohort of ~1000 placentas with similar measurement data. (**Table 9**) When comparing ALSPAC ASD cases and controls (**Table 10, Figures 6a-h,** small sample size), and when comparing high ASD risk EARLI placentas with low ASD risk NCS placentas (**Figures 7a-c**) there appear to be different trajectories of villous arborization from the center to the perimeter of the placental chorionic disk, with EARLI placentas showing reduced central placental disk thickness but greater preservation of that level of arborization extending to the perimeter, while NCS placentas show more variability throughout the distance from placental disk centroid to edge. This is consistent with our empirical DLA model of placental growth which predicted variability in perimeter would be correlated with variability in thickness/villous arborization. EARLI placentas have less perimeter variability and less variability in disk thickness. EARLI placentas are, however, thinner in the more central regions of the placenta near the umbilical cord insertion, the relatively "older" portions of the placenta.

9. There is a statistically significant **reduction** in placental weight (~100 g, 20% of the weight of a normal term placenta) for female ASD cases compared to female normal controls. (**Table 5**) We anticipated a decrease in volume compared to both groups of controls. However, there was no statistically significant difference in volumes. (**Table 5**) This suggests that the placentas of girls with ASD, which weigh less, but occupy the same volume, are "built" differently, with relatively reduced branches despite similar length of the fetal stem anchoring villi. This would be consistent with our

previous finding of an alteration in beta, a measure of the integrity of the placental vascular fractal, in ASD cases compared to female normal controls**.**

10. The relationship between placental chorionic surface vessels and the underlying placental disk parenchyma dependent on those vessels differ in ASD cases as compared to controls. This was demonstrated in an analysis of the undeformed ALSPAC 3D scans with companion flat 2D placental chorionic surface photographs., While the distribution of chorionic plate vessel segments did not differ between the two groups and there was no statistically significant difference in mean disk thickness between ASD cases and controls, both the maximum placental disk thickness and the standard deviation of placental disk thickness were significantly reduced significantly between ASD cases and controls. (**Figure 5, Table 12**) We interpret this as overall supportive of our global impression of ASD placentas being more constrained, less variable in shape, cord insertion, with more restricted arborization (reduced maximum thickness) and less "flexibility" in arborization (reduced variability in disk thickness).

These findings support our hypothesis that placentas in ASD show alteration of the branching structures known to be determined by the midtrimester (placental chorionic surface vascular networks) compared to terminal villi which are mainly formed after this period. Thus placental chorionic surface vascular network variance may parallel aberrant neuronal networks in ASD both in terms of altered placental chorionic surface vascular branching and in gestational period of effect.
While microscopic analysis of shape and structure was not a stated goal of this grant, because of the observation of reduction in placental weight without a comparable change in volume suggesting different "compositon" of villous parenchyma in ALSPAC ASD cases as compared to controls, and reports that villous maldevelopment (in the form of "trophoblast stromal inclusions", TSI), we have examined both the gross structure of microdissected terminal villous clusters and the terminal villous microvascular structure (the end-vascular capillary distribution of the surface chorionic arterial and venous networks), and neither appear to be simplified in ALSPAC ASD cases compared to matched controls.
Because of the potential value of any perinatal biomarker for ASD risk screening, we have continued to pursue shape analysis at the microscopic level by developing highly specific immunohistochemistry (IHC) approach for detection and classification of the villous distribution of cytokeratin-7 (CK-7), a marker of placental trophoblast, the villous "skin" (**Figures 11 a-d**). TSIs have been suggested to be more common in the placentas of newborns with an older sibling with ASD (thus comparable to our EARLI cohort), however, no study to date has examined a population based cohort of ASD placentas such as has been created by this grant, with ALSPAC cases and controls. A pilot blinded review of 80 slides, from 20 ASD cases and matched controls did not demonstrate an increased number of TSIs in our ALSPAC ASD cases. We consider this finding, albeit preliminary, to be significant. Our population is unique in that studied placentas searched for this villous feature belong to a population based cohort that includes case children with formally diagnosed ASD cases and controls known to be without neurodevelopmental disability. TSIs are suggested to mark increased villous surface complexity, with the greater surface irregularity leading to more common appearance of an inclusion of surface trophoblast epithelium in the villous core or stroma. Our cases are children actually diagnosed with (and not merely at risk for) ASD. Given our finding of bimodal placental chorionic surface vascular branching measures (majority sparse, a minority with increased complexity) in ALSPAC ASD cases, but not EARLI (high risk with case status yet to develop) placentas, we predict increased villous surface complexity would only mark a minority of ASD children, and potentially those with concurrent diagnoses in addition to ASD.

Our analysis method utilizes digitized slides, slides which have been processed such that the image information contained on them is converted into a viewable file on any computer screen. Our algorithm has set minimal criteria for irregularities of the villous surface and identification of regions of interest (ROIs) with potential TSIs. These regions of interest (ROIs) are saved as an annotation of the analyzed slide. The slide with annotation and the same region of a serial section stained with routine hematoxylin and eosin (the current published method for identification of TSIs) will be reviewed by specialist pathologists. Three

pathologists (Carolyn M. Salafia MD MS (PI), Theonia Boyd, MD, Harvard Medical School, and Drucilla J. Roberts, MD, Brigham and Women's Hospital, Boston, MA) are participating in validation of TSI identification on H&E and IHC stained slides. We expect some ongoing level of algorithm refinement to optimize the IHC computational algorithms for automated digitized slide review and to develop a validated algorithm for identification of TSIs in routine stains. Since the frequency of TSIs was reported only rarely as more than 3 per histological slide (<<1 of villi), our approach will reduce expert pathologists' time for slide review, validate diagnostic criteria for TSIs in routine H&E and in IHC slides, and confirm or refute the value of this marker as a perinatal predictor of ASD risk.

The differences between last year's observations and those from the final data result from our decision to exclude data from cases of deformed placentas in which placental chorionic surface and disk thickness (from digital photographs or 3D scans) were extrapolated from photographs or from 3D scans. We determined that our methods of decrumpling and uncurling shapes or slices, while seemingly mathematically straightforward, did not yield measures that were consistent with naked eye inspection of original images or the ruler measures provided in real time by Dr. Craig Platt at Bristol, UK, in the original processing of the placenta. The degree of extrapolation to placental areas that cannot be seen directly in the scan (areas in a folded shape being inaccessibly to the scan cameras) or are deformed (curled) in a digital image renders data which is not comparable to what is directly measured from well-preserved specimens. Since there were ~3 controls per ASD cases, the error caused by these failed assumptions had the greater effect of reducing variable shape measures in the larger population.

These findings support our original hypothesis that the placental vascular tree is altered in ASD, although heterogeneity in ASD diagnosis in the mid 1990's, and the effective small sample size, may limit the significance of our observations. We will continue to extend these methods to the EARLI cohort as they reach the age at which ASD diagnoses can be determined, and to population-based – and actively accruing-- case-control cohorts we have established in our home institutions. The alterations suggest a globally reduced flexibility of the placenta as it grows within the uterus, which may both mark the ASD placenta, and create a risky prenatal environment that may set the fetus up for injury with any subsequent exposure (e.g., inflammation, oxidative stress).

We clearly demonstrate that the placenta in ASD differs from population-based controls, and that with increased ASD risk (EARLI compared to NCS), similar differences are found. Discarding the placenta is a missed opportunity, in terms of perinatal biomarkers and in understanding the causal chain that leads to ASD.

<u>Original Proposal:</u>

ASD reflects a range of disordered and impaired brain development which leads to a lifelong course of behavioral and cognitive abnormalities. Diagnosis cannot formally be made prior to age two and at this point there is a lack of behavioral and biologic markers that we can use to predict its onset. Early predictors could lead to early interventions which might significantly improve the lives of those affected. We intend to use the fact that the same biochemistry that controls the branching of nerves also controls branching of blood vessels. Unlike the nerve networks in the living human brain, the branching of the blood vessels in a child's placenta (that is generally discarded after birth without any examination) can be photographed and dissected. Our methods have expressly focused on the capture of potentially key placental vascular features using equipment and procedures that could be performed at any hospital delivering a baby in the US. Thus, if successful, our work could lead to the routine examinations of placentas at birth to provide a noninvasive newborn screening test to identify children at high risk for developing ASD.

In this project we will measure the branching of larger blood vessels on the surface of the placenta (2D), the placental shape (that contains the placental vascular fractal), the branching structure of the fine vessels of the thickness of the placenta (3D), and analyze the maternal medical and gestational factors that may have led to differences observed between the ASD group, a group of children with other special educational

needs and healthy control children. We have developed and will apply new tools to analyze digital images of placental blood vessel branching, as well as the mathematics required to analyze the complex patterns of this placental branching architecture. In addition to its use as a biomarker, the application of these techniques has the potential to both clarify the pathologic anatomy of ASD, and to determine when during pregnancy ASD might have developed.

Any model generated in a single population will require validation prior to its general use in public health screening. Collection of a new cohort and confirmation of positive results from this study have been generated in each year of our award as preliminary data in families with an autistic child (in placentas of subsequently delivered infants who will begin to be able to be evaluated for ASD within the next 6 months). Thus, this research is being applied in current studies of high ASD risk siblings (EARLI), PI: Craig Newschaffer, PhD) and the Markers of autism risk in babies learning early signs, (. Marbles) (PI: Cheryl Walker, MD, UC Davis, Mind Institute) networks, and shows early promise of being able to rapidly contribute to our understanding of the likely pathways of disordered neurodevelopment in the highly heterogeneous spectrum of ASD.

Task: Placental processing: *P.I.: Carolyn M. Salafia, MD, MS, NYS Institute for Basic Research in Developmental Disabilities (IBR), 1050 Forest Hill Road, Staten Island, NY, 10314. Co-Investigators: Dr Craig Charles Platt, Consultant Perinatal Pathologist and Ms Roisin Armstrong University Hospitals Bristol NHS Foundation Trust and Professor Jean Golding, Sue Ring, PhD, Mr Colin Steer, Ms Amanda Carmichael, ALSPAC, University of Bristol, Bristol, UK. There is no animal or human use at any of the above addresses except for use of archived anonymized placental specimens only at ALSPAC.*

The specified placentas will be photographed and grossly processed according to protocols that Dr. Salafia previously implemented successfully in a birth cohort, and upon which placental protocols for the U.S. National Children's Study are based. These protocols will yield chorionic surface photographs that image the 2-D chorionic surface vascular tree and serially blocked regions of the placental parenchyma from which serial sections of histologic slides can be digitized to reconstruct the 3-D (finer) chorionic vascular branched tree.
Timeline: *The 392 placentas will be fully examined, dissected and tissues processed in the first 3 months of Year 1.*

Status: The final placental sample size now totals 348 placentas: 53 ASD cases, 145 non-ASD/non-SEN controls, and 150 SEN controls. The reasons for the sample size change have been previously noted. [1]

To measure placental shape and structure, the protocol included obtaining:

1. 3D scans of the whole placenta
2. 2D photographs of fetal surface and the sliced placental disk
3. Histology samples of umbilical cord, extraplacental membranes, and placental villous parenchyma

For the purposes of this proposal, we expected the ALSPAC Executive Committee to select materials from those placentas preserved flat in casks of formalin as shown to the PI during multiple visits to the ALSPAC placental storage facility. Unfortunately, the ALSPAC Executive Committee chose to provide the placentas from a separate cohort obtained from a private community hospital. These placentas were collected by ALSPAC staff and not preserved by the Department of Pathology with usual processing methods. Instead, they were placed in hard plastic buckets that were generally smaller in dimension than the placental chorionic plate surface. Once fixed, this resulted in generally moderate to severe deformation of the placental shape and surface. The placentas were also not completely covered with formalin preservative. This, combined with ill-fitting non-air-tight bucket lids, resulted in formalin evaporation and pigment deposition on histology slides created from tissue samples of this material. This deformation of shape affected our ability to analyze 3D meshes, the 2D photographs of the placental surfaces and slices, and the

formalin precipitation has rendered image segmentation of histology samples problematic.ALSPAC placental materials received included:

Total # of placentas received: 373 Total with DX: 348
Total # with analyzable 3D scans: 179 (51%) including 63 (35%) with some degree of deformation that has been manipulated within the 3D software
Total # with deformed scans that cannot be "meshed" 53 (15%)
Total # with no 3D mesh received 116 (33%)
Total number of fetal surfaces traced 160 (45%), which is 100% of those images that can be traced, with 192 cases (55%) providing unanalyzable photographs due to surface deformation or because no photographs were received.
Total number of placental slice images traced 149 (42%)

The PI analyzed 2D and 3D images and tissue samples from 223 cases from the ASD family study that is the EARLI network of Dr. Craig Newschaffer and colleagues. While these infants have, of course, not been diagnosed with ASD, they do reflect the placental arborization of families in which a tendency to the neuropathology that results in a diagnosis of ASD has been made. As the oldest of these infants was born in late 2009, these children will soon have all undergone standardized testing germane to a definitive ASD diagnosis. Furthermore, these children have undergone extensive developmental testing at 6 and 12 months and so continuous measures of ASD characteristics and precursors might also be examined prior to identification of the cases.

[1]The change from the original proposal is 3(~5%) of the mothers with children subsequently diagnosed with ASD had not given consent for the placentas to be part of subsequent research protocols. A higher percentage of the SEN controls (~ 10%) and normal (non-ASD/non-SEN) controls (~13%) had also not provided consent. Thus a total of 53 cases plus 18 special education needs controls matched controls and 23 non-ASD/ non-SEN controls were also not included in the sample of placentas for analysis.

SUBPROJECT 1: ANALYSIS OF 2-D CHORIONIC SURFACE VASCULATURE

P.I.: Carolyn M Salafia, MD, Institute for Basic Research (IBR), 1050 Forest Hill Road, Staten Island, NY, 10314.
Co-Investigators: Michael Yampolsky, PhD, Department of Mathematics, University of Toronto, 105 George St, Toronto, ON M5A 2N4, Canada; Dawn P. Misra, PhD, Wayne State University, 3939 Woodward Avenue, Detroit, MI, 48201; Richard K. Miller, PhD, Department of Obstetrics and Gynecology, University of Rochester Medical Center (URMC), 601 Elmwood Avenue, Room 7-7550, Rochester, NY, 14642. (Note that there is use OF WHAT at any of the above addresses; use of archived anonymized digitized files only).

The chorionic surface vascular tree (laid down early in gestation, consistent with critical exposures periods for valproate and thalidomide on ASD risk) will be extracted from the digital photographs of the chorionic surface.

Status: Significant differences in the placental chorionic surface networks have been obtained from the ALSPAC cohort and replicated in a comparison of placental chorionic surface vascular networks in a high ASD risk (EARLI) and low risk (NCS) cohorts. We noted a bimodal distribution of vascular branch point numbers in ALSPAC ASD cases, with the majority of ASD cases with reduced numbers and 6 cases with strikingly increased vascular branching, greater than 1 standard deviation above the mean expected for normal (ALSPAC control) and low ASD risk (NCS) infants' placentas (**Figure 1**). We speculate that this bimodality reflects heterogeneity in ASD diagnosis in the 1990's compared with contemporary practice, as Rett's Syndrome and Fragile X Syndrome were not distinguished from ASD proper at that time. Data were not available to confirm this; however, this will be the subject of future study by our group.

Figure 1. Distribution of numbers of arterial branch points in the chorionic surface vascular networks in ALSPAC ASD cases and controls.

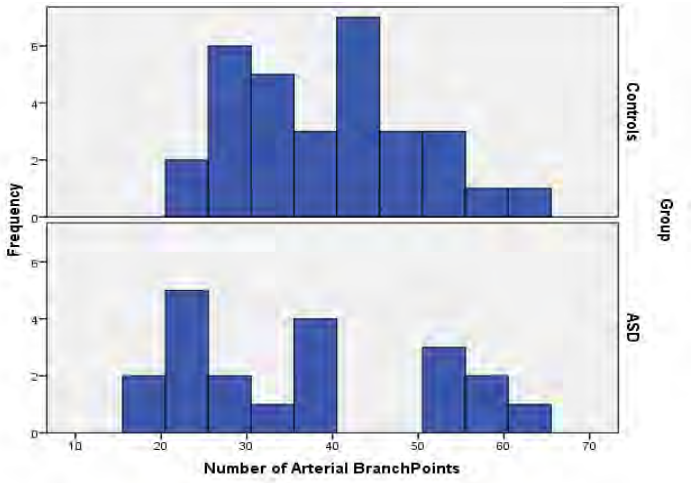

Excluding the 6 outliers, there are striking differences in the placental chorionic surface arterial networks, with similar but generally smaller effects seen in the venous networks. These differences consist of a total reduction in the number of branch generations (although not in a change in the number of vessels originating off the umbilical cord), a reduction of almost 42.5% in vascular branch points, reduced total vascular surface length and decreased placental chorionic surface vessel extension to the perimeter, and altered branching angles. (**Table 1**). The values for the ALSPAC ASD cases, excluding the distinct outliers, were similar to those found in the EARLI cohort (**Table 2**). In neither cohort was there a strong gender distinction; small sample sizes for female ALSPAC ASD cases limit the power of significance tests. ***All tables exclude the 6 hypervascular ASD cases.***

We used two other methods to explore aspects of the placental chorionic surface vessels networks, namely spline regression and data reduction/Principal Components Analysis. Multiple Adaptive Regression Splines (MARS, Salford Systems, CA, USA) examines data and determines whether relationships of given predictors to outcome measures are better represented by non-linear functions. Splines, points at which the predictor-outcome relationship changes, are not allowed to be discontinuous (i.e., the spline regression must be a single, if albeit broken, line). We have analyzed both the ALSPAC ASD cases and their controls, and the EARLI (high ASD risk) - NCS (low ASD risk) data sets of placental chorionic plate vessel variables. Spline regression determined that gender had no influence on the relationship among the 60 placental chorionic vessel measures, or the relationship of a subset of 6 variables (branch generation number, arterial branch point number, distance of vessels from the disk perimeter, distance between arteries and veins on the surface, branching angle, and vessel tortuosity) chosen because of highest loadings on extracted factors, given the limitations of small sample size) to birth weight variance, or ASD case/control status. In EARLI and NCS, separately and analyzed in combination, no difference in relationships of any one or group of placental chorionic plate vessel variables was attributable to infant gender.

The ALSPAC cohort may fail to detect significant correlations due to its limited sample size, but none of 6 factors identified independently in ALSPAC ASD cases and in controls were intercorrelated at $p<0.05$ after correction for multiple comparisons. Likewise, in EARLI and NCS, much larger cohorts, correlations between factors extracted to account for variance in placental chorionic surface vessel variables in EARLI were uncorrelated with a similar number of factors extracted from the same variables in the NCS cohort, nor was there an effect of gender on factor relationships.

Table 1 provides the descriptives and highlights variables that in univariate analyses differed between ALSPAC ASD cases and controls. It should be noted that there is a greater number of arterial variables that differed between ALSPAC ASD cases and controls, as well as the increased significance of these arterial measures, as compared to venous variables. While significance was attenuated in female ALSPAC ASD cases (due to the small sample size), trends were similar to those in male ALSPAC ASD cases (**Table 2**). We have similar findings in EARLI as compared to NCS (**Table 3**, **Figure 2 (a-c)**

Given that a major driving force in branching angiogenesis is oscillation or pulsatility of flow, we hypothesize that potentially the decreased electrical excitability *in vivo* of neurons treated with

valproate, a known risk factor for ASD when exposure is in the period in which major chorionic surface vascular networks are laid down, translates in changes in fetal heart rate variability that affect pulsatile flow on the placental surface in early pregnancy. We have found no association of number of branches off the umbilical cord insertion (the earliest developed and thus oldest) portions of the placental chorionic surface vascular networks in either ALSPAC ASD cases as compared to controls, or in EARLI compared to NCS. There appears to be no ASD- associated effect on the early vasculogenic period of placental vascular organization (<6 weeks gestation), with placental chorionic surface vascular correlations confined to the those elements of the chorionic surface vasculature laid down after the onset of the fetal heart beat.

Table 1. Descriptive statistics for selected placental chorionic surface vascular variables, with bolded items marking variables that differed significantly between ALSPAC ASD cases and controls.

		Mean	SD	Min	Max	P value
Arterial Surface Area	**Controls**	**29.6**	**7.9**	**16.8**	**49.0**	**.009**
	ASD	**23.0**	**6.2**	**15.2**	**39.6**	
Arterial Surface Area Ratio	**Controls**	**.12**	**.03**	**.08**	**.19**	**.045**
	ASD	**.11**	**.02**	**.08**	**.16**	
Arterial Number of Branch Generations	**Controls**	**10.5**	**1.9**	**7**	**15**	**.026**
	ASD	**9.1**	**1.6**	**6**	**12**	
Arterial Number of Branches off the Umbilical Cord	Controls	2.2	.6	1	3	.182
	ASD	2.5	.7	2	4	
Arterial Number of Branch Points	**Controls**	**40.0**	**10.9**	**23**	**63**	**.001**
	ASD	**28.2**	**8.1**	**18**	**40**	
Arterial Number of End Points	**Controls**	**42.2**	**10.7**	**26**	**65**	**.001**
	ASD	**30.7**	**7.8**	**21**	**42**	
Arterial Total length	**Controls**	**130.0**	**27.7**	**85.5**	**205.7**	**.002**
	ASD	**101.4**	**26.3**	**62.5**	**162.4**	
Arterial Volume	**Controls**	**2.91**	**1.23**	**1.30**	**6.19**	**.046**
	ASD	**2.17**	**.78**	**1.33**	**3.94**	
Arterial Mean Thickness	Controls	.15	.03	.10	.21	.558
	ASD	.15	.03	.12	.22	
Arterial SD of Thickness	Controls	.09	.02	.06	.14	.904
	ASD	.09	.02	.06	.12	
Arterial Mean Distance to Perimeter	**Controls**	**2.09**	**.52**	**1.22**	**3.59**	**.020**
	ASD	**2.48**	**.49**	**1.37**	**3.23**	
Arterial Mean Distance from Vascular End Point to Perimeter	**Controls**	**1.99**	**.42**	**1.26**	**2.94**	**.007**
	ASD	**2.38**	**.46**	**1.46**	**3.21**	
Venous Surface Area	**Controls**	**46.27**	**11.43**	**24.12**	**74.83**	**.018**
	ASD	**37.04**	**12.01**	**25.40**	**66.91**	
Venous Number of Branch Generations	Controls	10	2	7	15	.087
	ASD	9	1	7	11	
Venous Number of Branches off Umbilical Cord	Controls	3	1	2	4	.652
	ASD	3	1	2	3	
Venous Number of Branch Points	***Controls***	***41***	***14***	***23***	***66***	***.016***
	ASD	***31***	***11***	***14***	***54***	
Venous Total Length	***Controls***	***134.84***	***28.91***	***89.45***	***209.14***	***.005***
	ASD	***107.13***	***29.68***	***65.02***	***163.21***	
Venous Mean Distance to Perimeter	***Controls***	***2.03***	***.53***	***1.14***	***3.64***	***.017***
	ASD	***2.45***	***.52***	***1.29***	***3.24***	
Venous Mean Distance from	***Controls***	***2.01***	***.49***	***1.28***	***3.31***	***.033***

Vascular End Point to Perimeter	***ASD***	***2.36***	***.51***	***1.34***	***3.28***	
Arterial Mean Branch Angle	Controls	89.10	5.05	79.53	103.47	.575
	ASD	88.10	6.42	79.42	98.37	
Arterial SD of BranchAngle	Controls	51.65	2.34	47.72	56.43	.508
	ASD	51.10	2.97	44.07	55.83	
Arterial Minimum Branch Angle	***Controls***	***1.76***	***1.29***	***.32***	***5.02***	***.001***
	ASD	***4.10***	***3.31***	***.64***	***10.86***	
Arterial Maximum Branch Angle	Controls	176.7	.3.6	.042	.163	
	ASD	178.1	.1.35	.053	.116	.055

Table 2. Descriptive statistics for vascular variables, split by gender; bolded items mark variables that differed overall between ALSPAC ASD cases and controls (see Table 1). Male subgroup with 11 ASD cases and 24 controls, female subgroup with 3 ASD cases and 7 controls.

Gender			Mean	SD	Min	Max
Male	**Arterial Surface Area**	**Controls**	**29.28**	**6.58**	**19.31**	**46.24**
		ASD	**23.49**	**6.43**	**15.16**	**39.59**
	Arterial Surface Area Ratio	**Controls**	**.13**	**.02**	**.09**	**.19**
		ASD	**.11**	**.02**	**.08**	**.16**
	Arterial Number of Branch Generations	**Controls**	**10.79**	**1.96**	**7**	**15**
		ASD	**9.18**	**1.78**	**6**	**12**
	Arterial Number of Branches off the Umbilical Cord	Controls	2.25	.61	1	3
		ASD	2.55	.69	2	4
	Arterial Number of Branch Points	**Controls**	**40.25**	**9.64**	**24**	**60**
		ASD	**28.27**	**7.95**	**18**	**39**
	Arterial Number of End Points	**Controls**	**42.50**	**9.39**	**27**	**62**
		ASD	**30.82**	**7.67**	**21**	**41**
	Arterial Total length	**Controls**	**130.37**	**24.72**	**93.03**	**205.68**
		ASD	**101.45**	**26.16**	**62.53**	**162.40**
	Arterial Volume	**Controls**	**2.82**	**.99**	**1.30**	**4.87**
		ASD	**2.28**	**.84**	**1.40**	**3.94**
	Arterial Mean Thickness	Controls	.15	.03	.10	.21
		ASD	.15	.03	.12	.22
	Arterial SD of Thickness	Controls	.08	.02	.06	.14
		ASD	.09	.02	.06	.12
	Arterial Mean Distance to Perimeter	**Controls**	**2.01**	**.46**	**1.22**	**2.93**
		ASD	**2.57**	**.39**	**2.00**	**3.23**
	Arterial Mean Distance from Vascular End Point to Perimeter	**Controls**	**1.92**	**.42**	**1.26**	**2.94**
		ASD	**2.44**	**.40**	**1.76**	**3.21**
	Venous Surface Area	**Controls**	**44.80**	**9.76**	**27.89**	**72.02**
		ASD	**37.52**	**12.29**	**25.40**	**66.91**
	Venous Surface Area Ratio	**Controls**	**.19**	**.02**	**.15**	**.24**
		ASD	**.17**	**.03**	**.12**	**.24**
	Venous Number of Branch Generations	Controls	9.83	1.97	7	15
		ASD	8.82	1.33	7	11
	Venous Number of Branches off Umbilical Cord	Controls	2.50	.51	2	3
		ASD	2.55	.52	2	3
	Venous Number of Branch Points	**Controls**	**40.38**	**12.61**	**23**	**64**
		ASD	**29.91**	**8.86**	**14**	**42**
	Venous Total Length	**Controls**	**133.37**	**25.57**	**89.44**	**193.00**

		ASD	**106.24**	**27.81**	**65.02**	**163.21**
	Venous Mean Distance to Perimeter	**Controls**	**1.98**	**.48**	**1.14**	**2.88**
		ASD	**2.50**	**.41**	**2.0**	**3.23**
	Arterial Mean Branch Angle	Controls	89.68	5.19	79.53	103.47
		ASD	87.36	6.60	79.41	98.37
	Arterial SD of BranchAngle	Controls	51.43	2.48	47.72	56.43
		ASD	51.00	3.30	44.03	55.83
	Arterial Minimum Branch Angle	**Controls**	**1.94**	**1.35**	**.36**	**5.02**
		ASD	**4.56**	**3.57**	**1.11**	**10.86**
	Arterial Maximum Branch Angle	**Controls**	**178.38**	**1.16**	**175.40**	**180.00**
		ASD	**176.07**	**3.90**	**168.58**	**179.87**
Female	***Arterial Surface Area***	***Controls***	***30.65***	***12.08***	***16.75***	***48.99***
		ASD	***21.19***	***5.80***	***17.552***	***27.88***
	Arterial Surface Area Ratio	***Controls***	***.116***	***.03***	***.08***	***.16***
		ASD	***.099***	***.03***	***.08***	***.13***
	Arterial Number of Branch Generations	***Controls***	***9.57***	***1.72***	***7***	***12***
		ASD	***9.00***	***1.00***	***8***	***10***
	Arterial Number of Branches off the Umbilical Cord	Controls	2.14	.69	1	3
		ASD	2.33	.58	2	3
	Arterial Number of Branch Points	***Controls***	***39.00***	***15.42***	***23***	***63***
		ASD	***28.00***	***10.39***	***22***	***40***
	Arterial Number of End Points	***Controls***	***41.14***	***15.08***	***26***	***65***
		ASD	***30.33***	***10.12***	***24***	***42***
	Arterial Total Length	***Controls***	***128.93***	***38.57***	***85.48***	***190.73***
		ASD	***101.32***	***32.95***	***71.35***	***136.60***
	Arterial Volume	***Controls***	***3.22***	***1.93***	***1.40***	***6.19***
		ASD	***1.78***	***.45***	***1.33***	***2.23***
	Arterial Mean Thickness	Controls	.15	.03	.11	.21
		ASD	.14	.02	.13	.17
	Arterial SD of Thickness	Controls	.09	.02	.06	.12
		ASD	.08	.01	.07	.09
	Arterial Mean Distance to Perimeter	**Controls**	**2.34**	**.65**	**1.45**	**3.59**
		ASD	**2.15**	**.76**	**1.37**	**2.89**
	Arterial Mean Distance from Vascular End Point to Perimeter	**Controls**	**2.21**	**.39**	**1.49**	**2.65**
		ASD	**2.16**	**.72**	**1.46**	**2.90**
	Venous Surface Area	**Controls**	**51.30**	**15.80**	**24.12**	**74.83**
		ASD	**35.29**	**13.28**	**25.98**	**50.50**
	Venous Surface Area Ratio	**Controls**	**.20**	**.04**	**.12**	**.25**
		ASD	**.17**	**.06**	**.12**	**.24**
	Venous Number of Branch Generations	Controls	10.00	2.000	8	13
		ASD	9.00	2.000	7	11
	Venous Number of Branches off Umbilical Cord	Controls	2.86	.690	2	4
		ASD	2.33	.577	2	3
	Venous Number of Branch Points	Controls	43.57	18.35	25	66
		ASD	33.00	19.00	17	54
	Venous Total Length	Controls	140.01	40.39	89.71	209.14
		ASD	110.34	42.91	68.74	154.45
	Venous Mean Distance to Perimeter	Controls	2.20	.70	1.36	3.64
		ASD	2.27	.94	1.29	3.16
	Arterial Mean Branch Angle	Controls	87.11	4.27	81.78	92.29

		ASD	90.82	5.94	85.17	97.02
	Arterial SD of Branch Angle	Controls	52.36	1.72	50.48	54.27
		ASD	51.47	1.68	49.82	53.18
	Arterial Minimum Branch Angle	***Controls***	***1.12***	***.84***	***.32***	***2.63***
		ASD	***2.43***	***1.57***	***.64***	***3.60***
	Arterial Maximum Branch Angle	Controls	177.25	1.67	175.33	179.39
		ASD	178.86	.52	178.26	179.23

We find a reduced number of branch generations, as well as branch and terminal vascular points with reduced mean vascular caliber (of both arteries and veins). In addition, both arteries and veins terminate further from the surface perimeter, with greater variability in their termination relative to the disk perimeter. The distances between arteries and veins throughout their course are both greater and have greater variability. The placental chorionic vascular networks show reduced branching; we here also demonstrate **for the first time** that such variations in branching growth can be quantitated. **These differences are also meaningful regards to ASD.** They are large (e.g., ~40% reduction in branch points) observed in both sporadic ASD and increased familial ASD risk cohorts compared to their controls (ALSPAC ASD as compared to controls) or to a low risk cohort (EARLI as compared to NCS).

Table 3. Descriptive statistics for vascular variables, split by gender; bolded items mark variables that differed overall between EARLI and NCS cohorts. N: EARLI 44 male, 29 female, NCS 100 male 97 female.

Gender			Mean	SD	Min	Max	p value
Male	Arterial Surface Area	EARLI	31.94	49.24	19.64	49.24	.54
		NCS	30.91	64.11	14.70	64.11	
	Arterial Surface Area Ratio	EARLI	.12	.196	.000	.196	.40
		NCS	.12	.167	.068	.167	
	Arterial Number of Branch Generations	EARLI	**9.50**	**14**	**5**	**14**	**.001**
		NCS	**10.98**	**18**	**6**	**18**	
	Arterial Number of Branches off the Umbilical Cord	EARLI	2.09	4	1	4	.229
		NCS	2.21	4	1	4	
	Arterial Number of Branch Points	EARLI	**33.30**	**103**	**15**	**103**	**.000**
		NCS	**44.86**	**92**	**17**	**92**	
	Arterial Number of End Points	EARLI	**35.39**	**106**	**16**	**106**	**.000**
		NCS	**47.08**	**94**	**20**	**94**	
	Arterial Total length	EARLI	**121.54**	**214.52**	**62.57**	**214.52**	**.002**
		NCS	**138.96**	**234.35**	**80.34**	**234.35**	
	Arterial Volume	EARLI	**3.44**	**6.90**	**1.73**	**6.90**	**.032**
		NCS	2.919	8.33	.95	8.33	
	Arterial Mean Thickness	EARLI	**.17**	**.26**	**.000**	**.264**	**..000**
		NCS	**.14**	**.23**	**.099**	**.226**	
	Arterial SD of Thickness	EARLI	**.09**	**.13**	**.000**	**.13**	**.001**
		NCS	**.08**	**.12**	**.055**	**.12**	
	Arterial Mean Distance to Perimeter	EARLI	**2.34**	**3.50**	**1.29**	**3.50**	**.003**
		NCS	**2.12**	**3.34**	**1.29**	**3.34**	
	Arterial Mean Distance from Vascular End Point to Perimeter	EARLI	2.36	3.50	1.23	3.50	.057
		NCS	2.21	3.39	1.52	3.39	

	Arterial SD of Distance	EARLI		**.25**	**.48**	**1.67**	**.000**
	from Vascular End Point to Perimeter	NCS		**.18**	**.37**	**1.24**	
	Venous Surface Area	EARLI	41.18	73.30	21.05	73.301	.181
		NCS	38.10	94.20	14.92	94.195	
	Venous Surface Area Ratio	EARLI	.15	.20	.00	.199	.079
		NCS	.14	.22	.07	.220	
	Venous Number of Branch	**EARLI**	**9.27**	**15**	**5**	**15**	**.002**
	Generations	**NCS**	**10.76**	**20**	**5**	**20**	
	Venous Number of Branches off Umbilical Cord	EARLI	2.50	4	1	4	.59
		NCS	2.44	4	1	4	
	Venous Number of Branch Points	**EARLI**	**32.82**	**66**	**11**	**66**	**000**
		NCS	**45.37**	**98**	**16**	**98**	
	Venous Total Length	**EARLI**	**125.71**	**223.29**	**61.10**	**223.29**	**.007**
		NCS	**142.56**	**258.21**	**67.78**	**258.21**	
	Venous Mean Thickness	**EARLI**	**.20**	**.05**	**.001**	**.036**	**.000**
		NCS	**.17**	**.04**	**.09**	**.30**	
	SD of Mean Venous	**EARLI**	**.10**	**.03**	**.001**	**.09**	**.001**
	Thickness	NCS	.09	.02	.001	.036	
	Venous Mean Distance to Perimeter	**EARLI**	**.56**	**.08**	**1.28**	**3.66**	**.006**
		NCS	**.40**	**.04**	**1.51**	**3.17**	
	SD of Venous Mean	**EARLI**	**.85**	**.25**	**.52**	**1.46**	**.000**
	Distance to Perimeter	**NCS**	**.26**	**.03**	**.40**	**2.11**	
	Mean Distance from Arterial to Venous Vascular End Points	**EARLI**	**. 90**	**.22**	**.54**	**1.35**	**.000**
		NCS	**.70**	**.16**	**.0**	**1.21**	
	SD of Mean Distance from Arterial to Venous Vascular End Points	**EARLI**	**.74**	**21**	**.43**	**1.37**	**.000**
		NCS	**.61**	**.15**	**.32**	**1.16**	
	Arterial SD of Branch Angle	EARLI	51.17	56.26	45.06	56.26	.095
		NCS	51.98	57.48	45.98	57.48	
	Arterial Minimum Branch Angle	EARLI	2.08	7.54	.056	7.54	.227
		NCS	1.68	10.21	.041	10.21	
	Arterial Maximum Branch Angle	EARLI	177.57	180.00	169.42	180	.113
		NCS	178.15	180.00	171.97	18	
	Arterial Surface Area	EARLI	31.41	75.53	17.998	75.533	.47
		NCS	29.92	58.93	8.510	58.935	
	Arterial Surface Area Ratio	EARLI	.11	..03	.07	.20	.45
		NCS	.11	..026	.03	.18	
Female	**Arterial Number of Branch Generations**	**EARLI**	**8.83**	**13**	**6**	**13**	**000**
		NCS	**10.79**	**18**	**6**	**18**	
	Arterial Number of Branches off the Umbilical Cord	EARLI	2.24	4	1	4	672
		NCS	2.19	4	1	4	

Arterial Number of Branch Points	**EARLI**	**32.62**	**15.4**	**8**	**73**	**.000**
	NCS	**45.14**	**15.44**	**17**	**85**	
Arterial Number of End Points	**EARLI**	**34.86**	**15.28**	**10**	**75**	**.000**
	NCS	**47.32**	**15.29**	**19**	**85**	**85**
Arterial Total Length	**EARLI**	**122.27**	**37.84**	**61.65**	**200.75**	**.011**
	NCS	**142.49**	**36.76**	**82.60**	**264.78**	
Arterial Volume	**EARLI**	**3.41**	**1.94**	**1.58**	**11.19**	**.005**
	NCS	**2.64**	**.99**	**.61**	**5.85**	
Arterial Mean Thickness	**EARLI**	**.17**	**.03**	**.10**	**.24**	**.000**
	NCS	**.14**	**.02**	**.07**	**.20**	
Arterial SD of Thickness	**EARLI**	**.10**	**.02**	**.07**	**.14**	**.000**
	NCS	**.08**	**.01**	**.05**	**.11**	
Arterial Mean Distance to Perimeter	**EARLI**	**2.27**	**.48**	**1.08**	**3.11**	**.003**
	NCS	**2.00**	**.38**	**1.05**	**3.22**	
Arterial Mean Distance from Vascular End Point to Perimeter	**EARLI**	**2.42**	**.57**	**1.29**	**3.84**	**.000**
	NCS	**2.10**	**.37**	**1.30**	**3.242**	
Arterial SD of Distance from Vascular End Point to Perimeter	**EARLI**	**.86**	**.36**	**.34**	**1.86**	**.003**
	NCS	**.71**	**.17**	**.43**	**1.11**	
Venous Surface Area	**EARLI**	**46.12**	**15.79**	**18.88**	**90.31**	**.000**
	NCS	**37.99**	**11.85**	**10.53**	**78.55**	
Venous Surface Area Ratio	**EARLI**	**.17**	**.01**	**.10**	**.24**	**.000**
	NCS	**.14**	**.03**	**.05**	**.24**	
Venous Number of Branch	**EARLI**	**8.86**	**2.05**	**5**	**16**	**.003**
Generations	**NCS**	**10.27**	**2.23**	**6**	**18**	
Venous Number of Branches off Umbilical Cord	**EARLI**	2.52	.63	2	4	.376
	NCS	2.65	.72	2	4	
Venous Number of Branch Points	**EARLI**	**33.62**	**12.52**	**15**	**63**	**.001**
	NCS	**43.90**	**15.15**	**17**	**112**	
Venous Total Length	**EARLI**	**128.16**	**215.41**	**56.76**	**215.41**	**.036**
	NCS	144.05	243.64	75.80	243.642	
Venous Mean Thickness	**EARLI**	**.23**	**.04**	**.16**	**.33**	**. 000**
	NCS	**.17**	**.03**	**.06**	**.29**	
SD of Mean Venous Thickness	**EARLI**	**.12**	**.02**	**.07**	**.17**	**.000**
	NCS	**.09**	**.02**	**.06**	**.15**	
Venous Mean Distance to Perimeter	EARLI	2.18	.47	1.22	3.16	.016
	NCS	1.96	.40	1.01	3.20	
SD of Venous Mean Distance	EARLI	.77	.24	.42	1.53	.179
	NCS	.71	.20	.39	1.56	
SD of Mean Distance from Arterial to Venous Vascular End Points	EARLI	.89	.22	.53	1.50	.056
	NCS	.73	.16	.38	1.21	
Arterial SD of Branch Angle	EARLI	52.9	3.25	43.9	59.26	.285
	NCS	52.43	2.41	46.81	59.68	

Arterial Minimum Branch Angle	EARLI	1.83	2.05	.02	8.77	.112
	NCS	1.69	1.88	.03	11.40	
Arterial Maximum Branch Angle	EARLI	177.69	1.76	174.82	179.89	**.151**
	NCS	178.47	1.58	178.78	180.00	

Figure 2(a-c). (a) Placental chorionic surface photograph with traced arterial and venous networks; Traced arterial (b) and venous (c) networks extracted as unique layer.

Figure 3a-c. Examples of (a) "mean" arterial and venous distribution characteristics, NCS placenta; (b) arterial and venous distribution characteristics 1 SD above the mean, EARLI placenta; and (c) arterial and venous distribution characteristics at the mean, EARLI placenta.

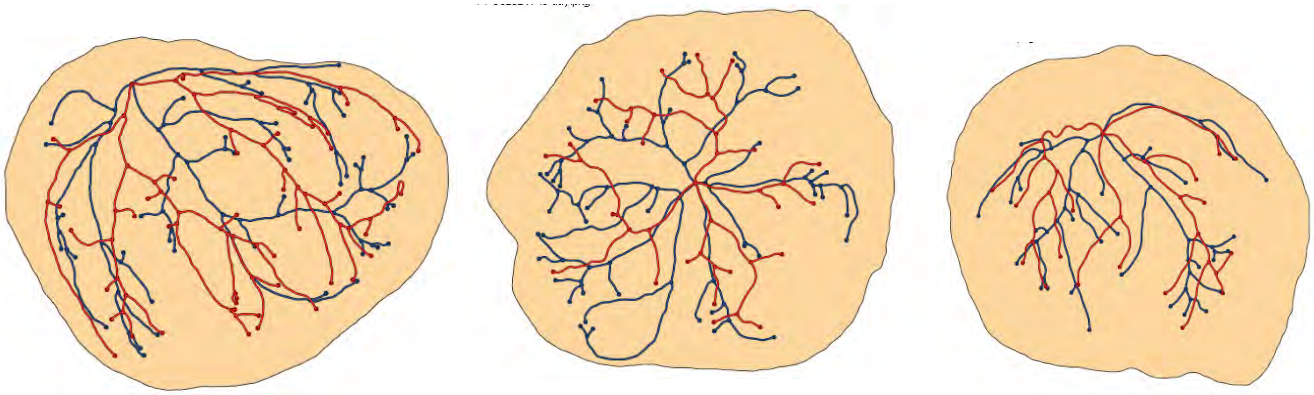

Status: We have identified significant differences in the placental chorionic surface vascular networks in ALSPAC ASD as compared to controls and have confirmed these observations in a data set at significantly increased risk of ASD (EARLI). Thus our observations may indicate the underlying genetic, environmental or epigenetic pathways that may be common to sporadic and also familial risk of ASD. These differences (e.g., reduced branching growth, decreased surface extension and greater arterio-venous distances) can be considered to share a theme of "parsimony". **The reduced length and surface area of these critical vascular networks is not of a degree to impact birth weight, but may place an at risk fetus at a disadvantage of lesser compensatory capacity and greater vulnerability to subsequent gestational stressors including inflammation and/or oxidative stress, gestational exposures that have been associated with ASD risk.**

We are prepared to move forward with studies in the EARLI cohort to identify potential candidate genes and polymorphisms that may covary with our measures of the placental chorionic surface vascular networks. We have been able to extract a larger number of variables from placental chorionic plate vascular networks but we do not yet have sufficient measures to allow application of methods of network analysis that compare patterns of features, such as used in facial recognition programs. However, we have maintained our

collaborations with Dr. Michael Yampolsky, and anticipate a hydrodynamic analysis of placental chorionic surface vessel patterns in early 2014.

The deformed chorionic plate surfaces limited such analyses in ALSPAC. However, the significant differences in ALSPAC ASD cases and controls, with all its caveats, and the EARLI and NCS as high and low ASD risk cohorts provide evidence that such networks merit study, and may be informative in the understanding of the genetic underpinnings of some ASD and the environmental or gene-environment interactions or epigenetics that underlie other ASD. A limitation of the current vascular protocol is that it is time consuming (~2.5 hours per placental chorionic surface network), and as such, would be difficult to apply to larger cohorts. We have continued to pursue work initiated in 2009 re: automation of vascular feature extraction from the placental chorionic surface photographs, now guided by our analyses that indicate which features may be. A number of features that distinguish EARLI from NCS placentas, such as the surface vascular density and the distance from vessel termination to the disk perimeter, are accessible to automated extraction from 2D photographs.

We have improved on a previous vascular recognition filtering process. The process is partly based on images' second-order characteristics and highlights image pixels from locally curvilinear structures while simultaneously decreasing non-vessel noise. The results, reported in Matthews Correlation Coefficient (MCC), comparing against the pathologist's ground truth tracings, have also been compared with an existing neural network approach. (**Figure 4-5)** The proposed enhancement process consistently outperformed the multiscale and neural network approaches in both accuracy and efficiency.

Since the process is completely automated, it provides measures that can be analyzed within seconds from a single well-prepared photograph. In brief, starting with a raw placenta image, we obtain the green channel information and stretch the intensity distribution by a linear transformation to highlight the extremely low and high intensities. The gray scale image is then converted to a binary image by thresholding the mean intensity value. The largest object in the image content is detected and filled in to create a continuous and compact domain. To create a smoother structure in the image boundary, morphological erosion is applied. The resulting image serves as a mask template and is overlayed on top of the original image to arrive at a cropped placenta image. Glare is then removed using a modified in-painting algorithm. The final image is what is utilized for the vessel extraction algorithms.

Vessel enhancing methods based on second-order characteristics uses eigenvalues of the Hessian to locally determine the likelihood that a pixel belongs to a vascular region. Note that the following discussion is intended for dark curvilinear structures with a brighter background. For bright objects with a darker background, the conditions of the eigenvalues (or the images) should be reversed. From an image's Hessian matrix, eigenvectors can be extracted corresponding to eigenvalues A1 and A2 satisfying $|A1| < |A2|$, respectively. If we associate $|Ai|$'s with the magnitude of curvatures, then u1 would likely point along with the direction where the vessel travels while u2 would point towards the edge of the vessel. These eigenvalues can then be used to define two "vesselness" measures. To eliminate the non-vessel noise that is picked up by the multiscale filter while maintaining the connected components in the vessel network, a curvilinear filter is used to further refine "vesselness". (**Figure 4**) This function highlights locally linear structure by controlling the width and length parameters, while penalizing neighborhood pixels that present non-cohesive structure. Notice that IF is a heuristic filter since it does not account for direction information. Since the orientation of the vessels varies across a single image, we create a library of curvilinear templates $\mathbf{W}k$'s corresponding to a collection of various orientations. The curvilinear filter identifies the linear regions from the multiscale filtered results. Additional mathematics enhance results by precluding negative values. The rationale is that the vessel pixels have dominating curvilinear filter responses than the noise pixels. Results are shown in **Figure 5.**

Figure 4. A box plot of maximum MCC values obtained via neural network [3] on each of 16 placentas. The best MCC value for the multiscale and the proposed curvilinear enhancement method

are also provided and are consistently superior to the neural network all cases. Figure 5. A visual comparison between the proposed and existing methods on a randomly chosen placenta patch.

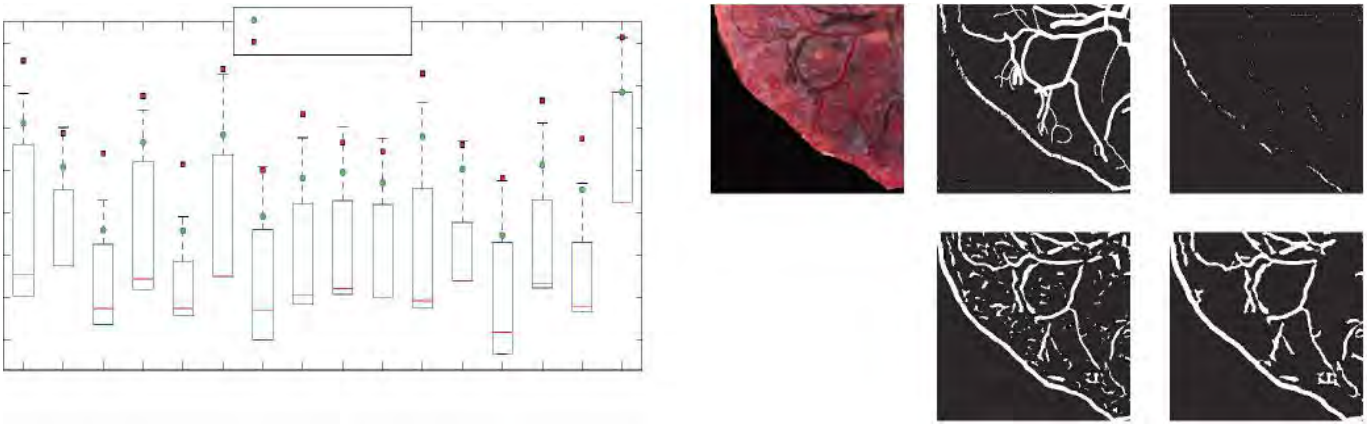

Figure 6. (a) An illustration for the conditions used in generating the curvilinear filter. (X, Y) is the pixel being analyzed, R is the vessel region, and w is the width of the filter. (b) The proposed curvilinear filter function, generated with w = 10 and l=15.

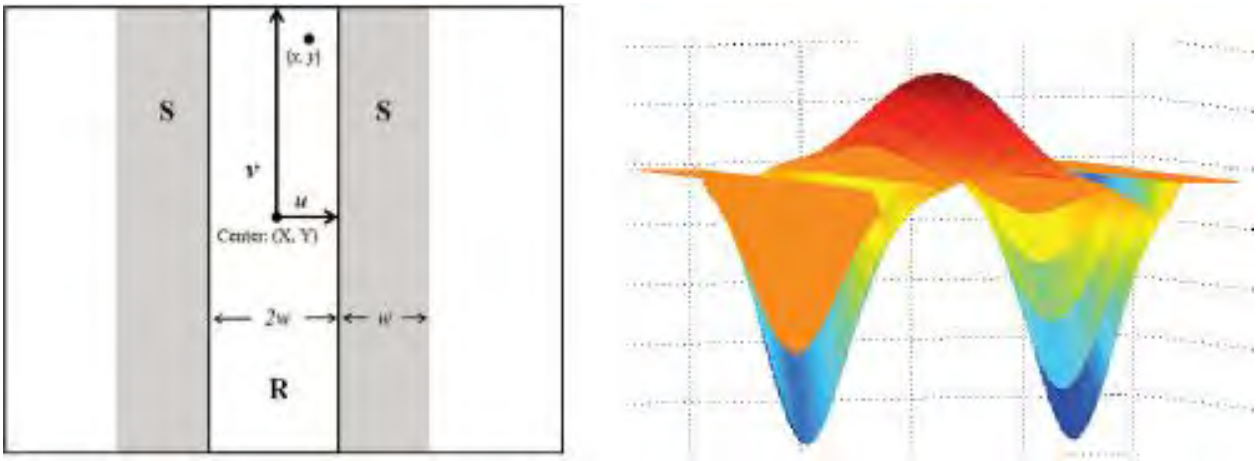

Accomplishments for this Subproject

We have documented significant differences of the chorionic surface vascular network in ASD as compared to neurodevelopmentally normal controls. Arterial features are more highly correlated with ASD than are venous features. Whether arterial outgrowth influences venous growth or whether arterial growth is more influenced by subtle changes in normal fetal physiology (such as neuronal activity and/or spontaneous electrical activity in cells of the fetal cardiac conduction system) is unclear and will be an aim in subsequent research. We have developed a preliminary method that may reliably and inexpensively extract features of vascular network structure that are germane to distinction of ASD risk, including branch numbers reflected in complexity of surface networks, and measures of extension of vessels toward the placental chorionic disk perimeter, reflecting lateral outgrowth of placental chorionic surface vessels to cover the whole placental chorionic disk.

SUBPROJECT 2: 3-D RECONSTRUCTION OF PLACENTAL VOLUME AS A PROXY FOR THE SHAPE OF THE CHORIONIC VASCULAR TREE

3D reconstructions of placental volume as a proxy for the shape of the chorionic vascular tree

Placental shapes, as captured in surface and slice images in the form of 3-D coordinate data, are created by rotating and translating the hand-traced 2D contours coordinates. Geometric descriptors will be easily extracted from the reconstructed shapes, such as surface area, volume, mean curvature, total curvature, shape moments, deviation from an average-shaped placenta, etc. These values will then be used in a classification approach, finding signatures for normal or abnormally shaped placentas, and to link these with our outcomes.

We have previously shown that2D shape information of the placenta is meaningful for health prediction: "initial findings indicate significant relationships between shape of the placental surface and newborn's birth weight as well as their gestational age." Therefore, since 3D shape information is a superset of what is available in 2D, one would expect that health prediction based on 3D shape information would be even better, and is certainly merits investigation.

3-D reconstructions of finer placental branching vasculature *Sets of blocks obtained from placental parenchyma centered on a diving chorionic placental vessel will be serially sectioned as follows: Slides 1-3 H&E, 4-5 retained for possible future immmunohistochemistry (IHC) stains, 6-8 stained with H&E, 9-10 retained unstained, etc.*

1. *The stained slides will be digitized and the series registered using standard registration techniques. Since villous branching is driven by vascular branching in the fetal systems, we need only to register the (larger) villus, simplifying the task of registration.*
2. *The registered 3-D structure will be pruned of the terminal villi, development of which is by simple capillary extension and therefore do not reflect the mechanism of growth we are targeting. This radically simplifies the fine chorionic vascular tree.*
3. *These 3-D networks will be transformed and analyzed as in Subproject 1, above.*

Status:
Our empirical models[1] and our direct research[2] indicate that both these features have their origin before the mid-trimester (irregular shape) and by 11-14 weeks gestation (umbilical cord insertion).

We have demonstrated the following:

1. There is a statistically significant difference in ALSPAC ASD placental chorionic surface shape, with **reduced** maximum radius, and **reduced** standard deviation of the radius of the chorionic surface shape, compared to placentas of neurodevelopmentally normal control children. (**Table 4**) This contrasts with last year's report (see discussion, following).

2. There is a statistically significant **reduced** eccentricity of the umbilical cord insertion, as compared to placentas of neurodevelopmentally normal control children. (**Table 5**) This contrasts with last year's report (see discussion, following).

3. After stratification by gender, these findings are also generally preserved, although significance is attenuated among females with ASD due to the small sample size. (**Tables 4-5**)

4. Differences in these measures carry over into the range of the ASD phenotypes, with significant differences in placental shape features when stratifying on either social understanding phenotype or on "repetitive stereotyped behaviour" phenotype. (**Tables 6-7**)

5. There are no statistically significant differences in the slice dimensions of ALSPAC ASD placentas as compared to the control group although the limited sample size in ALSPAC may restrict inference. (**Table 8**) However, EARLI placentas have significantly different slice dimensions when compared to a large birth cohort of ~1000 placentas with similar measurement data. (**Table 9**) When comparing ALSPAC ASD cases and controls (**Table 10, Figures 6a-h,** small sample size), and when comparing high ASD risk EARLI placentas with low ASD risk NCS placentas (**Figures 7a-c**) there appear to be different "trajectories of villous arborization from the center to the perimeter of the placental chorionic disk, with EARLI placentas showing reduced central placental disk thickness but greater preservation of that level of arborization extending to the perimeter, while NCS placentas show more variability throughout the distance from placental disk centroid to edge. This is consistent with our empirical DLA model of placental growth which predicted variability in perimeter would be

correlated with variability in thickness/villous arborization. EARLI placentas have less perimeter variability and less variability in disk thickness. EARLI placentas are, however, thinner in the more central regions of the placenta near the umbilical cord insertion, the relatively "older" portions of the placenta.

6. There is a statistically significant reduction in placental weight (~100 g, 20% of the weight of a normal term placenta) for female ASD cases compared to female normal controls. (**Table 5**) We anticipated a decrease in volume compared to both groups of controls. However, there was no statistically significant difference in volumes. (**Table 5**) This suggests that the placentas of girls with ASD, which weigh less, but occupy the same volume, are "built" differently, with relatively reduced branches despite similar length of long fetal stem anchoring villi. This would be consistent with our previous finding of an alteration in beta, a measure of the integrity of the placental vascular fractal in ASD cases compared to female normal controls**.**

7. The relationship between the placental chorionic surface vessel and the underlying placental disk parenchyma dependent on that vessel differ in ASD cases as compared to controls. This was demonstrated in an analysis of the undeformed ALSPAC 3D scans with companion flat 2D placental chorionic surface photographs., While the distribution of chorionic plate vessel segments did not differ between the two groups and there was no statistically significant difference in mean disk thickness between ASD cases and controls, both the maximum placental disk thickness and the standard deviation of placental disk thickness were significantly reduced significantly between ASD cases and controls. (**Figure 5, Table 12**) We interpret this as overall supportive of our global impression of ASD placentas being more constrained, less variable in shape, cord insertion, with more restricted arborization (reduced maximum thickness) and less "flexibility" in arborization (reduced variability in disk thickness).

The differences between last year's observations and these final data are caused by our decision to exclude data from cases in which placental chorionic surface, disk thickness (from digital photographs or 3D scans) were extrapolated from deformed placentas. We determined that our methods of decrumpling and uncurling shapes or slices, while seemingly mathematically straightforward, did not yield measures that were consistent with naked eye inspection of original images or the ruler measures provided in real time by Dr Craig Platt at Bristol in the original processing of the placenta. The degree of extrapolation to placental areas that cannot be seen directly in the scan (areas in a folded shape being inaccessibly to the scan cameras) or are deformed (curled) in a digital image) yields data that is not comparable to what is directly measured from well-preserved specimens.

The assumptions resulted in placental variable values that marked a shape more regular in all dimensions than was the actual case as determined by inspecting of scan and digital photographs. Reanalyzing the data combined with inspection of each set of placental images forces us to reject the conclusion that ASD placentas, or EARLI (high ASD risk) placentas, have either greater surface irregularity or cord eccentricity; in fact, the reverse is true.

Table 4. ALSPAC measures are derived from 2D placental chorionic surface and slice photographs, with 31 ASD cases compared to 59 developmentally unremarkable controls. ***Males, N=26 ASD, N= 50 controls females 5 ASD, 9 controls***

	Mean ± sd			
	ASD cases	Normal controls	Difference (ASD vs. normal)	p-value

Birthweight (g)				
Overall	3506 ± 368	3507 ± 521	-1	.99
Males,	3533 ± 380.7	3479 ± 532.2	+54	.64
Females	3360 ± 283.2	3660 ± 452	-300	.21
Placental weight (g)				
Overall	463 ± 107	473 ± 85	-10	.59
Males	470.89 ± 93.5	460.97 ± 75.6	-9.90	.62
Females	419.8 ± 168.8	545.9 ± 104.1	-126	.11
Placental volume (cm^3)				
Overall	487 ± 121	513 ± 108	-26	.24
Males	493 ± 119	515 ± 111	-22	.39
Females	447 ± 141	540 ± 111	-126	.18
Gestational age (weeks)				
Overall	39.8 ± 1.3	39.4 ± 1.7	+0.4	.31
Males	39.78 ± 1.4	39.3 ± 1.8	+0.48	.26
Females	39.80 ± .84	40.0 ± 1.0	-.2	.71
Umbilical distance from centroid (cm)				
Overall	2.97 ± 1.67	3.73 ± 1.88	-0.75	0.059
Males*	**2.80 ± 1.61**	**3.70 ± 1.96**	**-0.90**	**0.042**
Females	3.91 ± 1.90	3.85 ± 1.43	0.06	0.95
Radius minimum (cm)				
Overall	5.2 ± 1.74	4.58 ± 1.84	0.62	0.13
Males*	**5.43 ± 1.67**	**4.52 ± 1.91**	**0.91**	**0.041**
Females	3.95 ± 1.72	4.94 ± 1.41	-0.99	0.27
Radius maximum (cm)				
Overall*	**11.98 ± 1.99**	**13.01 ± 2.14**	**-1.03**	**0.027**
Males	**3.95** ± 1.72	**4.94** ± 1.41	**-.98**	**0.055**
Females	12.14 ± 2.22	13.30 ± 1.54	-1.16	0.27
Radius standard deviation				
Overall*	**2.13 ± 1.09**	**2.65 ± 1.17**	**-0.52**	**0.04**
Males*	**2.02 ± 1.05**	**2.64 ± 1.22**	**-0.61**	**0.031**
Females	2.71 ± 1.21	2.74 ± .88	-0.03	0.95
Radius Fourier 1				
Overall	**1.43 ± .77**	**1.79 ± .85**	**-0.36**	**0.052**
Males*	**1.36 ± .75**	**1.77 ± .88**	**-0.42**	**0.042**
Females	1.84 ± .83	1.86 ± .64	-0.02	0.94
Radius Fourier 2				
Overall	0.31 ± .20	0.39 ± .22	-0.08	0.08
Males*	**0.29 ± .19**	**0.39 ± .22**	**-0.10**	**0.046**
Females	0.43 ± .30	0.41 ± .18	0.02	0.87
Perimeter (cm)				
Overall	56.09 ± 6.11	57.19 ± 5.37	-1.10	0.38
Males	56.53 ± 6.24	56.98 ± 5.63	-0.49	0.75
Females	53.72 ± 5.73	58.36 ± 3.6	-4.64	0.07
Area (cm^2)				
Overall	233.5 ± 49.0	240.8 ± 39.7	-7.36	0.44
Males	237.5 ± 50.1	239.04 ± 41.3	-1.51	0.90
Females	**211.4** ± 39.8	**250.7** ± 29.4	**-39.3**	**0.056**
Maximum Diameter (cm)				
Overall	18.67 ± .39	19.22 ± 1.8	-0.55	0.21

Males	18.82 ± 2.31	19.12 ± 1.92	-0.30	0.54
Females*	**17.89** ± 1.68	**19.78** ± .98	**-1.89**	**0.019**

*p<0.05
**p<0.01
Negative differences == ASD cases smaller dimensions than controls.

Table 5. ALSPAC Male ASD where all ASD cases are compared to male controls. The placental measures derived from 2D placental chorionic surface and slice photographs.

	Mean ± sd			
	ASD cases	Normal controls	Difference (ASD vs. normal)	p-value
Umbilical distance from centroid (cm)	**2.80±1.61**	**3.70±1.96**	**-0.91**	**0.04**
Radius minimum (cm)	**5.43±1.68**	**4.52±1.91**	**0.91**	**0.04**
Radius maximum (cm)	11.95±1.99	12.96±2.25	-1.01	0.06
Radius standard deviation (cm)	**2.02±1.05**	**2.64±1.23**	**-0.61**	**0.03**
Radius Fourier 1	**1.36±0.75**	**1.77±0.88**	**-0.42**	**0.04**
Radius Fourier 2	**0.29**±	**0.39**±	**-0.10**	**0.046**

Negative differences indicate ASD cases have smaller dimensions than controlsThe findings of more regular chorionic plate shape and less eccentric umbilical cord insertion correlate with specific ASD phenotypes. (**Table 6-7**).

Table 6. Comparisons within ALSPAC male ASD cases stratifying on social understanding phenotype.* Placental measures are derived from 2D placental chorionic surface and slice photographs.

	Mean ± sd			
	Social Understanding <-1.0 (n=19)	Social Understanding ≥-1.0 (n=5)	Difference	p-value
Umbilical distance from centroid (cm)	2.59±1.49	4.05±1.73	-1.46	0.07
Radius minimum (cm)	**5.66±1.45**	**3.72±1.71**	**1.93**	**0.02**
Radius maximum (cm)	11.87±1.66	12.71±2.62	-0.84	0.38
Radius standard deviation (cm)	1.89±0.97	2.84±1.14	-0.94	0.07
Radius Fourier 1	1.26±0.71	1.92±0.79	-0.66	0.08
Radius Fourier 2	**0.26±0.15**	**0.46±0.24**	**-0.20**	**0.03**
Perimeter irregularity calculated from the cord insertion site	**1.93±1.03**	**3.09±1.36**	**-1.16**	**0.047**
Umbilical cord distance from the centroid (cm)	**2.32±1.00**	**4.07±2.13**	**-1.75**	**0.01**
Symmetry of the placental chorionic shape about the umbilical cord insertion	**0.39±0.21**	**0.62±0.23**	**-0.23**	**0.04**

*Social understanding phenotype variables centered on zero, more negative numbers are more “autistic”. Negative differences indicate that ASD cases <-1.0 (more “autistic”) have smaller dimensions than those above cutpoint (less “autistic”).

Table 7. Comparisons within ALSPAC male ASD cases stratifying on social understanding phenotype. Placental measures are derived from 2D placental chorionic surface and slice photographs.

	Mean ± sd			
	Repetitive	Repetitive	Difference	p-

	Stereotyped Behavior <0 (n=19)	Stereotyped Behavior ≥0 (n=5)		value
Umbilical distance from centroid (cm)	**2.53±1.57**	**4.25±1.10**	**-1.71**	**0.03**
Radius minimum (cm)	**5.65±1.49**	**3.75±1.60**	**1.91**	**0.02**
Radius maximum **(cm)**	11.90±1.98	12.60±1.38	-0.70	0.47
Radius standard deviation (cm)	**1.87±1.03**	**2.92±0.71**	**-1.05**	**0.04**
Radius Fourier 1	**1.24±0.73**	**2.03±0.51**	**-0.79**	**0.03**
Radius Fourier 2	0.30±0.21	0.33±0.09	-0.03	0.75
Umbilical cord distance from the centroid (cm)	2.40±1.41	3.76±1.17	-1.36	0.06
Symmetry of the placental chorionic shape about the umbilical cord insertion	**0.37±0.21**	**0.68±0.23**	**-0.31**	**0.005**

Repetitive Stereotyped Behavior centered on zero, more negative numbers are more "autistic". Thus " negative" differences indicate that ASD cases <0 (more "autistic") have smaller dimensions than those above cutpoint (less "autistic").

Effect sizes are similar or larger than for ASD vs. normal comparisons but not as statistically significant, probably due to reduced power given smaller N's for within-ASD comparisons. No placental differences were seen within male ASD cases by distribution of other phenotypic behaviors such as cognition. No differences were seen between male SEN subjects and male controls (data not shown). No differences were seen within male SEN subjects by phenotype distribution. (data not shown).

Table 7. ALSPAC ASD newborns' placentas (N=32) are compared to ALSPAC controls (N=52). The measures were derived from 2D placental chorionic surface and slice photographs.

	Mean ± sd			
	ASD cases	Normal controls	Difference	p-value
Mean Thickness				
Overall	2.05 ± .32	2.09 ± .33	-.04	0.26
Males,	2.19 ±.40	2.27 ± .45	-0.08	0.38
Females	2.00 ± 1.10	2.27 ± .52	-0.27	0.18
SD of Thickness				
Overall	.57 ± .12	.60 ± .12	-0.20	.31
Males	1.00 ±.000	1.02 ± .13	-0.02	0.49
Females	1.00 ± .000	1.00 ± .000	0	1.00
Maximum Thickness				
Overall	2.77 ± .41	2.88 ± .43	-0.20	0.26
Males	4.55 ± .93	4.63 ± .99	-.13	0.69
Females	4.20 ± .45	4.45 ± .69	-.25	0.47

We did not observe significant differences between the average disk thickness or other permutations of this measure (in relation to the chorionic plate surface, i.e., the length of the slice) in ALSPAC ASD cases as compared to their matched controls. However, our impression from the comparison of EARLI (high ASD risk) cases to a much larger birth cohort, the University of North Carolina Pregnancy Infection and Nutrition (UNC PIN) with low ASD risk, found significant differences (**Table 8**). The "linear deviation from the average width" and the same quantity normalized to length were calculated from a traced central slice. To simplify the procedure, endpoints were placed on the traced slice to distinguish the chorionic plate (fetal) and basal plate (maternal) surfaces. The lengths of these two curves are calculated in cm. Adding markers to the curves allows calculation of the distance between the $_i$th point on each of the two curves. The average

value is the average of that distance, the average width. If we calculate the width W_i and also $|W_i - W_{avg}|$ and take the average, the quantity is the linear deviation from average width. Divided by the slice length (average of the two curve lengths) yields the linear deviation from average width relative/ length.

Table 8. 127 EARLI newborns' placentas are compared to >1100 University of North Carolina Pregnancy Infection and Nutrition (UNC-PIN) Study controls. The measures were derived from 2D placental chorionic surface and slice photographs. The EARLI data was updated from 2011.

	UNC	EARLI	p-value
Fourier 1	**3.23±1.81**	**4.07±2.34**	**.002**
Displacement/Diameter (cm)	**.164±.091**	**.204±.12**	**.002**
Sigma	**1.106±.492**	**2.680±1.47**	**.000**
Average (Avg.) Width (cm)	**2.08±.38**	**1.74±.27**	**.000**
Linear Deviation from the Average Width (cm)	**.34±.111**	**.364±.135**	**.001**
Linear Deviation from the Average Width (Relative)/Length	**.020±.007**	**.019±.007**	**.001**

There is normally some thinning over this distance as the placenta transitions from the arborized placental disk to the thin chorion of the extraplacental membranes. Slice characteristics were extracted from undeformed 3D scans. The observed differences in mean disk thickness would be significant with a sample size of 38 per group (**Table 9**). We next tested for differences in the pattern of change of disk thickness from the centroid of the placental shape to its edge. (**Figures 7a-h)** The differences in the ratio of disk thickness at the placental disk's geometric center (centroid) to the thickness at the margin (**Table 9**) would be significant with 25 per group. The ASD cases have a trend to reduced overall disk thickness but are thicker, relative to the disk edge. This means that there is reduced natural "taper" or transition of the placental chorionic disk, fully arborized to an average 2+ cm thick, to the 1 mm thick extraplacental membranes that continue off the placental chorionic disk to contain the fetus until birth.

Table 9. ALSPAC ASD newborns' placentas (N=20) are compared to ALSPAC controls (N2=29). The measures were derived from undeformed 3D placental scans.

		Mean	SD	Min	Max
MeanThickness	Controls	2.36	.31	1.72	3.11
	ASD	2.20	.42	1.63	3.45
Ratio of thickness at Centroid/Thickness at Perimeter	Controls	9.50	2.64	4.19	15.58
	ASD	10.38	2.82	6.77	17.33

We have compared the trajectory of disk thickness change in EARLI and NCS placentas and find that there is a relative reduction in central disk thickness and a greater preservation of that measure to the perimeter in EARLI, while thickness is more variable in NCS with a greater per cent reduction in disk thickness as a function of distance from the disk perimeter. (**Figures 8a-c)**

Figures 7a-h. Comparison of trajectories of change in thickness as a function of the fractional distance from the perimeter, (L) Controls, (R) ASD cases, as calculated from the umbilical cord insertion point (IP) or the geometric center of the placental surface area (centroid).

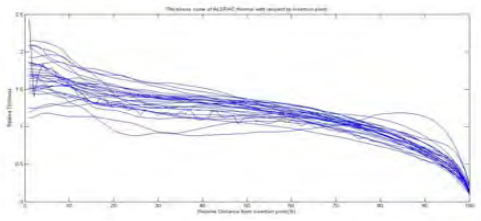

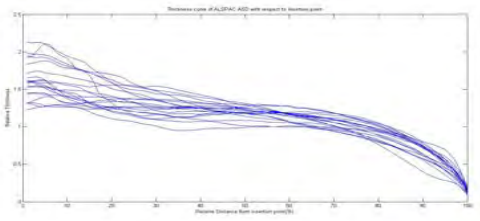

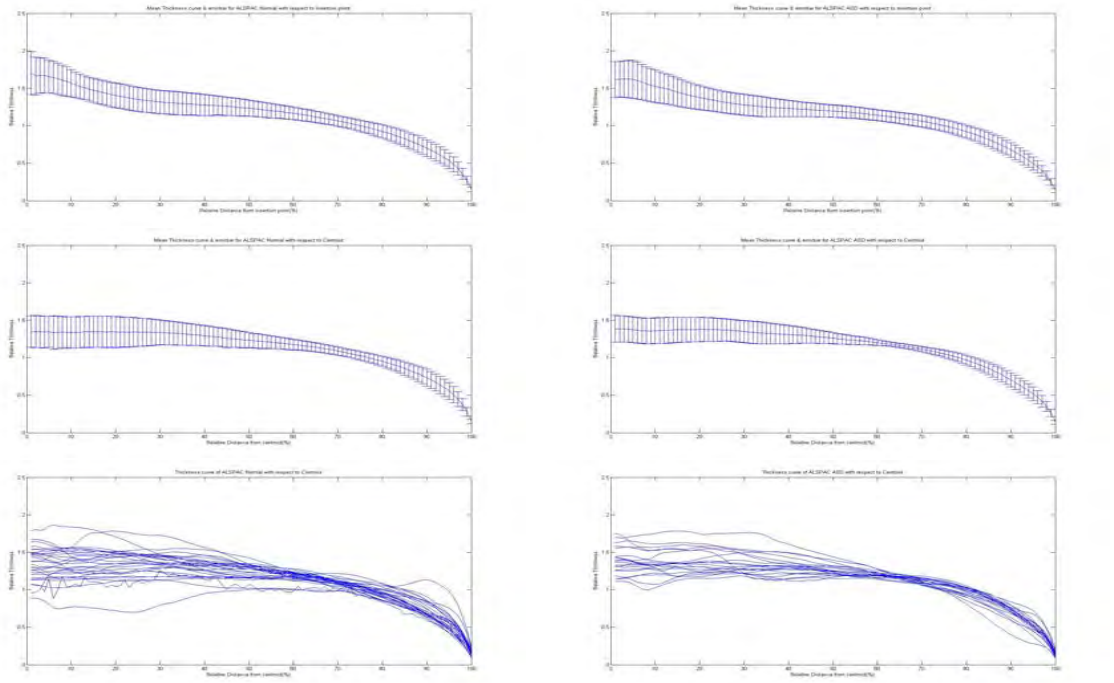

Figure 8 a-c (a, top left) Actual change in disk thickness from centroid to edge in EARLI (red) and NCS (blue) placentas. Figure (b, top right). Mean change in disk thickness from centroid to edge in EARLI (red) and NCS (blue) placentas. Figure (c, bottom left). Standard deviation of change in disk thickness from centroid to edge in EARLI (red) and NCS (blue) placentas.

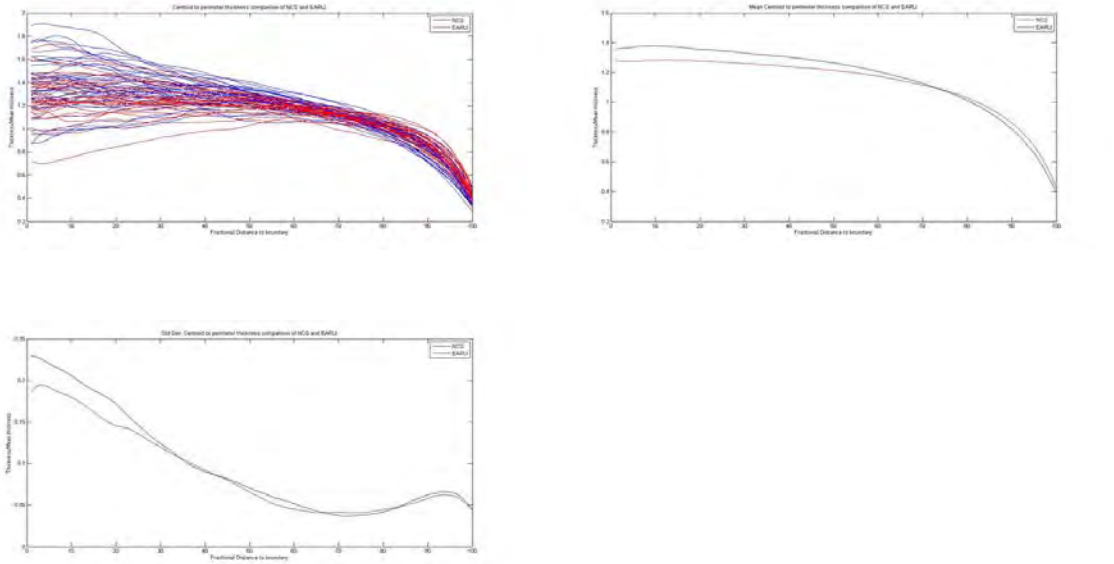

.

The placental chorionic plate vessel networks overlie the placental parenchyma. The placental chorionic plate vessels provide branches that dive deep into the parenchyma to branch to form the fetal stem vessels and the placental functional units that terminate in the villous capillary networks that are the site of all oxygen and nutrient exchange between the mother's and the fetal bloodstreams. The 3D scans of the placental volumes can be rendered as polar maps of the placental thickness (on the y-axis) and the umbilical cord insertion (along the x-axis). In effect, the polar maps provide a step-by step "map" of placental growth and development out from the umbilical cord insertion (the initial site of placental vasculogenesis), with each step on the y-axis reflecting placental growth at t=0, t=1 and t=2, etc. When the chorionic plate surface vessel networks, as extracted from the traced 2D photographs, are overlaid on the placental "thickness map", the relationship between the overlying chorionic plate vessels and the subjacent placental parenchyma is made explicit (**Figure 9**). Chorionic plate vessels are largest in caliber at their origin from the umbilical cord insertion, and progressively decrease in caliber as branches are dropped off to develop into the placental

functional units underlying the chorionic plate. We postulated that the relationship between the placental chorionic surface vessel and the underlying placental disk parenchyma dependent on that vessel would differ in ASD cases as compared to controls.

Figure 9. Polar projection of a 3D placental scan overlaid with placental chorionic surface vascular tracing obtained from companion 2D photograph. The colors of the map indicate disk thickness; the colors of the vessels indicate their caliber on the surface.

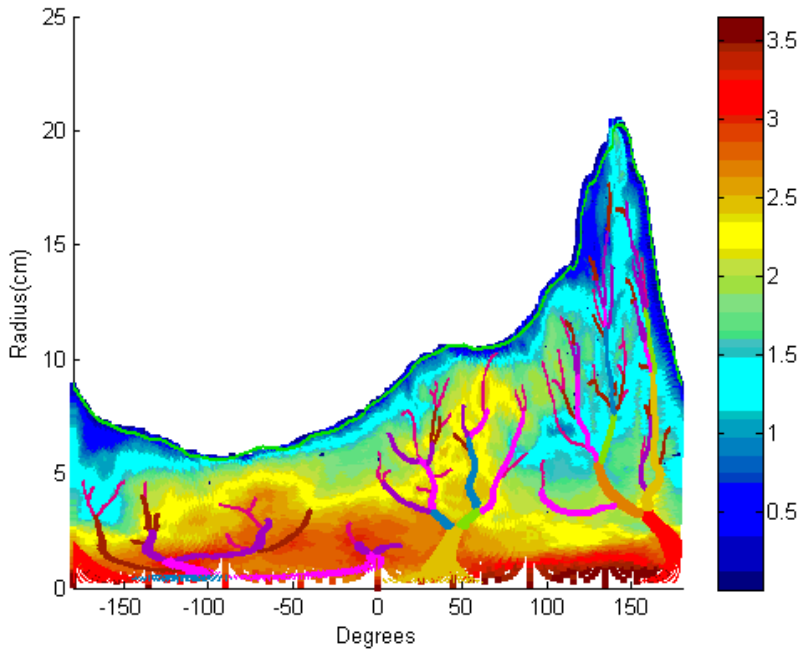

This was demonstrated in an analysis of the undeformed ALSPAC 3D scans with companion flat 2D placental chorionic surface photographs. Chorionic plate vessels were marked by vessel caliber using pen colors. The color corresponded with pixel width, which translates directly into vessel diameters. As can be seen in **Table 12**, the distribution of chorionic plate vessel calibers was not different between the two groups, (p=0.51), although, as described above, the surface vascular networks in ASD placentas were shorter in total length with fewer branch generations. Given our previous findings of no statistically significant difference between ASD cases and controls in mean disk thickness in the available scans, any association of placental chorionic plate vessel diameters with disk thickness would imply deviation from what is likely a critical relationship between the placental chorionic surface vessel and the subjacent parenchyma of arborized villi. Both the maximum placental disk thickness and standard deviation of placental disk thickness associated with any given placental chorionic surface vessel caliber were significantly reduced between ASD cases and controls. We interpret this as consistent with what we have observed in terms of the generally reduced flexibility in placental growth in ASD placentas, with more regular shapes, more central cord insertions and now both a "cap" on placental villous arborization (maximum disk thickness) for placental chorionic surface vessels of any given caliber, and reduced variability placental villous arborization (standard deviation of disk thickness).

Table 12. Correlations of chorionic plate vessel characteristics and underlying placental disk thickness; Control chorionic vessel segment N=231, ASD chorionic vessel segment N=158.

		Mean	SD	Min	Max	P value
Chorionic Plate Vessel Diameter	Control	.247	.130	.048	.600	.51
	ASD	.256	.132	.057	.523	
Average Placental Disk Thickness	Control	2.800	.643	1.598	4.925	.30
	ASD	2.729	.717	1.308	4.907	
SD of Placental Disk Thickness	**Control**	**.574**	**.248**	**.052**	**1.261**	**.000**
	ASD	**.474**	**.249**	**.085**	**1.720**	
Maximum Disk Thickness	**Control**	**3.901**	**.704**	**2.545**	**6.267**	**.000**
	ASD	**3.630**	**.724**	**2.189**	**5.557**	
Min Disk Thickness	Control	1.418	1.021	.000	4.474	.088

	ASD	1.599	1.037	.000	4.257	
Total Surface Area	Control	3.135	2.066	.238	13.686	.40
	ASD	2.954	2.081	.323	14.859	

This can be explained biologically in one of two ways, if variability in placental shape features is the result of variability in the intrauterine environment as the placenta is established and matures:

1. **Either fetuses who will have diagnoses of ASD made in childhood have unusually uniform maternal environments, so that placental shape variability is not needed to be invoked as a response, or**
2. **The placentas of fetuses who will have diagnoses of ASD made in childhood have restricted ability to vary aspects of placental growth that allow compensation for the normal and variability in the maternal uterine environment.**

Since there is no evidence that mothers who deliver children who will be diagnosed with ASD have less complicated pregnancies, or have more uniform uterine environments throughout gestation, we propose that the ASD placenta is less able to compensate for normal intrauterine variability, and may thus not only mark children at ASD risk, but also provide a mechanism for fetal injury, if reduced compensatory capacity leaves the fetus of infant more vulnerable to other stressors such as inflammation or oxidative stress.

In pursuit of understanding what changes in placental structure can account for the observed the relationship of volume to weight, we moved to the formalin fixed slices provided by Dr Craig Platt, and selected portions of the disk that might provide preliminary insights into possible structural changes. We pursued these studies in light of the report of abnormal villous configurations resulting in the appearance of "trophoblast stromal inclusions" (TSIs) were more common in placentas of children at risk for ASD (a population roughly comparable to our EARLI cohort, of placentas from newborns in families with an older sibling already diagnosed with ASD). If such findings were more common in a population with an approximately 20% risk of ASD (Craig Newschaffer, personal communication), we anticipated a clear cut difference between ALSPAC ASD and control placentas, that might be appreciable in confocal microscopic analysis of the distal villi, or, alternatively, in placental histopathology slides.

We first turned to the actual placental tissue of ALSPAC ASD cases and controls. We developed a standardized dicing approach to 2 mm samples extracted from central placental slices avoiding fetal stem villi. These specimens could also be stained to highlight the villi (**Figure 10a**) or compartments within villi. (**Figure 10-b)** Thus these samples would be enriched for terminal villi, villi that predominantly develop after the midtrimester. Using a stereomicroscope, one observer performed dissection of these samples blinded to case/control status. 1853 microdissected villous clusters were extracted from 11 controls and 971 from 7 ALSPAC ASD cases. Individually, these two classes of clusters could be distinguished by a two-fold difference in standard deviation, a reflection of sample heterogeneity. (**Figure 13**)

Figure 10 a-b. a) Microdissected villous fragment stained with eosin (green); retained erythrocytes can be seen within villous capillaries (red). b) Microdissected villous fragment stained with cytokeratin-8 (red) to mark villous trophoblast outlines and CD-31, an endothelial marker that highlights villous capillaries (green).

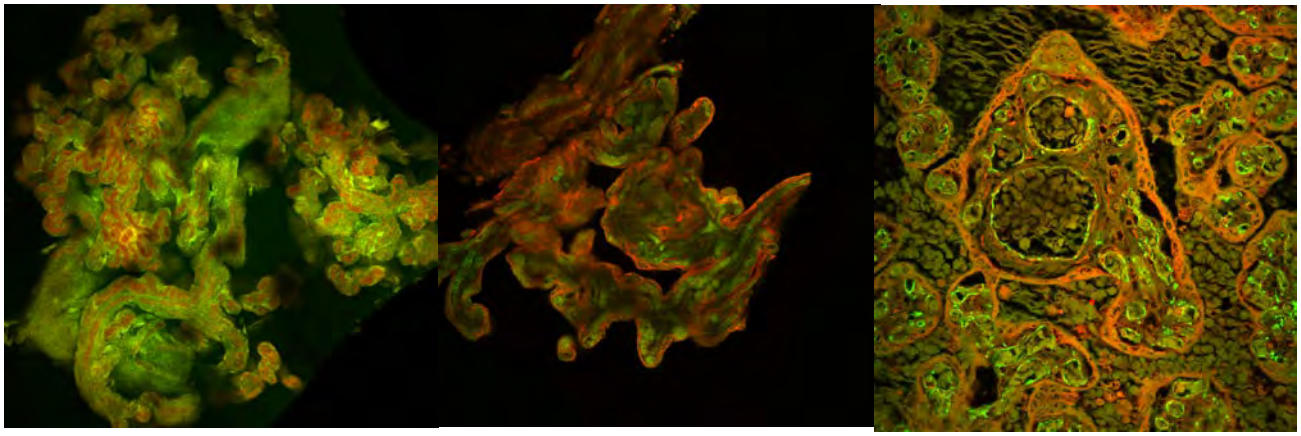

Heterogeneity of this type is less in ASD microdissected villous clusters. However, the se clusters came from 11 controls and 7 cases; the aggregated data examining the difference in means for each placenta analyzed did not show a significant difference, whether analyzed as continuous data or categories. The distributions are highly skewed (large standard deviation relative to the mean, **Figure 14).** Thus we have no *a priori* basis to expect differences in terminal villous branching structure that might be expected if the villous surfaces were more irregular (and thus had greater likelihood of cutting the villous surface so as to catch an "island" of trophoblast epithelium within the villous stroma, a "TSI)".

Table 13. Descriptives of all microdissected villous clusters without consideration of repeated measures (samples drawn from 11 ALSPAC control and 7 ALSPAC ASD placentas, Mann Whitney U test).

		N	Mean	SD	Min	Max	P value
Area	Controls	1853	1376	3144	100	60339	.474
	ASD	971	1077	1600	201	19798	
Perimeter	Controls	1853	236	269	45	3878	.308
	ASD	971	209	176	58	1556	
Area/Perimeter	Controls	1853	3.49	1.14	1.94	9.53	.136
	ASD	971	3.39	1.00	1.94	8.85	

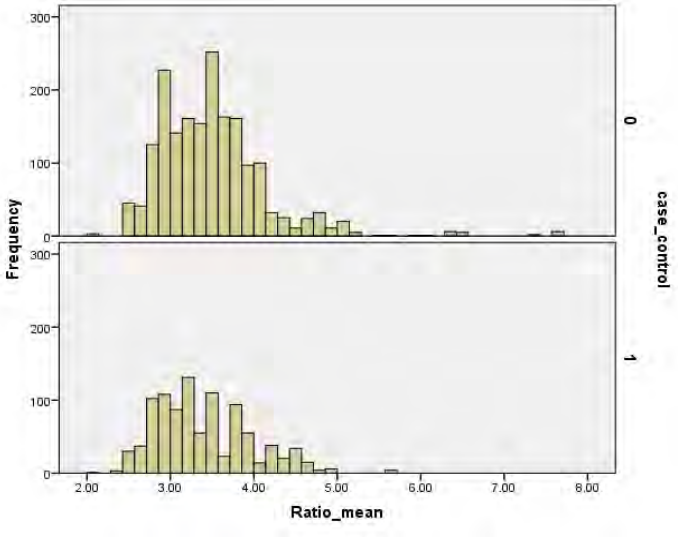

Figure 14. Distributions of Area/Perimeter ratios of dissected microclusters from 11 ALSPAC controls and 7 ALSPAC ASD cases.

We next turned to the routine histopathology slides for ASD cases and controls. From 20 ASD cases and their matched controls, two slides per case were selected from the 6 slides archived per case and provided to the PI blinded to case status. We first tested the diagnostic criteria for TSIs. Time to review one slide averaged 15 but ranged up to 35 minutes. This was due to the difficulty, in manual slide review, of being confident that every field in the slide was reviewed, and all fields reviewed once. To assure that no duplicate TSIs were scored, we elected to document each scored TSI with a photomicrograph of its region of interest. This increased reviewer time 10 minutes per slide. Despite these protocols intrarater reliability was poor with variation of >100% in the number of TSIs identified by the same reviewer.

For this reason, we have elected to identify TSIs using IHC in an immunohistochemistry (IHC) based method for automated slide review, with regions of interest as identified by cytokeratin-7 (CK7) immunoreactivity, a specific marker of the trophoblast, isolated by algorithm from the whole digitized slide. The ALSPAC H&E slide archive has been digitized; thus, each histology slide exists as a digital file of from 500-1100 MB. Our IHC protocol includes the retention of the coordinates of regions of interest (ROIs) containing a solid area of IHC immunoreactivity separated by at least 2 stromal nuclei from the overlying trophoblast epithelium, as an annotation of the analyzed slide. The slide with annotation and the same region of a serial section stained with routine hematoxylin and eosin (the current published method for identification of TSIs) will be reviewed by for specialist pathologist review.

Three pathologists (Carolyn M. Salafia, MD MS (PI), Theonia Boyd, MD, Harvard Medical School, and Drucilla J Roberts, MD, Brigham and Women's Hospital, Boston, MA) are participating in validation of TSI

identification on H&E and IHC stained slides. We expect some ongoing level of algorithm refinement to optimize the H&E and IHC computational algorithms for automated digitized slide review and to develop

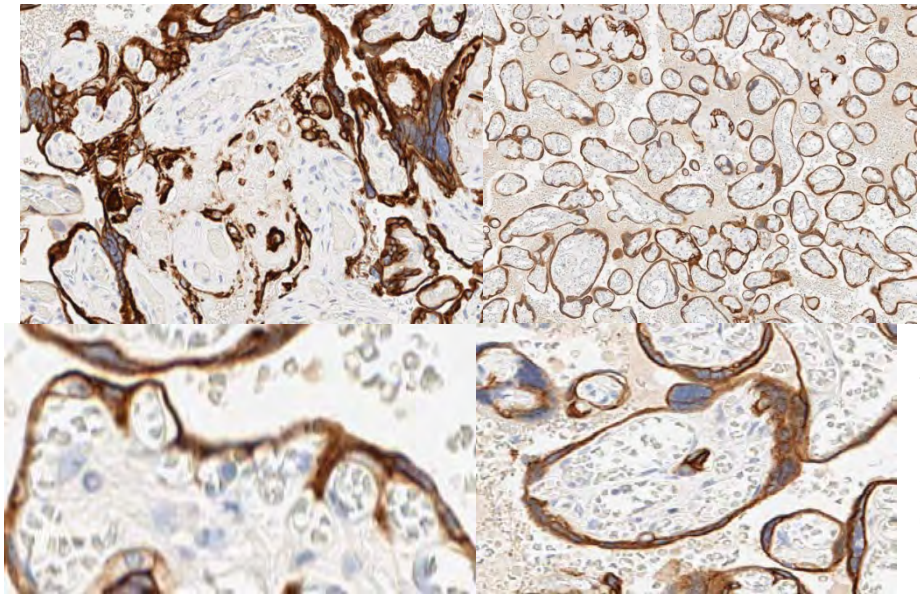

Figures 11 a-d. CK-7 IHC staining of contemporary placental pathology specimens. A. CK-7 outlining of chorionic villi, with isolated CK-7 positive cytotrophoblast enmeshed in perivillous fibrin. B. Low magnification view of CK-7 IHC with one villus with apparent TSI. C. Irregular (scalloped) villous outline suggested being a precursor to TSI. High magnification view of apparent TSI found in (B).

a validated algorithm for identification of TSIs in routine stains. Since the frequency of TSIs was reported only rarely to more that 3 per histological slide (<<1% of villi), our approach will reduce expert pathologists' time for slide review, and validate diagnostic criteria for TSIs in routine H&E and in IHC slides, and that will provide reliable and reproducible analysis to confirm or refute the value of this marker as a perinatal predictor of ASD risk, with CK-7 as the definitive identifier of trophoblast and determinant of the epithelial origins of stromal cell clusters (TSIs).

These studies do not approach analyses of the larger fetal stem villi, those whose development may e particularly compromised when beta, the fractal dimension that relates normal birth weight and placental weight, deviates from 0.75. We have joined with Marcelo Magnasco, Ph.D. (Professor, Mathematical Physics Laboratory, Rockefeller University, New York) and George Merz, Ph.D., Head of Image Analysis and Microscopy at IBR, and are pursuing analyses at the stem villous levels via two methods.

Previously, Dr Magnasco, in an attempt to study the fine structure of the human liver, realized that registration of serial sections of even this solid organ was not possible from histology slides since the shear on the tissue caused by the microtome distorted each section just enough to preclude registration. We have identified lobules of placental functional units from the slices of ALSPAC placentas provided by Dr. Craig Platt. We have experimented with the best protocol for immunofluorescent labeling of the villous trophoblast surface (with CK-7 antibodies) and the stem and villous endothelium (via CD 31antibody). (e.g., **Figure 12 c**) Dr. Magnasco's protocols allow for evaluation of frozen formalin fixed tissue in a sucrose density matched medium. The tissue face is imaged with a high resolution camera under fluorescent light. Next, the slices are and the new tissue surface is imaged. It is these serial faces of the tissue, undistorted by microtome shear stress that will be segmented and registered to reproduce a virtual placental fetal stem villous "tree". Neurolucida ™ will be used to register the sections and recreate the 3D villous tree structure.

Our second approach is a continuation of our work using Definiens Developer™. Thomas Haberichter, Ph.D., former Senior Scientist at Definiens has committed 20% effort over the next 6 months to compile algorithms that will allow translation of Dr. Merz's 3D reconstruction of images collected via the laboratory of Dr. Magnasco, and to update the image segmentation algorithms initially piloted in 2006. Once the 3D reconstruction is completed, the model can be virtually sliced to mimic the orientations of routine 2D

histology slides. Also model parameters can be manipulated to understand the genesis of observed 2D patterns of branching arborization in our ALSPAC and our EARLI histology slides.

The color image segmentation of routinely stained hematoxylin and eosin stained slides in the ALSPAC cohort has been expected to be difficult:

- aging of tissues after 20 years preservation in formalin alters staining characteristics of key components, especially loss of the normal red-orange staining of erythrocytes and instead a pale pink coloration of these cells that is virtually indistinguishable from connective tissue
- formalin evaporation precipitates opaque black formalin on tissues, obscuring tissue details and further complicating segmentation.

The basic principle that we use for segmentation is that the slide background is white. Thus an approach is to determine for every pixel a scalar quantity describing how white that pixel is, and then comparing this quantity to a threshold. The details then are in how to compute the scalar quantity and how to set the threshold. For different applications and purposes, we adapt suitable thresholds and quantity for the specific characteristics. Edge detection of complex villous trees remains problematic in routine stained slides. We will continue to pursue this path toward placental villous image segmentation outside of the scope of this year of no-cost extension. However, in order to complete our tasks, we have elected to simplify the villous images to render segmentation a far simpler task, by use of cytokeratin staining. (**Figures 12 a-c**) The four images below show routine staining and CK-7 IHC at 4x and 20x magnifications. At even 20x magnification, the villi are crowded and intervillous (maternal) erythrocytes make distinction of villous boundaries (essential for villous segmentation) problematic. However, CK-7 IHC outlines the villous borders, and simplifies segmentation, and can be employed both in microclusters (see above) and of the exact microcluster preserved as a histologic sample. (**Figure 12c**) We have shifted from focusing on extraction of the villous interface with the maternal intervillous space to extraction of the interface between villous stroma and trophoblast epithelium. This will consistently reduce the estimated villous caliber/area, but will provide clear segmentation between image elements (villi) with trophoblast covered surfaces.

Figure 12 a-c. a) Routine hematoxylin and eosin stained tissue section showing central large villous stem flanked by tiny terminal villi. b) IHC for CK-7, serial section, with same central large fetal stem flanked by tiny terminal villi. c) IHC for CK-7 (red) and CD-31 (green, immunofluorescence darkfield examination).

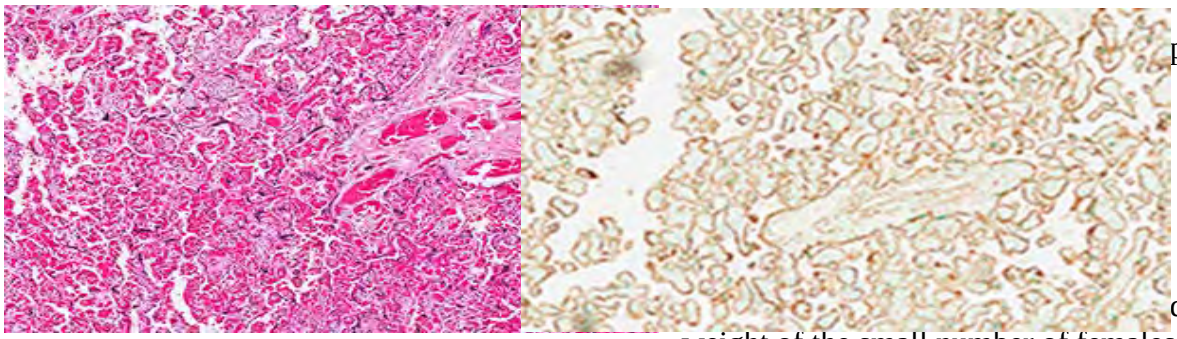

pe of image difference in weight of the small number of females with ASD and their female controls, male controls, and males with ASD. Given that there was a statistically significant reduction in placental weight (~100 g, 20% of the weight of a normal term placenta) in placentas of females with ASD cases compared to female controls, we anticipated a decrease in volume compared to both groups of controls. However, there was no statistically significant difference in volumes of ALSPAC ASD cases and controls groups. This is true for the all ASD females as well as when restricting the sample to children born at term gestation or adjusting for gestational age. This was not the result of outliers in either distribution. We did not find similar effects in males. While males represent the vast majority of ASD cases, it appears that there may be differences within ASD by sex. This suggests that the placentas of girls with ASD, which weigh less, but occupy the same volume, are “built” differently, with relatively reduced branches despite similar length of long fetal stem anchoring villi. This would be consistent with our previous

finding of an alteration in beta, a measure of the integrity of the placental vascular fractal in ASD cases compared to female normal controls.

In summary, in this project we observed significant differences in placental chorionic surface shape (reflecting lateral chorionic vascular extension), and placental disk thickness initially identified in the first EARLI family placentas analyzed in 2011 have been confirmed in the ALSPAC cohort. This supports the hypothesis that deviations in placental angiogenesis are correlated with ASD as diagnosed in ALSPAC and can be also demonstrated in placentas of EARLI newborns that have not yet been diagnosed with ASD. Future exciting research will determine whether the differences in EARLI placentas are confined to that percentage of children in such high risk families who will eventually be diagnosed with ASD by 2 years of age, or whether high risk families have global and basic differences in angiogenesis (in which case EARLI newborns will share deviations from the standard patterns of vascular growth we have documented in low risk birth cohorts). This will allow more targeted investigation of genes and gene-environment interactions in gestation that may be central to genesis of ASD risk.

Accomplishments for this Subproject

Significant differences in placental chorionic surface shape (reflecting lateral chorionic vascular extension), and placental disk thickness initially identified in the first EARLI family placentas analyzed in 2011 have been confirmed in the ALSPAC cohort. This supports the hypothesis that deviations in placental angiogenesis are correlated with ASD as diagnosed in ALSPAC and can be also demonstrated in placentas of EARLI newborns that have not yet been diagnosed with ASD. Future exciting research will determine whether the differences in EARLI placentas are confined to that percentage of children in such high risk families who will eventually be diagnosed with ASD by 2 years of age, or whether high risk families have global and basic differences in angiogenesis (in which case EARLI newborns will share deviations from the standard patterns of vascular growth we have documented in low risk birth cohorts). This will allow more targeted investigation of genes and gene-environment interactions in gestation that may be central to genesis of ASD risk.

SUBPROJECT 3: EPIDEMIOLOGY OF GESTATIONAL MODIFIERS OF PLACENTAL VASCULAR STRUCTURE AND ASD RISK

P.I: W. Ted Brown, MD, PhD, IBR; Co-Investigators: Carolyn M Salafia, MD, IBR; Eric London, MD, IBR; Dawn P. Misra, PhD, Department of Family Medicine and Public Health Services, Wayne State University School of Medicine, 101 E. Alexandrine, Room #203, Detroit, MI, 48201 (no animal or human use at any of the above addresses; use of archived anonymized data only).

Given the final limitations of sample size, it would not be reasonable to pursue multivariate analyses of relationships among placental features and gestational exposures or maternal medical or gestation factors in regards to ASD case/control status.

KEY RESEACH ACCOMPLISHMENTS

This project has, despite the obvious issues with specimen quality, provided the first population based analysis of placental growth and development in children diagnosed with ASD compared to population based controls. Given recent claims that there is placental villous maldevelopment in placentas of children at risk for but not diagnosed with ASD, these data, of a comparatively "regular" placental shape, reduced cord eccentricity and reduced villous arborization, speak against increased villous complexity. We have searched for villous maldevelopment using confocal microscopy at the terminal villous level and have found no evidence of altered villous development in this late gestational stage placental feature. We have, at no additional cost, continued to incorporate EARLI high risk newborn's placentas into data analysis, which in Year 1 provided our first evidence supporting the hypothesis that placental structure is measurably different in ASD cases, as well as potentially in their families, reflecting genetic predisposition to altered patterns of angiogenesis or altered susceptibility to factors that modify angiogenesis. Methods for volume reconstruction and estimation from 3D mesh and 2D photographs have been validated in the National Children's Study, a significant cost savings to this project. An algorithm has been developed for the automated selection of ROIs of a digitized IHC slide stained to identify CK7 a specific marker for trophoblast which allows for more rapid review of whole slides and more consistent TSI diagnosis, both of which will, if our analysis supports the association of increased numbers of TSI with ASD, provide an inexpensive and reliable tool for TSI quantitation. The principles underlying the components of this algorithm (positive pixel discrimination, object discrimination with labeling of villous structures by size and histology characteristics, annotation of slides with ROI selection of areas meeting algorithm criteria for dedicated review by expert pathologist) are readily translatable to our goals of clarifying the possible association of other placental exposures (acute inflammation, chronic inflammation and oxidative stress) with ASD case status.

Our findings are:

1. **The chorionic surface vasculature in most cases of ASD differs from that of controls.** The differences in the placental chorionic surface networks are most striking in the arterial networks, with similar but generally smaller effects seen in the venous networks. These differences consist of a total reduction in the number of branch generations although not in a change in the number of vessels originating off the umbilical cord, a reduction of almost 42.5% in vascular branch points, total vascular surface length and failed extension of the chorionic vessels over the full surface of the placenta chorionic plate (measured by an increased distance of vessels from the perimeter), and altered angles of vascular branching. (**Table 1**). These reductions are common to ASD males and ASD females. (**Table 2**)

2. **There is a striking bimodal distribution of chorionic surface vascular parameters within ALSPAC ASD cases**, with the majority showing a ~40% reduction of chorionic surface branch points compared to controls but 6 cases with markedly increased placental chorionic surface branching, greater than one standard deviation above the mean for normal controls. (**Figure 1**) The two groups of ALSPAC ASD cases cannot be distinguished by gender, gestational age or extremes of birth weight or placental weight. We speculate, since pertinent data are not available from ALSPAC, that this reflects heterogeneity within the ASD population as it was determined in the early-mid 1990's, and that these ASD "outliers" with marked surface hypervascularity are cases of ASD diagnosed in genetic syndromes that currently are excluded from the spectrum of ASD (e.g., Fragile X, Rett's Syndrome, etc). These cases have been excluded from all analyses (including (1), above). We propose this because in the ALSPAC cohort, the ASD sparse-vascularized group shares essentially the identical mean and SD of placental chorionic surface branch points with the high ASD risk EARLI (Early Autism Longitudinal Investigation) cohort of newborns in families with an older child who has an ASD diagnosis (**Table 3**), while the ALSPAC controls and the low ASD risk National Children's Study have essentially identical chorionic vascular parameters. **Figure 2a-c** presents the original photograph from which placental

chorionic surface vascular networks are traced with the completed tracing, extracted, on the right, as arterial and venous networks. **Figures 3a-c** includes representative chorionic surface vascular networks of NCS placentas, and ASD placentas both with arterial branchpoints at the mean and 1 SD above the mean.

3. **No gender dimorphism** of vascular network structure is appreciated in ALSPAC ASD cases or neurodevelopmentally normal controls in EARLI as a whole or stratified by gender. (**Tables 2-3**)

4. **There is a statistically significant difference in ALSPAC ASD placental chorionic surface shape**, with **reduced** maximum radius, and **reduced** standard deviation of the radius of the chorionic surface shape, compared to placentas of neurodevelopmentally normal control children. (**Table 4**) This contrasts with last year's report (see discussion, following).

5. **There is a statistically significant reduced eccentricity of the umbilical cord insertion**, as compared to placentas of neurodevelopmentally normal control children. (**Table 5**) This contrasts with last year's report (see discussion, following).

6. **After stratification by gender, these findings are also generally preserved**, although significance is attenuated among females with ASD due to the small sample size. (**Tables 4-5**)

7. Differences in these measures carry over into the range of the ASD phenotypes, with **significant differences in placental shape features when stratifying on either social understanding phenotype or on "repetitive stereotyped behaviour" phenotype**. (**Tables 6-7**)

8. **There are no statistically significant differences in the slice dimensions of ALSPAC ASD placentas as compared to the control group** although the limited sample size in ALSPAC may restrict inference. (**Table 8**) However, EARLI placentas have significantly different slice dimensions when compared to a large birth cohort of ~1000 placentas with similar measurement data. (**Table 9**) When comparing ALSPAC ASD cases and controls (**Table 10, Figures 6a-h,** small sample size), and when comparing high ASD risk EARLI placentas with low ASD risk NCS placentas (**Figures 7a-c**) there appear to be different "trajectories of villous arborization from the center to the perimeter of the placental chorionic disk, with EARLI placentas showing reduced central placental disk thickness but greater preservation of that level of arborization extending to the perimeter, while NCS placentas show more variability throughout the distance from placental disk centroid to edge. This is consistent with our empirical diffusion-limited aggregation (DLA) model of placental growth (see References, Yampolsky et al) which predicted variability in perimeter would be correlated with variability in thickness/villous arborization. EARLI placentas have less perimeter variability and less variability in disk thickness. EARLI placentas are, however, thinner in the more central regions of the placenta near the umbilical cord insertion, thus the older portions of the placenta.

9. **There is a statistically significant reduction in placental weight (~100 g, 20% of the weight of a normal term placenta) for female ASD cases compared to female normal controls.** (**Table 5**) We anticipated a decrease in volume compared to both groups of controls. However, there was no statistically significant difference in volumes. (**Table 5**) This suggests that the placentas of girls with ASD, which weigh less, but occupy the same volume, are "built" differently, with relatively reduced branches despite similar length of long fetal stem anchoring villi. This would be consistent with our previous finding of an alteration in beta, a measure of the integrity of the placental vascular fractal in ASD cases compared to female normal controls**.**

10. The relationship between the placental chorionic surface vessel and the underlying placental disk parenchyma dependent on that vessel differ in ASD cases as compared to controls. This was

demonstrated in an analysis of the undeformed ALSPAC 3D scans with companion flat 2D placental chorionic surface photographs., While the distribution of chorionic plate vessel segments did not differ between the two groups and there was no statistically significant difference in mean disk thickness between ASD cases and controls, **both the maximum placental disk thickness and the standard deviation of placental disk thickness were significantly reduced significantly between ASD cases and controls**. (**Figure 5, Table 12**) We interpret this as overall supportive of our global impression of ASD placentas being more constrained, less variable in shape, cord insertion, with more restricted arborization (reduced maximum thickness) and less "flexibility" in arborization (reduced variability in disk thickness).

11. For this reason, we have examined the **terminal villous structure (the end-vascular capillary distribution of the surface chorionic arterial and venous networks) and the structure does not appear to be simplified in ALSPAC ASD cases** compared to matched controls.

These findings support our hypothesis that placentas in ASD will show alteration of the branching structures known to be determined by the midtrimester (placental chorionic surface vascular networks) compared to terminal villi which are mainly formed after this period. Thus placental chorionic surface vascular network variance may parallel aberrant neuronal networks in ASD both in terms of altered placental chorionic surface vascular branching and in gestational period of effect.

Additionally the differences in placental chorionic surface vascular networks (e.g., reduced branching growth, decreased surface extension and greater arterio-venous distances) have considered to share a theme of "parsimony". The reduced length and surface area of these critical vascular networks is not of a degree to impact birth weight, but may place an at risk fetus at a disadvantage of lesser compensatory capacity and greater vulnerability to gestational stressors including inflammation and/or oxidative stress, gestational exposures that have been associated with ASD risk.

While microscopic analysis of shape and structure was not a stated goal of this grant, because of the observation of reduction in placental weight without a comparable change in volume suggesting different "compositon" of villous parenchyma in ALSPAC ASD cases as compared to controls, and reports that villous maldevelopment (in the form of "trophoblast stromal inclusions", TSI), we have examined both the gross structure of microdissected terminal villous clusters and the terminal villous microvascular structure (the end-vascular capillary distribution of the surface chorionic arterial and venous networks), and neither appear to be simplified in ALSPAC ASD cases compared to matched controls (**11, above**).

However, because of the potential value of any perinatal biomarker for ASD risk screening, we have continued to pursue shape analysis at the microscopic level by developing highly specific immunohistochemistry (IHC) methods for cytokeratin-7 (CK-7), a marker of placental trophoblast, the villous "skin" (**Figures 11 a-d**). TSIs have been suggested to be more common in the placentas of newborns with an older sibling with ASD (thus comparable to our EARLI cohort), however, no study to date has examined a population based cohort of ASD placentas such as has been created by this grant, with ALSPAC cases and controls. A pilot blinded review of 80 slides, from 20 ASD cases and matched controls did not demonstrate an increased number of TSIs in our ALSPAC ASD cases. We consider this finding, albeit preliminary, to be significant. Our population is unique in that studied placentas belong to case children with formally diagnosed ASD and controls known to be without neurodevelopmental disability searched for this villous feature. TSIs are suggested to mark increased villous surface complexity, with the greater surface irregularity leading to more common appearance of an inclusion of surface trophoblast epithelium in the villous core or stroma. Our cases are children actually diagnosed with (and not merely at risk for) ASD. Given our finding of bimodal placental chorionic surface vascular branching measures (majority sparse, a minority with increased complexity) in ALSPAC ASD cases, but not EARLI placentas, we predict increased

villous surface complexity would only mark a minority of ASD children, and potentially those with concurrent diagnoses in addition to ASD.

Our analysis method utilizes digitized slides, slides which have been processed such that the image information contained on them is converted into a viewable file on any computer screen. Our algorithm has set minimal criteria for irregularities of the villous surface and identification of regions of interest (ROIs) with potential TSIs. These regions of interest (ROIs) are saved as an annotation of the analysed slide. The slide with annotation and the same region of a serial section stained with routine hematoxylin and eosin (the current published method for identification of TSIs) will be reviewed by specialist pathologists. Three pathologists (Carolyn M. Salafia, MD MS (PI), Theonia Boyd, MD, Harvard Medical School, and Drucilla J. Roberts, MD, Brigham and Women's Hospital, Boston, MA) are participating in validation of TSI identification on H&E and IHC stained slides. We expect some ongoing level of algorithm refinement to optimize the IHC computational algorithms for automated digitized slide review and to develop a validated algorithm for identification of TSIs in routine stains. Since the frequency of TSIs was reported only rarely to more that 3 per histological slide (<1 of villi), our approach will reduce expert pathologists' time for slide review, validate diagnostic criteria for TSIs in routine H&E and in IHC slides, and confirm or refute the value of this marker as a perinatal predictor of ASD risk.

The differences between last year's observations and these final data result from our decision to exclude data from cases in which placental chorionic surface, disk thickness (from digital photographs or 3D scans) were extrapolated from photographs or 3D scans of deformed placentas. We determined that our methods of decrumpling and uncurling shapes or slices, while seemingly mathematically straightforward, did not yield measures that were consistent with naked eye inspection of original images or the ruler measures provided in real time by Dr Craig Platt at Bristol, UK, in the original processing of the placenta. The degree of extrapolation to placental areas that cannot be seen directly in the scan (areas in a folded shape being inaccessibly to the scan cameras) or are deformed (curled) in a digital image renders the data not comparable to what is directly measured from well-preserved specimens. Since there were ~3 controls per ASD cases, the error caused by these failed assumptions had the greater effect reducing variable shape measures in the larger population.

These findings support our original hypothesis that the placental vascular tree is altered in ASD, although heterogeneity in ASD diagnosis in the mid 1990's, and the effective small sample size, may limit the significance of our observations. We will continue to extend these methods to the EARLI cohort as they reach age at which ASD diagnoses can be determined, and to population-based – and actively accruing-- case-control cohorts we have established in our home institutions. The alterations suggest a globally reduced flexibility of the placenta as it grows within the uterus, which may both mark the ASD placenta, and create a risky prenatal environment that may set the fetus up for injury with any subsequent exposure (e.g., inflammation, oxidative stress).

REPORTABLE OUTCOMES

An abstract of ALSPAC and EARLI chorionic disk and slice results was presented at the International Federation of Placenta Association Meeting, Hiroshima, Japan, September 2012, and the EARLI chorionic vascular data is being prepared for presentation at the Society for Gynecological Investigation (SGI), Meeting in March 2013.

1. There was a statistically significant reduction in placental weight (~100 g) for female ASD cases compared to female normal controls. This is true for the overall sample of females as well as when restricting the sample to children born at term gestation or adjusting for gestational age. This was not the result of outliers in either distribution. We did not find similar effects in males. While males represent the vast majority of ASD cases, it appears that there may be differences within ASD by sex.

2. The influence of gestational age on placental weight also appears to differ by sex. In multiple linear regression analyses predicting placental weight by case/control status and gestational age, we also saw that gestational age had a strong effect on placental weight for males but not for females.

3. There was no statistically significant difference in the smaller placental dimension for ASD cases compared to normal controls among males or females However, the estimated difference among the girls (~0.82 cm) was approximately two times larger than among the boys (~0.43 cm)

4. Based on these placental differences between males and females with diagnoses of ASD, β, a marker of placental functional efficiency as well as placental fractal structure, was calculated for the ALSPAC cohort. Beta did not differ between boys with ASD (0.755$\pm$0.0239) and those without such a diagnosis (0.753$\pm$0.0202). However β did differ between girls with ASD (0.733$\pm$0.0354) and those without such a diagnosis (0.760$\pm$0.0161, p=0.001). By contrast, β did differ by gestational age in boys (point estimate of effect=-0.002, p=0.009). The association of altered β in girls with ASD persisted after adjustment for gestational age (point estimate of effect of ASD "case" status=0.03, p=0.01), and there was no independent effect of gestational age on β in girls (p=0.53).

Abstracts were presented at The International Federation of Placental Associates (IFPA 2013), Whistler, CA, September 11-14, 2013

1. Chorionic vascular structure and placental functional efficiency (beta) differ in high and low ASD risk placental cohorts
2. Mapping placental topology from 3D scans, the graphic display of variation in arborization across gestation
3. Placental terminal villi complexity in cases of autism spectrum disorder & their matched controls

Five peer-reviewed Publications (see attached in appendices)

CONCLUSION

This project brought together and standardized materials from international groups studying the importance of the placenta's role as a potential biomarker of ASD. The ALSPAC placenta sample from the UK remains the largest collection of placentas from a population cohort in which neurodevelopmental examinations were universally applied and placentas were archived. The partnering of resources provision by the Department of Defense and the State of NewYork at the Research Foundation for Mental Hygiene, Inc., located at the Institute for Basic Research in Developmental Disabilities provided a successful environment for this project to be conducted. Despite the large number of deformed specimens provided to the research team, we have capitalized on our exhaustive analytic experience with the UNC-PIN study (R, the NCS Formative Research Study (NIH-NCS-LOI-BIO-2-18) , and the EARLI cohort to provided replicated evidence of aberrant early placental angiogenesis in terms of surface expansion and stem villous arborization, and have new evidence of dir5ect abnormality of chorionic vascular network, in terms of reduced branch generations and vascular surface density that may be vascular counterparts of the altered neuronal connectivity documented in ASD.

Most importantly, our analyses confirm our hypothesis that placental structure varies between ASD cases and in families with an autistic sibling, compared to a large birth cohort. To date most placentas are still discarded as medical waste. **We clearly demonstrate that the placenta in ASD differs from population-based controls, and that with increased ASD risk (EARLI compared to NCS), similar differences are found. Discarding the placenta at birth is a missed opportunity, in terms of the continued refinement of a screening set of perinatal biomarkers, as well as in regards to contributions towards understanding the causal chain that leads to ASD.**

The differences in placental chorionic surface vascular networks (e.g., reduced branching growth, decreased surface extension and greater arterio-venous distances) can be considered to share a theme of "parsimony". The reduced length and surface area of these critical vascular networks is not of a degree to impact birth weight, but may place an at risk fetus at a disadvantage of lesser compensatory capacity and greater vulnerability to gestational stressors including inflammation and/or oxidative stress, gestational exposures that have been associated with ASD risk. Thus, the abnormal placenta we have documented may be a perinatal biomarker and also on the causal pathway to the persistent neuronal injury that has been suggested to underlie ASD.

REFERENCES

1. Niswander K, Gordon M. The Collaborative Perinatal Study of the National Institute of Neurological Diseases and Stroke: the Women and Their Pregnancies. Philadelphia, PA: W.B. Saunders, 1972.
2. Kleiber M. The Fire of Life: An Introduction to Animal Energetics. Revised ed. s.l. Robert E. Krieger Saunders Publ. Co, Philadelphia PA. 1975.
3. Baker AM, Braun JM, Salafia CM, Herring AH, Daniels J, Rankins N, Thorp JM. Risk factors for uteroplacental vascular compromise and inflammation. Am J Obstet Gynecol. 2008 Sep; 199(3):256.e1-9.
4. James GBW, Brown H, editors. Scaling in Biology. Santa Fe Institute studies in the sciences of complexity proceedings. New York, NY: Oxford UniversityPress; 2000. p. 368.
5. Yampolsky M, Salafia CM, Shlakhter O, Haas D, Eucker B, Thorp JM. Modeling the variability of shapes of a human placenta. Placenta 2008;29(9): 790–7
6. Salafia CM, Maas E, Thorp JM, Eucker B, Pezzullo JC, Savitz DA. Measures of placental growth in relation to birth weight and gestational age. Am J Epidemiol. 2005. Nov 15; 162(10):991-8.
7. Yampolsky M, Salafia CM, Shlakhter O, Haas D, Eucker B, Thorp J. Centrality of the Umbilical Cord Insertion in a Human Placenta Influences the Placental Efficiency. Placenta. 2009 30(12):1058-64.
8. Jen-Mei Chang, Amy Mulgew, Carolyn Salafia, A Geometric Approach to Study the Relationship between Maternal and Fetal Characteristics and Shape of Placental Surfaces,under review.
9. Sertel, Kong, Catalyurek, Lozanski, Saltz, Gurcan. Histopathological Image Analysis Using Model-Based Intermediate Representations and Color Texture: Follicular Lymphoma Grading. J Sign Process Syst. 2009; 55(1-3):169-183.

APPENDICES

PI’s Biosketch
Peer-Reviewed Publications
Abstract Posters

BIOGRAPHICAL SKETCH

Provide the following information for the Senior/key personnel and other significant contributors.
Follow this format for each person.

NAME Salafia, Carolyn Margaret	POSITION TITLE Director, Placental Analytics, LLC
eRA COMMONS USER NAME Salafiacm	

EDUCATION/TRAINING

INSTITUTION AND LOCATION	DEGREE *(if applicable)*	MM/YY	FIELD OF STUDY
Dartmouth College	A.B.	06/76	French Literature
Duke University School of Medicine	M.D.	06/80	Medicine
Mailman School of Public Health, Columbia University	M.S.	6/01	Biostatistics

A. Positions and Honors

08/2007- present Director, Placental Analytics, LLC.
7/2008- present Research Scientist, Institute for Basic Research in Developmental Disabilities, NYS DOH, Staten Island, New York.
2/07 -6/08 Research Scientist, New York University School of Medicine
7/2003- 1/07 Assistant Professor of Epidemiology, Joseph P. Mailman School of Public Health
7/02- 6/03 Postdoctoral Research Fellow and Assistant in Clinical Psychiatry, Department of Psychiatry, Columbia University
07/98- 06/01 Professor of Pathology and Pediatrics at CPMC, Columbia University College of Physicians and Surgeons, New York, NY.
06/96-06/98 Associate Professor of Pathology, Department of Pathology, Albert Einstein Medical College, Bronx, NY, (joint appointment with Department of Pathology, Mount Sinai Medical Center, New York, NY).
02/94-05/96 Section Chief, Perinatal Pathology, Perinatology Research Facility, Associate Professor of Pathology and Obstetrics & Gynecology, Georgetown University Medical Center, Washington, DC

Honors

2/2010 Biomedical Imaging Workshop, National Science Foundation Sponsored Fellow, Institute of Pure and Applied Mathematics, UCLA
03/08-06/08 Optimal Shapes Conference, National Science Foundation Sponsored Fellow, Institute of Pure and Applied Mathematics, UCLA
03/07-07/07 Random Shapes Conference, National Science Foundation Sponsored Fellow, Institute of Pure and Applied Mathematics, UCLA
2001, NARSAD Young Investigator Award (Honorable Mention Klerman Award, 2007, for research excellence).
1999, POR (Patient Oriented Research) Scholarship for Masters in Science (Biostatistics), Joseph L. Mailman School of Public Health, Columbia University.
1990, American Board of Pathology, Pediatric Pathology Subspecialty Boards
1985 American Board of Pathology, Anatomic and Clinical Pathology Boards

B. Selected Peer-reviewed Publications (selected from 100 peer-reviewed publications)

Most relevant to the current application

1. Yampolsky M, Salafia CM, Shlakhter O, Haas D, Eucker B, Thorp J. Centrality of the Umbilical Cord Insertion in a Human Placenta Influences the Placental Efficiency. Placenta. 2009 30(12):1058-64.

2. Misra DP, Salafia CM, Miller RK, Charles AK.Non-Linear and Gender-Specific Relationships Among Placental Growth Measures and The Fetoplacental Weight Ratio.Placenta. 2009 30(12):1052-7.
3. Yampolsky M, Salafia CM, Shlakhter O, Haas D, Eucker B, Thorp J. Modeling the variability of shapes of a human placenta. Placenta. 2008 Sep;29(9):790-7.
4. Salafia CM, Misra D, Miles JN. Methodologic Issues in the Study of the Relationship between Histologic Indicators of Intraamniotic Infection and Clinical Outcomes. Placenta. 2009 Nov;30(11):988-93.
5. Buhimschi IA, Zambrano E, Pettker CM, Bahtiyar MO, Paidas M, Rosenberg VA, Thung S, Salafia CM, Buhimschi CS. Using Proteomic Analysis of the Human Amniotic Fluid to Identify Histologic Chorioamnionitis. Obstet Gynecol. 2008 Feb;111(2):403-412.
.

Additional recent publications of importance to the field (in chronological order).

1. Salafia CM, Yampolsky M. Metabolic scaling law for fetus and placenta, Placenta. 2009; 30(5):468-71.
2. Baker AM, Braun JM, Salafia CM, Herring AH, Daniels J, Rankins N, Thorp JM. Risk factors for uteroplacental vascular compromise and inflammation. Am J Obstet Gynecol. 2008 Sep;199(3):256.e1-9.
3. Baptiste-Roberts K, Salafia CM, Nicholson WK, Duggan A, Wang NY, Brancati FL. Gross placental measures and childhood growth. J Matern Fetal Neonatal Med. 2008 Dec 9:1-11.
4. Coall DA, Charles AK, Salafia CM. Gross placental structure in a low-risk population of singleton, term, first born infants. Pediatr Dev Pathol. 2008 May-Jun;12(3):200-10.
5. Baker AM, Braun JM, Salafia CM, Herring AH, Daniels J, Rankins N, Thorp JM. Risk factors for uteroplacental vascular compromise and inflammation. Am J Obstet Gynecol. 2008 Sep;199(3):256.e1-9.
6. Baptiste-Roberts K, Salafia CM., Nicholson WK., Duggan A, Wang NY, Brancati FL. Maternal risk factors for abnormal placental growth: the national collaborative perinatal project. BMC Pregnancy and Childbirth 2008, **8**:44.
7. Salafia CM, Zhang J, Miller RK, Charles AK, Shrout P, Sun W. Placental growth patterns affect birth weight for given placental weight. Birth Defects Res A Clin Mol Teratol. 2007 Feb 7.
8. Salafia CM, Maas E, Thorp JM, Eucker B, Pezzullo JC, Savitz DA. Measures of placental growth in relation to birth weight and gestational age.Am J Epidemiol. 2005 Nov 15;162(10):991-8.
9. Salafia CM, Maas EM. The twin placenta: framework for gross analysis in fetal origins of adult disease initiatives. Paediatric and Perinatal Epidemiology 2005(Suppl. 1): 23–31.
10. Ghidini A, Salafia CM. Gender differences of placental dysfunction in severe prematurity. Br J Obstet Gynecol, 2005; 112:140-44.

The Prevalence and Distribution of Acute Placental Inflammation in Uncomplicated Term Pregnancies

CAROLYN M. SALAFIA, MD, CRISTINE WEIGL, BS, AND LESTER SILBERMAN, MD

The clinical relevance of histologic evidence of acute ascending intrauterine infection has been called into question by descriptions of "silent" chorioamnionitis. The described frequencies of silent chorioamnionitis in normal and abnormal pregnancies vary widely because of differences in the definition of a normal pregnancy, methods of placental examination, and pathologic criteria. Therefore, we examined placentas from 161 uncomplicated gestations for the presence and severity of acute inflammation in the amnion, chorion-decidua, chorionic plate, and umbilical cord using strict gross and microscopic protocols. Indicators of amniotic fluid infection, specifically umbilical cord inflammation, amnionitis, and inflammation within the chorionic plate were present in 0, 1.2, and 4% of the cases, respectively. Silent chorioamnionitis was rare. There was a statistical association between the presence of acute inflammation and the occurrence of labor at term. Methods of tissue sampling that included a more extensive examination of the site of membrane rupture resulted in an increased frequency of diagnosis of acute inflammation at the site of rupture in vaginal deliveries at term. ***(Obstet Gynecol 73:383, 1989)***

A histologic diagnosis of chorioamnionitis is associated with an increased risk of preterm delivery and neonatal sepsis,[1] conditions that remain among the leading causes of perinatal morbidity and mortality in developed countries.[2–5] Despite a statistically significant relationship between the presence of histologic chorioamnionitis and the isolation of organisms from the amniotic fluid,[6] clinically "silent" chorioamnionitis is also reported frequently,[7] calling the clinical relevance of such a diagnosis into question.[2] Part of the controversy is due to the wide variation in reported prevalence of acute inflammation of the placenta, membranes, and cord, which ranges from as low as 4.8% to as high as 48.8%.[2] Fox[2] suggested that reasons for this discrepancy include variations in methods of tissue sampling, pathologic diagnostic criteria, socioeconomic status, and obstetric practices. Ideally, if one were able to control for many of these variables, one could make a true assessment of the prevalence of subclinical acute inflammation of the placenta in uncomplicated pregnancies. This approach is critical to proper evaluation of the significance of acute inflammation in pregnancies complicated by shortened gestation, labor abnormalities, or fetal distress.

A low-risk and high-socioeconomic-level community hospital population is one in which uniformity of obstetric practice is the general rule, and may be unique among populations currently reported in the literature. We conducted this study to determine the frequency of diagnosis of acute intrauterine inflammation in pregnancies with uneventful antepartum, intrapartum, and postpartum courses in our community hospital population, and to examine the effects of our method of tissue sampling on the diagnosis of acute inflammation.

Materials and Methods

Since 1983, placental pathologic study has been a routine part of the evaluation of any complicated pregnancy, delivery, or neonatal course at the Danbury Hospital. Clinical data are collected on standard Hollister data forms, by which past medical, prenatal, intrapartum, and neonatal data are recorded in a checklist format. All deliveries with any clinically relevant maternal, fetal, or neonatal complications routinely have placental histopathologic examination. A consecutive series of 161 uncomplicated term deliveries form the basis of this data set. These included 103 uncomplicated vaginal deliveries, including two oxytocin inductions and five oxytocin stimulations, and 58 cases of cesarean delivery, 35 in which labor did not begin (cesarean section − labor) and 23 deliveries

From the Departments of Laboratory Medicine and Obstetrics and Gynecology, Danbury Hospital, Danbury, Connecticut.

0029-7844/89/$3.50

Table 1. Grading System for Acute Intrauterine Inflammation

Amnion and chorion-decidua
Grade 1—One focus of at least five PMNs
Grade 2—More than one focus of grade 1 inflammation, or at least one focus of five to 20 PMNs
Grade 3—Multiple and/or confluent foci of grade 2
Grade 4—Diffuse and dense acute inflammation
Umbilical cord
Grade 1—PMNs within the inner third of the umbilical vein wall
Grade 2—PMNs within the inner third of at least two umbilical vessel walls
Grade 3—PMNs in the perivascular Wharton jelly
Grade 4—Panvasculitis and funisitis extending deep into the Wharton jelly
Chorionic plate
Grade 1—One focus of at least five PMNs in subchorionic fibrin
Grade 2—Multiple foci of grade 1 in subchorionic fibrin
Grade 3—Few PMNs in connective tissue or chorionic plate
Grade 4—Numerous PMNs in chorionic plate, and chorionic vasculitis

PMNs = polymorphonuclear leukocytes.

following the spontaneous onset of labor (cesarean section + labor). Cesarean section − labor consisted exclusively of elective repeat cesarean section in multiparous patients. No data were available concerning the degree of cervical dilatation at the time of cesarean section. The cesarean section + labor group comprised patients whose membranes ruptured spontaneously and in whom the duration of labor was less than 100 minutes. The mean gestational age was equivalent for all methods of delivery.

Tissue sampling and histologic examination were performed without knowledge of clinical data. The method of placental examination involved a modification of the method of Benirschke,[8] in which two samples of membranes are taken, one a standard membrane roll and the second a rim of membranes from the site of membrane rupture, as determined by gross examination. We noted the presence of acute inflammation of the extraplacental membranes, cord, and chorionic plate, and graded the severity of the inflammation at each site. Any tissue that contained cells clearly identifiable as polymorphonuclear leukocytes was graded as positive for acute inflammation, using a scale of 1+ to 4+ (Table 1; Figures 1–4). The amnion was graded as a separate tissue because it is frequently separated from the chorion and decidua mechanically in the course of delivery, and a tissue section may not include amnion and chorion-decidua samples juxtaposed in utero. Although it has been standard practice to localize inflammation to either the chorion or decidua, we chose to describe patterns of acute inflammation in this tissue. In certain cases, polymorphonuclear leukocytes were present in the decidua with minimal decidual destruction and demonstrated a directed migration toward the amnion and amniotic fluid space. At tissue interfaces, such as the junction of cellular and connective-tissue chorion, this migration appeared to be impeded, and polymorphonuclear leukocytes piled up at this interface. This pattern was termed "marginating" (Figure 3). "Nonmarginating" choriodeciduitis was defined as any other distribution of polymorphonuclear leukocytes in chorion and decidua. Frequently, nonmarginating in-

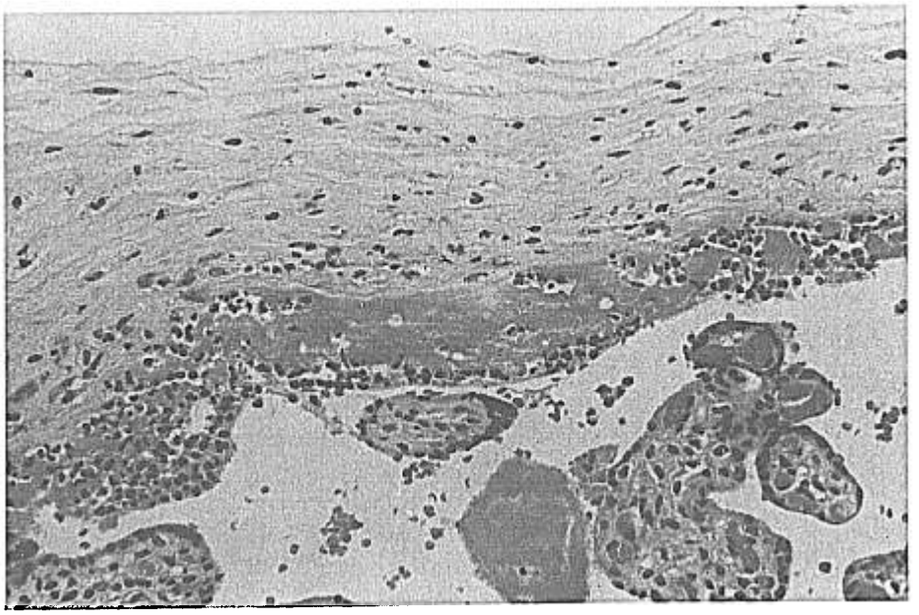

Figure 1. Chorionic plate: maternal polymorphonuclear leukocytes in subchorionic fibrin and focally invading the chorionic plate, grade 2 (H&E, × 10).

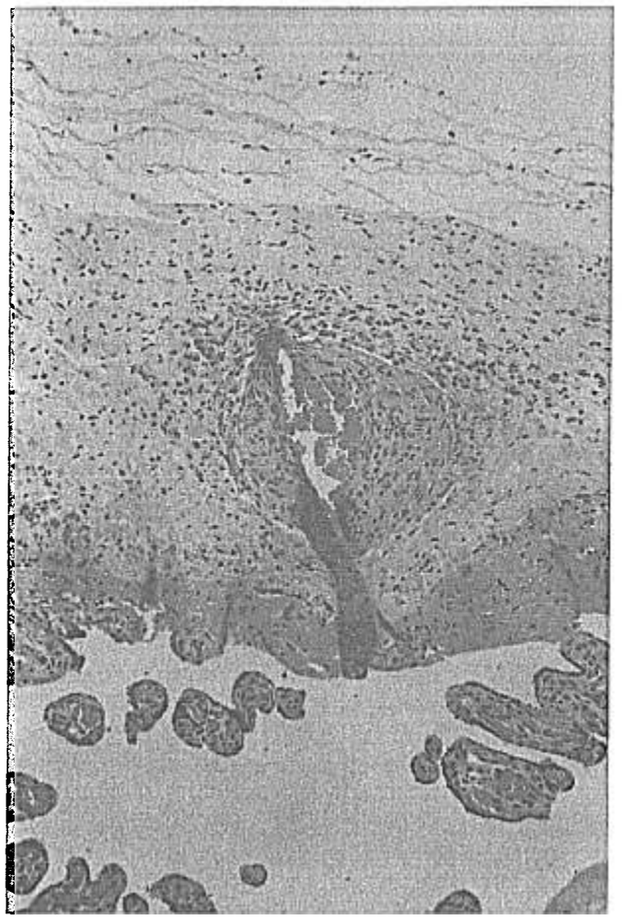

Figure 2. Chorionic plate: maternal infiltrate in subchorionic fibrin with fetal vasculitis, grade 4 (H&E, × 10).

flammation appeared as a destructive decidual inflammatory process (Figure 4) in which the chemotactic stimulus for maternal polymorphonuclear leukocyte migration appeared to be located in the decidua.

Statistical analysis used the χ^2 technique, with Fisher correction for small sample sizes where applicable.

Results

Table 2 summarizes the distribution of acute inflammation in the membranes, chorionic plate, and umbilical cord. Acute inflammation involving the amnion and umbilical cord occurred rarely, with frequencies of 1.2 and 0%, respectively. The two cases of amnionitis occurred in association with normal vaginal delivery. Whereas mild acute inflammation of the intervillous fibrin beneath the chorionic plate was fairly common, only 4.3% (seven of 161) showed inflammation of the chorionic plate itself (grade 3 or 4). The frequency of acute marginating choriodeciduitis was 2.5% (four of 161); the small number of cases precluded analyses of association with other sites of acute inflammation. Seven women who delivered vaginally had labor induced or stimulated with oxytocin. The placentas from these deliveries showed a random occurrence of grade 1 acute inflammation of chorion-decidua only. These cases are included in the vaginal delivery group in all tables and analyses.

The prevalence of acute inflammation of the chorion-decidua was as high as 54% (56 of 103) at the site of membrane rupture in vaginal delivery cases, but was

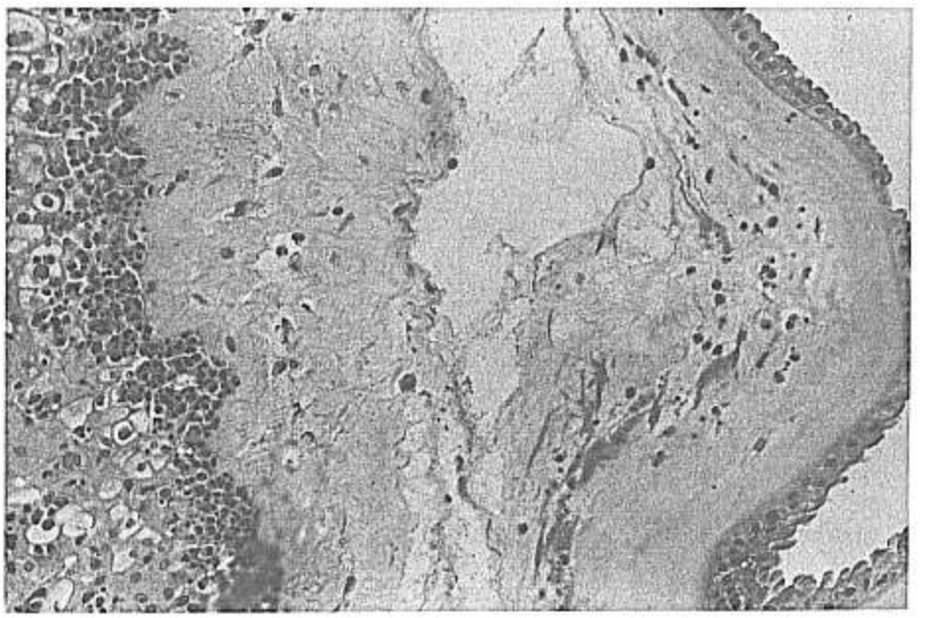

Figure 3. Marginating choriodeciduitis with maternal polymorphonuclear leukocytes at the junction of the cellular and connective tissue chorion and sparsely present within amnion, grade 3 (H&E, × 20).

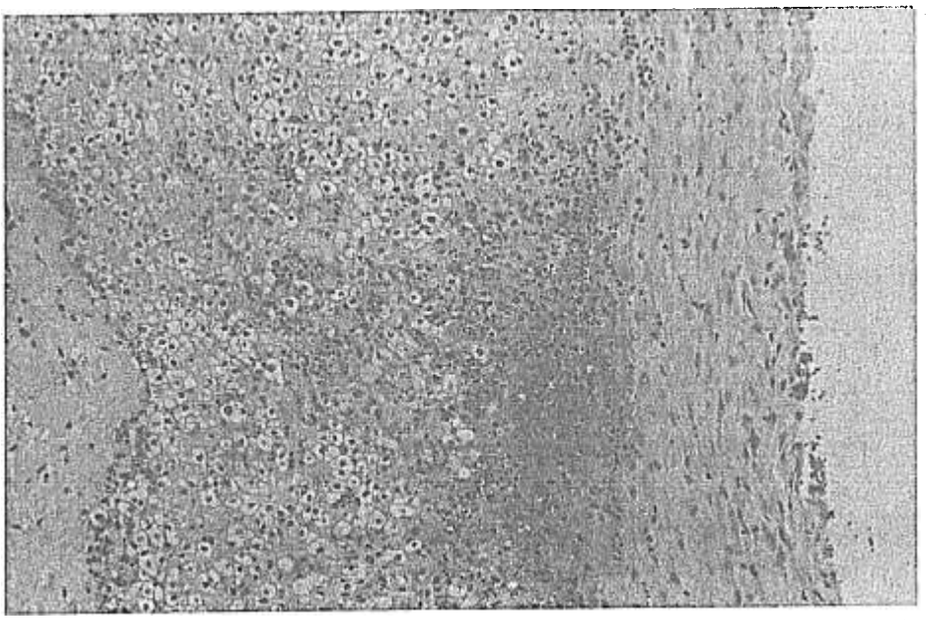

Figure 4. Predominantly nonmarginating deciduitis with decidual destruction, grade 2 (H&E, × 10).

present in only 36% (21 of 58) of the cesarean section cases (Table 3). This represents a statistically significant difference between vaginal delivery and cesarean section cases ($\chi^2 = 4.9$; $P = .02$). In both vaginal and cesarean deliveries, we observed significantly fewer examples of higher grades of choriodecidual inflammation, and the pattern was almost uniformly nonmarginating (Tables 4 and 5). Cesarean section cases with labor demonstrated an increased prevalence of acute inflammation over those without labor, which was statistically significant in the membrane roll ($\chi^2 = 6.3$; $P = .01$). We found no difference in the prevalence of inflammation of the chorionic plate; again, grades of acute inflammation describing other than a sprinkling of polymorphonuclear leukocytes within subchorionic fibrin were rare in all cases.

We evaluated the site of tissue sampling for its effect on the rate of detection of acute inflammation. Sampling of membranes from the pericervical area is expected to yield a higher prevalence of acute inflammation because of potential colonization of the membranes by the cervicovaginal flora. In addition, the site of spontaneous membrane rupture is expected to demonstrate an increase in acute inflammation because of the effect of membrane inflammation on the

Table 2. Prevalence and Distribution of Acute Inflammation in the Placenta According to Grade

	Total (N = 161)	Grade 1+	2+	3+	4+
Membranes—site of rupture					
Amnion	2 (1%)	1 (0.5%)	0	0	1 (0.5%)
Chorion-decidua	77 (48%)	70 (91%)	3 (4%)	1 (1%)	3 (4%)
Membrane roll					
Amnion	1 (0.6%)	0	0	1	0
Chorion-decidua	61 (38%)	57 (93%)	3 (5%)	1 (2%)	0
Chorionic plate	44 (27%)	35 (79%)	2 (5%)	5 (11%)	2 (5%)
Umbilical cord	0	0	0	0	0

Percent grades of inflammation indicate percent of total samples with inflammation in that tissue. Because cases may have been positive in both site of rupture and membrane roll, the total number of positive membranes is greater than the total number of cases.

Table 3. Prevalence and Distribution of Acute Inflammation in the Placenta by Mode of Delivery

	Total (N = 161)	Vaginal (N = 103)	CS − labor (N = 35)	CS + labor (N = 23)
Membranes—site of rupture				
Amnion	2 (1%)	2 (2%)	0	0
Chorion-decidua	77 (48%)	56 (54%)	11 (31%)	10 (43%)
Membrane roll				
Amnion	1 (0.6%)	1	0	0
Chorion-decidua	61 (38%)	42 (41%)	8 (22%)	11 (48%)
Chorionic plate	44 (27%)	23 (22%)	13 (37%)	8 (35%)
Umbilical cord	0	0	0	0

CS = cesarean section.

Percent grades of inflammation indicate percent of total samples with inflammation in that tissue. Because cases may have been positive in both site of rupture and membrane roll, the total number of positive membranes is greater than the total number of cases.

process of membrane rupture.[9] In the cesarean section cases with intact membranes, the site of artificial membrane rupture is distant from the cervix. The membrane sample from the site of surgical incision into the membranes would represent a random sample, similar to the sample taken in a membrane roll. A lower prevalence of acute inflammation and agreement in diagnoses of acute inflammation would be expected in the two random membrane samples taken in cesarean section cases. Of the 58 cesarean section cases, 21 showed acute inflammation at the site of rupture and 19 showed acute inflammation in the membrane roll. In the 103 vaginal deliveries, 56 pericervical samples demonstrated acute inflammation, compared with 39 membrane roll samples. We made an additional 17 diagnoses of acute choriodeciduitis (30%) given a more extensive sampling of pericervical tissues, for an increase of 43.5%.

We noted an equal prevalence of acute inflammation at each week of gestation from 37–42 weeks (data not shown). Examination of the prevalence of acute inflammation in cases differing by mode of delivery also failed to show an effect of gestational age (data not shown).

Discussion

Whereas other studies have reported up to 70% of cases of chorioamnionitis as being clinically silent,[10] this study indicates that if the definition of a normal delivery excludes all forms of fetal distress, truly silent histologic inflammation of the amnion is rare, occurring in only 1–2% of cases (two of 161). Umbilical vasculitis/funisitis, grade 3 inflammation of the chorionic plate, and acute amnionitis have been correlated strongly with the isolation of organisms from amniotic fluid obtained by amniocentesis.[6] Preliminary data also indicate that acute marginating choriodeciduitis is correlated with intra-amniotic infection (Romero RJ, Salafia CM, unpublished observations). Marginating choriodeciduitis, chorionitis, umbilical vasculitis, and amnionitis—histologic indicators of significant intra-amniotic bacterial colonization and amniotic fluid infection—are rare in uncomplicated term pregnancies.

Inflammation of the chorionic plate has been used as the sole criterion in the diagnosis of chorioamnionitis,[11] with chorioamnionitis defined as the presence of no fewer than four polymorphonuclear leukocytes per high-power field in the chorionic plate. However, low grades of chorionitis, acute inflammation confined to the subchorionic fibrin, were not consistently associated with a positive culture.[6] In this study, every case graded as positive for inflammation in the chorionic plate also had associated inflammation in the chorion and decidua. This strong correlation suggests that this mildest degree of chorionic plate inflammation may be a response to the earliest stage of intra-amniotic infection, in which minimal numbers of intra-amniotic organisms are present. Alternatively, an inflammation based in the decidua may result in the "contamination" of the amniotic fluid with chemotactic factors, which then elicit the migratory response from maternal polymorphonuclear leukocytes in the intervillous space. The low prevalence of marginating choriodeciduitis suggests that the primary site of generation of chemotactic stimuli was usually not the amniotic fluid, and supports the latter interpretation. Certain cases of low-grade chorionitis may therefore represent amniotic fluid inflammation rather than infection proper.

Acute deciduitis, without inflammation of chorion, has been excluded in several other studies of acute inflammation.[11–14] Acute inflammation confined to the decidua, and of the mildest grade, constituted most of the diagnoses of acute inflammation (70 of 77 at the site of membrane rupture; 57 of 61 in the membrane roll). Schneider[15] found acute deciduitis in 85% of spontaneously delivered placentas, which is consistent with our observations. Fox[2] suggested that, given its prevalence, acute deciduitis may be a physiologic phenomenon of no significance. Acute inflammation was most

Table 4. Grade of Acute Choriodecidual Inflammation at the Site of Rupture According to Method of Delivery

	Total	Grade 1+	Grade 2–4+
Vaginal (N = 103)	56	51 (91%)	5 (9%)
CS + labor (N = 23)	10	9 (90%)	1 (10%)
CS − labor (N = 35)	11	10 (91%)	1 (9%)

CS = cesarean section.
Percent grades of inflammation indicate percent of total samples with inflammation in that tissue.
Vaginal *vs* CS − labor: χ^2 = 4.65, P = .03, odds ratio = 2. Other comparisons not significant.

Table 5. Grade of Acute Choriodecidual Inflammation at the Membrane Roll According to Method of Delivery

	Total	Grade 1+	Grade 2–4+
Vaginal (N = 103)	42	40 (95%)	2 (5%)
CS + labor (N = 23)	11	10 (91%)	1 (9%)
CS − labor (N = 35)	8	7 (88%)	1 (12%)

CS = cesarean section.
Percent grades of inflammation indicate percent of total samples with inflammation in that tissue.
Vaginal *vs* CS − labor: χ^2 = 4.12, P = .04, odds ratio = 2.5; CS + labor *vs* CS − labor: χ^2 = 6.3, P = .01, odds ratio = 4.2.

prevalent in the pericervical tissues at the site of membrane rupture in women delivering vaginally (56 of 103), and was significantly more frequent than in cesarean section cases with no labor and intact membranes. The prevalence of acute inflammation in pericervical tissues may simply be due to the proximity of these tissues to the vaginal flora throughout the course of labor. Alternatively, pericervical membrane infection, through actions of bacterial digestive enzymes on the connective-tissue component of the amnion, chorion, and decidua,[9] may play a role in membrane rupture at term.

We did not perform amniotic fluid or placental cultures in this study. Therefore, any assumption of an infective etiology of the observed acute inflammation must be examined critically. Noninfective etiologies of chorioamnionitis have been proposed; as summarized by Fox,[2] these include fetal hypoxia, changes in the pH of amniotic fluid, maternal immunologic reaction to fetal tissues, the irritative effects of meconium, or a nonspecific response to the poor condition of the infant. The present study specifically excludes cases of fetal hypoxia or acidosis, clinically detectable passage of meconium, or compromised fetuses or neonates. We did not examine amniotic fluid pH, and did not assess maternal-fetal immunologic incompatibility. However, there is no reason to suspect pH abnormalities of amniotic fluid in this normal group. Maternal-fetal immunologic incompatibility has been associated with poor pregnancy outcome in several studies[16,17]; again, these outcomes are specifically excluded here.

Staples et al[18] have demonstrated the development of a polymorphonuclear leukocyte infiltrate in sheep decidua after oophorectomy. They suggested that the decrease in circulating and intrauterine progesterone levels after oophorectomy leads to a decrease in progesterone-mediated immunosuppression, permitting the intrauterine infiltration. Romero et al have reported a drop in both absolute levels of intra-amniotic progesterone and the estrogen/progesterone ratio in amniotic fluid of women in labor, compared with nonlaboring women (Romero RJ, Scoccia B, King Y, Hobbins JC, Benveniste R. Evidence for a local change in the estrogen/progesterone ratio in human parturition. Abstract, Society of Perinatal Obstetricians, February 1988). Although it may be reasonable to attribute a proportion of acute deciduitis in the pericervical tissues to ascending infection, low-grade polymorphonuclear leukocyte infiltrates distant from the site of rupture may reflect the effects of an intrapartum decline in progesterone levels. The polymorphonuclear leukocyte infiltrate observed by Staples et al was shown to be dependent upon the presence of fetal tissues in the uterus, and may be considered a manifestation of a maternal rejection response to fetal alloantigenicity.

Acute inflammation has been linked to the spontaneous onset of labor prior to term,[1] and in this context is considered almost exclusively to have an infectious etiology.[2,3,5] Complex hormonal priming, a shift in favor of promotion of prostaglandin production with increasing gestational age, and modifications of the myometrial cell itself cause labor to be initiated progressively more easily with advancing gestation.[19] This study observed statistically significant associations of acute decidual inflammation with the presence of labor at term, independent of the eventual method of delivery. Even cesarean section cases with labor lasting less than 100 minutes showed more frequent acute deciduitis than those without labor. The severity of acute deciduitis noted in the present study is dramatically lower than that noted in association with premature onset of labor prior to 37 weeks' gestation (Salafia CM, unpublished observations). This would be expected, given the more complete preparation of the term uterus for the initiation of labor.[20] To initiate labor at 27 weeks by a mechanism involving acute inflammation may require a greater degree of inflammation than that required to initiate labor at term. Whether a mild degree of acute decidual inflammation, a potential source of intrauterine prostaglandins, contributed to labor onset, or whether a labor-triggered decline in progesterone levels permitted the infiltrate in response to fetal antigens, cannot be determined by this study. The increased frequency of pericervical acute inflammation suggests that ascending (transcervical) infection plays a role in the genesis of the histologic lesions observed.

References

1. Guzick DS, Winn K. The association of chorioamnionitis with preterm delivery. Obstet Gynecol 1985;65:11–6.
2. Fox H. The pathology of the placenta. Philadelphia: WB Saunders, 1978. (Bennington JL, ed. Major problems in pathology; vol 7).
3. Naeye RL. Causes and consequences of chorioamnionitis. N Engl J Med 1975;293:40–1.
4. Naeye RL. Causes of perinatal mortality in the U.S. Collaborative Perinatal Project. JAMA 1977;238:228–9.
5. Russell P. Inflammatory lesions of the human placenta. I. Clinical significance of acute chorioamnionitis. Am J Diagn Gynecol Obstet 1979;1:127–37.
6. Dong Y, St. Clair PJ, Ramzy I, Kagan-Hallet KS, Gibbs RS. A microbiologic and clinical study of placental inflammation at term. Obstet Gynecol 1987;70:175–82.
7. Hauth JC, Gilstrap LC III, Hankins GDV, Connor KD. Term maternal and neonatal complications of acute chorioamnionitis. Obstet Gynecol 1985;66:59–62.
8. Benirschke K. A review of the pathologic anatomy of the human placenta. Am J Obstet Gynecol 1962;84:1595–622.

9. Sbarra AJ, Selvaraj RJ, Cetrulo CL, Feingold M, Newton E, Thomas GB. Infection and phagocytosis as possible mechanisms of rupture in premature rupture of the membranes. Am J Obstet Gynecol 1985;153:38–43.
10. Hawrylyshyn P, Bernstein P, Milligan JE, Soldin S, Pollard A, Papsin FR. Premature rupture of membranes: The role of C-reactive protein in the prediction of chorioamnionitis. Am J Obstet Gynecol 1983;147:240–6.
11. Naeye RL, Dellinger WS, Blanc WA. Fetal and maternal features of antenatal bacterial infections. J Pediatr 1971;79:733–9.
12. Naeye RL. Amniotic fluid infections, neonatal hyperbilirubinemia, and psychomotor impairment. Pediatrics 1978;62: 497–503.
13. Zhang J, Kraus FT, Aquino TI. Chorioamnionitis: A comparative histologic, bacteriologic and clinical study. Int J Gynecol Pathol 1985;4:1–10.
14. Fox H, Langley FA. Leucocytic infiltration of the placenta and umbilical cord: A clinico-pathologic study. Obstet Gynecol 1971;37:451–8.
15. Schneider L. Uber vorkommen und bedeutung leukocytarer infiltrate im ablosungsvereich der spontan geborenen placenta. Arch Gynaekol 1970;208:247–53.
16. Labarrere C, Althabe O, Telenta M.Chronic villitis of unknown etiology in placentae of idiopathic small for gestational age infants. Placenta 1982;3:309–18.
17. Jenkins DM, Need JA, Scott JS, Morris H, Pepper M. Human leukocyte antigens and mixed lymphocyte reaction in severe pre-eclampsia. Br Med J 1978;2:542–4.
18. Staples LD, Heap RB, Wooding FBP, King GJ. Migration of leucocytes into the uterus after acute removal of ovarian progesterone during early pregnancy in the sheep. Placenta 1983;4:339–50.
19. Garfield RE. Control of myometrial function in preterm versus term labor. Clin Obstet Gynecol 1984;27:572–91.
20. Casey ML, Winkel CA, Porten JC, MacDonald PC. Endocrine regulation of the initiation & maintenance of parturition. Clin Perinatol 1983;10:709–21.

Address reprint requests to:
Carolyn M. Salafia, MD
Department of Laboratory Medicine
Danbury Hospital
24 Hospital Avenue
Danbury, CT 06810

Received June 1, 1988.
Received in revised form July 15, 1988.
Accepted July 25, 1988.

AMERICAN JOURNAL OF PERINATOLOGY/VOLUME 14, NUMBER 7 August 1997

FETAL BUT NOT MATERNAL SERUM CYTOKINE LEVELS CORRELATE WITH HISTOLOGIC ACUTE PLACENTAL INFLAMMATION

Carolyn M. Salafia, M.D.,[*†§] *David M. Sherer, M.D.,*[*‡] *Catherine Y. Spong, M.D.,*[*‡] *Sean Lencki, M.D.,*[‡] *Gary S. Eglinton, M.D.,*[‡] *Vinita Parkash, M.D.,*[#] *Edith Marley, M.D.,*[†] *and Janice M. Lage, M.D.*[†]

ABSTRACT

Our objective was to determine if placental histologic acute inflammation is related to maternal and fetal serum cytokine levels in preterm labor, using a data set previously constructed blinded to histopathologic information. To this goal in 1992, 32 consecutive patients at 20–36 weeks with progressive labor and tocolytic failure were recruited. Maternal serum sampled during the active phase of labor, and fetal (umbilical vein) serum were assayed by ELISA for levels of soluble interleukin-1 β (IL-1ß), soluble interleukin-2 receptor (IL-2 R), and interleukin 6 (IL-6) (T-Cell Diagnostics). Acute placental inflammation was scored by two groups blinded to clinical data, and the average scores analyzed for relationships to serum cytokine levels. Weighted kappa values, reflecting interobserver agreement in scoring of acute inflammation, were: amnion 0.84; choriodecidua 0.84; umbilical cord 0.85; and chorionic plate 0.73. Fetal levels of IL-1ß and IL-2 R were higher with grade 3–4 acute amnionitis than with grades 0–2 ($p = 0.022$ and $p = 0.023$). Fetal levels of all three cytokines were higher in grade 3–4 umbilical vasculitis (IL-1ß $p = 0.008$, IL-2 R $p = 0.01$, and IL-6 $p = 0.03$). In contrast, maternal serum cytokine levels were not associated with presence or severity of histologic evidence of acute placental inflammation. Histologic acute inflammation was not related to duration of labor, interval from membrane rupture to delivery, and presence or duration of antibiotic therapy. We conclude that fetal serum, but not maternal serum cytokine levels, are correlated with histologic evidence of acute placental inflammation, and may reflect a predominant placental origin of the cytokines.

Keywords: Acute ascending infection; placental pathology; interleukins; maternal serum; fetal serum

Despite decades of intensive investigation, preterm delivery remains a primary cause of perinatal morbidity and mortality, with an incidence essentially unchanged for 30 years.[1,2] The contribution of intrauterine infection to at least a subset of these preterm births has been well-detailed in the past decade, using clinical criteria for defining intra-amniotic infection,[3,4] and histologic markers of acute inflammation in amnion, choriodecidua, chorionic plate, and umbilical cord.[5–7] Recent studies have supported the hypothesis that inflammatory cytokines contribute to the pathogenesis of several of the most important neonatal sequelae of prematurity (i.e., intraventricular hemorrhage, periventricular leukomalacia, and neonatal death).[8–10] Histologic measures of acute inflammation are correlated with elevated amniotic fluid levels of interleukins 1 and 8 and tumor necrosis factor,[11] and may be more sensitive in-

*Perinatal Research Facility, Departments of [†]Pathology and [‡]Obstetrics and Gynecology, Georgetown University Medical Center, Washington, DC; [§]Montefiore Medical Center, Albert Einstein College of Medicine, Bronx, New York; and the [#]Department of Pathology, Yale University School of Medicine, New Haven, Connecticut

Reprint requests: No reprints available

dicators of intra-amniotic infection than clinical diagnoses of chorioamnionitis.[12] The purpose of the present study was to correlate histopathology of acute inflammation with cytokine levels of (IL)1-ß, IL-6, and IL-2-receptor (IL-2 R) in a data set of samples of maternal and fetal serum obtained in cases with preterm labor refractory to tocolysis. We also examined the reproducibility of the histologic diagnosis and grading of maternal and fetal inflammatory lesions indicating acute ascending infection.

METHODS AND MATERIALS

In 1992, 32 consecutive patients in preterm labor were recruited. The clinical characteristics of this population have been previously reported.[13] Inclusion criteria were: gestational age between 20 and 36 weeks with active and progressive labor with failure of tocolysis or with contraindications for tocolysis, such as advanced cervical dilatation, chorioamnionitis, ruptured membranes, or fetal compromise. Intramuscular steroids were not administered to laboring patients or patients with diagnosis of chorioamnionitis. Cases of preeclampsia, known or suspected maternal viral infection, human immunodeficiency virus seropositivity, or positive urine cultures were excluded. All patients had urine cultures obtained at admission. Gestational age at delivery was based on reliable menstrual dating or early ultrasonography. Retrospective chart review extracted maternal demographic features, documentation of antepartum antibiotic administration and duration of administration, and duration of active labor and membrane rupture prior to delivery. Antibiotic therapy was administered if admission culture yielded a pathogen, or in the presence of a clinical diagnosis of chorioamnionitis (defined by a maternal temperature >38°C, and at least one of the following: maternal tachycardia >100 beats/min, uterine tenderness, white blood cell count >15,000, and foul-smelling vaginal discharge). Maternal serum was sampled during the active phase of labor, and fetal serum was obtained from the umbilical vein at birth, and stored at −70 prior to batched runs of enzyme-linked immunoassays (ELISA) for cytokine levels (pg/mL or IU/mL), of soluble IL-2 R, IL-6, and IL-1ß (T-Cell Diagnostics, Cambridge, MA) as previously described. All assays were run without knowledge of the maternal, placental, or neonatal data.

Histology slides from the 32 cases of preterm birth were retrieved from pathology archives. The slides included 31 sections of amnion, 32 sections of umbilical cord, 30 sections of choriodecidua, and 31 sections of chorionic plate. In nine cases (28%), the samples of the chorionic plate did not include chorionic (fetal) vessels, so the fetal inflammatory response was assessed in the umbilical cord only. The published guidelines for diagnosing and scoring acute amnionitis, choriodeciduitis, chorionitis, and umbilical vasculitis[14] were provided without additional instructions to two separate junior faculty-level investigators (E.M. and V.P.) who scored the histologic slides. Because tissue necrosis may obscure tissue detail and complicate diagnosis, the presence and extent of tissue necrosis was recorded. The scores were returned to the guideline author and entered into a database. A weighted Kappa statistic was performed to assess not only concordance of scoring, but the extent of discordance between scores (e.g., a discordance between grade 1 and grade 4 carried greater weight than a discordance between grade 1 and grade 2).

Serum cytokine distributions were tested for normality by the Kolmogonov–Smirnov test (Statview 4.5, Abacus Concepts, Berkeley, CA). Variables not normally distributed were analyzed using nonparametric methods. Kruskal–Wallis tests, Spearman rank correlation. If log-transformation normalized the data, parametric methods (analysis of variance [ANOVA]and regression) were used. $p < 0.05$ was considered as significant. Results are expressed as mean ± standard error.

RESULTS

The demographics of this population have been previously reported.[13] Briefly, 21 patients were of African-American descent, mean maternal age was 28 ± 5 years, and gestational age at delivery was 29 ± 5 weeks. The mean duration of the interval from membrane rupture to delivery was 92 ± 150 hr, and active labor lasted a mean of 6 ± 5 hr. Seventy-two percent (23 of 32) of patients received antepartum antibiotics, 7 (30%) for more than 48 hr prior to delivery. The data regarding acute inflammation scores were first analyzed to determine concordance and reliability of acute inflammation scoring. The weighted Kappa values, reflecting extent of interobserver agreement in the scoring of the precise

Table 1. Summary of Fetal and Maternal Serum Cytokine Levels

	Mean	*SD*	*SE*	*Count*	*Minimum*	*Maximum*
Fetal [IL-1]	93.4	116	23.7	24	undetectable	480
Fetal [IL-2R]	989.3	614.1	116.1	28	300	3100
Fetal [IL-6]*	37.7*	93.3*	18.7*	25	undetectable	400
Maternal [IL-1]	53.4	53.4	10.5	26	undetectable	160
Maternal [IL-2 R]*	440.6*	405.3*	71.7*	32	100	2100
Maternal [IL-6]*	71.9*	353.6*	62.5*	32	undetectable	2000

*Indicates non-normally distributed variables.

Table 2. Summary of Significant Relationships of Increasing Grade of Acute Inflammation to Maternal and Fetal Serum Cytokine Levels

	Maternal AI			*Fetal AI*
	Acute Amnion Inflammation	*Choriodecidual Inflammation*	*Chorionic Plate Inflammation*	*Umbilical Vasculitis*
Fetal serum levels				
IL-1	0.0065*	0.035	0.88	0.33
IL-2 R	0.40	0.51	0.68	0.13
IL-6*	0.74	0.54	0.83	0.04*
Maternal serum levels				
IL-1	0.41	0.61	0.78	0.78
IL-2 R	0.09	0.66	0.73	0.73
IL-6*	0.60	0.93	0.87	0.53

*Kruskal–Wallis Test.

grade of acute inflammation in each tissue were as follows: amnion 0.84; choriodecidua 0.84; umbilical cord 0.85; and chorionic plate 0.73. Table 1 presents the raw data for amnion and umbilical cord scoring. Seventy-five of 77 diagnoses (97.4%) were concordant for the diagnosis of presence of acute inflammation. Sixteen (50%) of the cases were scored as grade 4 amnionitis, and 17 (51%) scored as grade 4 umbilical vasculitis. Twenty-six percent (20 of 77) of the total scores were discordant for inflammation grade. Eleven (50%) of the discordant scores involved the severe end of the inflammation scale (grades 3 and 4) and would not have modified the diagnosis of high-grade inflammation. In all of the 11 cases, multifocal or diffuse tissue necrosis was present, which distorted the histologic characteristics and might have contributed to discrepancy in interpretation. The two scores were averaged to provide the score used in subsequent analyses.

Table 1 describes the observed distributions of fetal and maternal serum cytokine levels. Tables 2 and 3 list the significant relationships of histologic measures of maternal and fetal acute inflammation to maternal and fetal serum cytokine levels. Considering the full scale of grades of acute inflammation (grades 0–4), the only significant correlations were between acute amnion inflammation and increased fetal serum IL-1ß levels ($p = 0.007$), and umbilical vasculitis and increased fetal serum IL-6 levels ($p = 0.04$). When the severity of acute inflammation was dichotomized into none or mild (grades 0–2) and severe (grades 3–4), fetal serum levels of IL-1ß and IL-2 R were related to severe acute amnion inflammation ($p = 0.022$ and $p = 0.023$, respectively) and severe umbilical vasculitis ($p = 0.008$, $p = 0.01$, respectively), and IL-6 was associated with severe umbilical vasculitis ($p = 0.03$). Acute inflammation of choriodecidua or chorionic plate was not related to either maternal or fetal serum cytokine levels. Presence and severity of acute maternal and fetal histologic inflammation were independent of administration of antepartum antibiotics, the duration of active labor, and the interval from membrane rupture to delivery.

DISCUSSION

Both histologic maternal inflammation (in the amnion), and histologic fetal inflammation (in the umbilical cord) were related to fetal (umbilical venous) serum cytokine levels, while no histologic characteristics were related to maternal serum cytokine levels. These associations were independent of latency from membrane rupture to delivery, duration of active labor, and antibiotic administration.

Table 3. Significant Relationships Of Grade 3–4 Acute Inflammation Compared to Grade 0–1+ Acute Inflammation to Maternal and Fetal Serum Cytokine Levels

	Maternal AI			*Fetal AI*
	Severe Acute Amnion Inflammation	*Severe Choriodecidual Inflammation*	*Severe Chorionic Plate Inflammation*	*Severe Umbilical Vasculitis*
Fetal serum levels				
IL-1	0.022	0.26	0.18	0.008
IL-2 R	0.023	0.26	0.15	0.01
IL-6*	0.24	0.29	0.18	0.03
Maternal serum levels				
IL-1	0.17	0.27	0.15	0.45
IL-2 R*	0.083	0.62	0.73	0.63
IL-6*	0.17	0.48	0.36	0.14

*Kruskal–Wallis Test.

The lack of association between maternal serum cytokine levels and histologic evidence of acute inflammation may reflect the predominantly local (paracrine) effects of cytokines. Our correlations between fetal serum cytokine levels and histologic acute inflammation are based on umbilical venous serum samples. Therefore, they may demonstrate a correlation between fetal physiological response and histologic acute inflammation. Alternatively, umbilical venous samples may be more representative of the placental state than fetal physiology. Indeed, the placenta is a well recognized source of a wide range of cytokines including interleukin-1[15] and interleukin-6.[16] Whether these placentally derived cytokines have any impact(s) on the fetus is unknown. Placentally generated cytokines could have no fetal systemic effects due to rapid clearance, or could contribute to the changes in fetal well-being, which may occur in the context of intraamniotic infection.[17] Fetal serum cytokine levels have been reported to identify cases at risk for early onset sepsis.[18] Future studies of fetal serum cytokines in relation to fetal/neonatal disease must clearly distinguish umbilical venous and arterial samples, because they may reflect completely different sources of cytokine generation and therefore possibly different modalities for optimal intervention. Whether placentally derived cytokines can have fetal systemic effects is an important question for clinicians working to reduce neonatal morbidity associated with acute ascending infection. The lack of correlation of antibiotic administration with fetal serum cytokine levels and with severity of histologic acute inflammation may raise questions as to how much antibiotics improve the fetoplacental environment in acute ascending infection, at least from the viewpoint of reducing production or fetal exposure to potentially deleterious cytokines.

We also demonstrate that a scoring system of histologic acute inflammation can be learned—from a printed set of guidelines alone—with a high level of reproducibility. The interobserver concordance was not, however, perfect. The grading system was devised for study of uncomplicated term deliveries. When acute inflammation is severe, neutrophils become "too numerous to count," and finer distinctions cannot be made. Also severe acute inflammation is associated with tissue destruction, which hampers the assessment of neutrophil presence and number. The highest grade (grade 4) of acute inflammation was seen in at least half of our cases, with the corollary of extensive tissue damage. A modification of this histologic grading to include the extent of tissue necrosis will further increase the reproducibility of histologic grading, especially in cases of preterm birth, when acute inflammation can be most severe. Clinicians should be able to rely on high interobserver concordance in the diagnosis of histologic markers of acute intra-amniotic infection, because such diagnoses can be made reliably, and with a minimum of training.

We conclude that fetal umbilical venous cytokine levels are correlated with the presence and severity of placental lesions of acute inflammation, which can be reliably and reproducibly diagnosed.

REFERENCES

1. Gabbe S, Niebyl J. *Obstetrics and Problem Pregnancy*. New York: Churchill-Livingston; 1986:1029
2. Leveno KJ, Little BB, Cunningham FG. The national impact of ritodrine hydrochloride for inhibition of preterm labor. Obstet Gynecol 1990;76:12–15
3. Romero R, Sirtori M, Oyarzun E, Avila C, Mazor M, Callahan R, Sabo V, Athanassiades A, Hobbins JC. Prevalence, microbiology, and clinical significance of intraamniotic infection in women with preterm labor and intact membranes. Am J Obstet Gynecol 1989;161:817–24
4. Skoll A, Moretti M, Sibai B. The incidence of positive amniotic fluid cultures in patients with preterm labor with intact membranes. Am J Obstet Gynecol 1989;161:813–16
5. Romero R, Salafia CM, Athanassiadis AP, Hanaoka S, Mazor M, Sepulveda W, Bracken M. The relationship between acute inflammatory lesions of the preterm placenta and amniotic fluid microbiology. Am J Obstet Gynecol 1992;166:1382–8
6. Guzick DS, Winn K. The association of chorioamnionitis with preterm delivery. Obstet Gynecol 1985;65:11–15
7. Hillier SL, Witkins SS, Krohn MA, Watts DH, Kiviat NB, Eschenbach DA. The relationship of amniotic fluid cytokines and preterm delivery, amniotic fluid infection, histologic chorioamnionitis, and chorioamnion infection. Obstet Gynecol 1993;81:941–8
8. Salafia CM, Minior VK, Rosenkrantz TS, Pezzullo JC, Cusick W, Vintzileos AM. Maternal, placental and neonatal associations with early germinal matrix/intraventricular hemorrhage in infants born at 32 weeks gestation. Am J Perinatol 1995;12:427–34
9. Leviton H. Preterm birth and cerebral palsy: Is tumor necrosis factor the missing link? Develop Med Child Neurol 1993;35:553–6
10. Hillier SL, Krohn MA, Kiviat NB, Watts DH, Eschenbach DA. Microbiologic causes and neonatal outcomes associated with chorioamnion infection. Am J Obstet Gynecol 1991;165:955–61
11. Potter NT, Kosuda L, Bigazzi PE, Fleming AD, Vintzileos AM, Homon C, Salafia CM. Relationships among cytokines (IL-1, TNF and IL-8) and histologic markers of acute ascending intrauterine infection. J Mat Fet Med 1992;1:142–7
12. Gibbs RS, Romero R, Hillier SL, Eschenbach, Sweet RL. A review of premature birth and subclinical infection. Am J Obstet Gynecol 1992;166:1515–28
13. Lencki SG, Maciulla MB, Eglinton GS. Maternal and umbilical cord serum interleukin levels in preterm labor with clinical chorioamnionitis. Am J Obstet Gynecol 1994;170:1345–51
14. Salafia CM, Weigl C, Silberman L. The prevalence and distribution of acute placental inflammation in uncomplicated term pregnancies. Obstet Gynecol 1989;73:383–9
15. Flynn A. Stimulation of interleukin-1 production from placental monocytes. Lymphokine Res 1984;3:1–5
16. Kauma SW, Turner TT, Harty JR. Interleukin-1 Beta stimulates interleukin-6 production in placental villous core mesenchymal cells. Endocrinology 1994;134:457–60
17. Fleming AD, Salafia CM, Vintzileos AM, Rodis JF, Campbell WA, Bantham KF. The relationships amongst umbilical arterial velocimetry, fetal biophysical profile and placental inflammation in preterm premature rupture of the membranes. Am J Obstet Gynecol 1991;164:38–41
18. Lehrnbecher T, Schrod L, Kraus D, et al. Interleukin-6 receptor in cord blood in the diagnosis of early onset sepsis in neonates. Acta Paediatrica 1995;84:806–8

American Journal of Perinatology

VOLUME 14 NUMBER 8 SEPTEMBER 1997

PLACENTAL PATHOLOGY AND ANTIPHOSPHOLIPID ANTIBODIES: A DESCRIPTIVE STUDY

Carolyn M. Salafia, M.D., and F. Susan Cowchock, M.D.*†*

ABSTRACT

We described placental pathology in antiphospholipid antibody (APL) syndrome, APL and no history of recurrent pregnancy loss, and in treated and untreated pregnancies of APL syndrome. Thirty-nine pregnancies of 28 patients were studied: 23 placentas delivered from 23 women with APL (13 with APL syndrome and 10 with serological APL); 8 untreated miscarriages before APL diagnosis from 6 of the 13 patients with APL syndrome and 1 of 10 with serological APL; and 8 miscarriages by 5 additional women before APL syndrome diagnosis. Histopathology was reviewed by a pathologist blinded except to gestational age. Contingency tables and analysis of variance (ANOVA) considered $p < 0.05$ significant. Comparing the placentas delivered at >18 weeks' gestation, excessive perivillous coagulation, avascular terminal villi, and chronic villitis/uteroplacental vasculitis tended to be more common in treated APL syndrome than serological APL cases ($p = 0.07$). Of the 16 miscarriages before diagnosis of APL, 11 were lost at <18 weeks' gestation. None had pathology typical of APL, but 4 of 11 (36%) had chronic intervillositis. Five of 16 miscarriages before the diagnosis of APL were miscarried between 18–22 weeks. Three of 5 (60%) miscarried after 18 weeks had multifocal uteroplacental thromboses, compared to 6 of 13 (46%) treated pregnancies with APL syndrome and 0 of 10 cases with serological APL.

Keywords: Antiphospholipid antibodies; placental pathology; uteroplacental vessels; coagulation

Antiphospholipid antibodies (APL) are associated with recurrent thrombotic events, thrombocytopenia, and with repeated fetal deaths.[1] The term APL syndrome has been used when APL are associated with one or more of these events. The detection of these antibodies in patients with histories of poor pregnancy outcome indicates an increased risk of additional pregnancy losses. However, the tests (immunoassays for anticardiolipin antibodies and/or prolongation of phospholipid-dependent clotting times) lack specificity. These tests detect a broad family of antibodies of varying specificities for phospholipid and phospholipid-protein complexes.[2] The predictive value of positive APL tests in general obstetric populations at low risk for fetal loss is poor. The mechanisms underlying those fetal deaths associated with pathological APL are unknown.

The placental lesions reported to occur in cases of APL-associated fetal loss include a wide

*Department of Pathology, Montefiore Medical Center, Bronx, New York; †Departments of Medicine & ‡Obstetrics and Gynecology, Thomas Jefferson University Medical School, Philadelphia, Pennsylvania

Reprint requests: Dr. Salafia, Associate Professor of Pathology, Montefiore Medical Center Weiler Hospital, 1825 Eastchester Road, Bronx, NY 10461

range of uteroplacental vascular lesions, including uteroplacental thrombosis,[3] fibrinoid necrosis of the vessel wall and atherosis,[4] as well as placental damage such as infarct and fibrosis secondary to uteroplacental vascular disease. The latter includes placental infarction and hypovascular fibrosed villi.[5] These changes are also described in placentas from patients with systemic lupus erythematosus, who may have had associated APL.[5,6] The predominance in older reports of coagulation-associated placental pathology is one reason for the current use of heparin in the treatment of APL during pregnancy. Generally, only placentas from patients with the APL syndrome have been studied. No previous report has compared pathological findings in placentas from APL women without clinical or obstetric symptoms (serological APL) to those from women with the APL syndrome, or compared placentas from prospectively ascertained and treated pregnancies to those from prior untreated pregnancies. This study compares placental pathological findings in pregnancies of women in whom the finding of APL may have been coincidental (a group defined serologically but without a history of thrombosis, thrombocytopenia, or repeated fetal losses, $N = 10$), to placentas from pregnancies of APL women with history of 2 or more prior fetal losses ($N = 13$). The serological APL group was treated with 80-mg aspirin daily or given no specific treatment, while those with APL syndrome were treated with heparin or prednisone plus 80-mg aspirin daily.

METHODS AND MATERIALS

Patient Population

In the context of treatment trials[7] of the effects of therapy on APL-associated pregnancy loss, permission to obtain tissue or prepared blocks and slides from placentas delivered from enrolled patients was part of the consent form approved by participating Institutional Review Boards. The goal of the treatment trials was to compare the pathology after treatment with aspirin plus either heparin or prednisone in patients with APL syndrome and 2 or more prior losses and those of women with APL but no history of recurrent pregnancy loss (serological APL) treated with aspirin or usual obstetric care.[7] The criteria for diagnosis and confirmation of APL were the same for all women whose pregnancies were studied. Immunoassays for IgM and IgG class anticardiolipin antibodies were performed at collaborating institutions and repeated at least once. Positive results were confirmed if either value was at or above 2.0 multiples of the median. Tests for lupus anticoagulants included activated partial thromboplastin times, or dilute Russell viper venom times. Prolongation of clotting times more than 2 SDs above the normal mean were confirmed by 1:1 dilution of the sample with fresh-frozen plasma to exclude clotting factor deficiencies. Patients were considered to be APL positive if either or both tests were repeatedly positive.

One group of patients represented a subset of the published treatment trial.[7] Thirteen of the 20 (65%) pregnancies delivered of women with APL syndrome in this trial were available for study, as were 10 of 19 (53%) placentas delivered of women with serological APL. None of the patients with serological APL had only IgM anticardiolipin. Six of the 13 women with APL syndrome also had one pretreatment miscarriage available for review, and one of the women with serological APL had two prior untreated miscarriages available for review. Clinical data are presented in Table 1.

We also requested permission to review slides or blocks from prior pregnancies of women enrolled in other trials of therapy for APL and whose laboratory testing demonstrated the above described diagnostic abnormalities. Five women had a total of 8 untreated miscarriages prior to diagnosis of APL syndrome available for review. Therefore, a total of 16 untreated miscarriages from then undiagnosed women were included in the study. These patients had APL detected and at the time of presentation for therapy had at least two prior miscarriages.

Placental Examination

Placental examination was performed by a single blinded pathologist (C.M.S.) on 16 of the 23 prospectively studied placentas. Placentas were weighed after removal of adherent blood and umbilical cord. Presence, number, and estimated volumes of infarct and intervillous thrombus were recorded. Four sections of grossly normal placenta

Table 1. Comparison of Clinical Data from Patients Whose Placentas from Prospectively Ascertained and Treated Pregnancies Underwent Systematic Pathologic Examination

	APL Syndrome	*Serological APL*
Average number of prior losses	3.5 (45 of 13)*	0.4 (4 of 10)
Prior live birth(s)	23% (3 of 13)	80% (8 of 10)
Medical complications	23% (4† of 13)	0% (0 of 10)
IgG ACL	69% (9 of 13)	50% (5 of 10)
Lupus anticoagulant	46% (6 of 13)	30% (3 of 10)

*p calculated using two-tailed Fisher's Exact or t-tests.
†Thrombosis (3), Systemic Lupus Erythematosus (1).

were examined microscopically for perivillous fibrin deposition, chorionic and fetal stem vessel thrombi, avascular villi, and chronic villitis/intervillositis. Sections of the basal plate included decidual segments of uteroplacental vessels. The remaining 7 placentas from prospectively ascertained pregnancies were studied in local hospitals; reports of gross examinations and 21 slides from these 7 cases were reviewed. Tissue sampling from the 16 preenrollment untreated pregnancy losses was performed at referring hospitals. Ninety-four hematoxylin and eosin stained slides from the 16 cases were examined and diagnoses made according to published criteria.[5,8] Lesions were scored as absent or normal/present or excessive for gestational age. Placental lesions were grouped as: (1) uteroplacental vascular pathology and secondary villous damage, (2) lesions involving coagulation, and (3) lesions of chronic inflammation.

1. Uteroplacental vascular pathology and secondary villous damage. Uteroplacental vascular pathology included the uteroplacental lesions, and the villous lesions which may be the result of uteroplacental vascular pathology. Specific lesions of the uteroplacental vessels were fibrinoid necrosis/atherosis and absent or incomplete physiological conversion of the basal spiral vasculature. The latter diagnosis was made when the normal endovascular trophoblast destruction of the muscular and elastic components of the decidual spiral vessels did not occur or was incomplete.[8] Incompletely converted vessels retained muscle and elastic in their walls and resembled spiral vessels of the late luteal phase endometrium.[9] Lesions considered to be indirect effects of uteroplacental vascular pathology included villous infarcts,[10] terminal villous fibrosis, and terminal villous hypovascularity.[11,12] Infarcts were considered as single or multiple, and lesions of villous fibrosis and hypovascularity were subjectively scored as mild or severe (e.g., Fig. 1). To prevent multiple classification of lesions, two types of uteroplacental vascular lesions, occlusive vascular thrombi and chronic uteroplacental vasculitis, were assigned to the categories of coagulation-related lesions and chronic inflammation, respectively.
2. Lesions involving coagulation. Coagulation-related lesions were grouped by anatomical location within the placenta: (1) maternal circulation, (2) villous trophoblast surface, or (3) within the feto-placental circulation. The coagulation-related lesion identified in the maternal circulation was occlusive uteroplacental vascular thrombus. On the placental surface, initiation of coagulation results in deposition of fibrin on the villous trophoblast surface and around villi ("perivillous fibrin deposition"). Some perivillous fibrin is present in normal placentas.[9] Excessive perivillous fibrin deposition, with entrapment of >20% of villi in any one slide in perivillous fibrin, was considered pathological. Lesions reflective of coagulation within the fetoplacental circulation were thrombi within chorionic or fetal stem vessels, and/or occlusion in the microcirculation demonstrated by foci of avascular terminal villi.
3. Lesions of chronic inflammation. Chronic inflammation was also distinguished by anatomical location. In maternal tissues, chronic inflammatory lesions included uteroplacental vasculitis (defined as a mononuclear infiltrate within the maternal vessel wall of either the basal or parietal decidua)[13] and dense decidual infiltrates with a plasma cell component. Chronic perivillous inflammation was labeled chronic intervillositis.[14] Villi with a stromal mononuclear cell infiltrate were diagnosed as chronic villitis.[15]

Diagnoses in cases of early pregnancy losses were made according to previously published criteria.[16] These criteria considered the integrity of the villous circulation, the proportion of nucleated to anucleated erythrocytes, and the presence and ex-

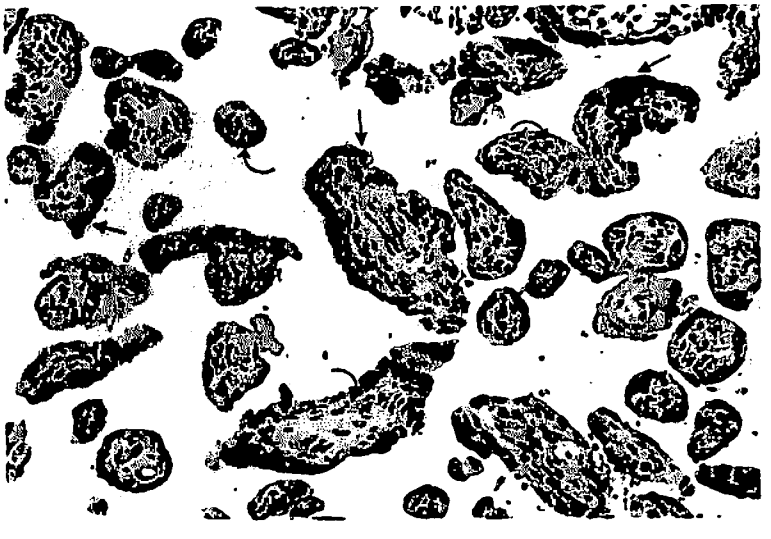

Figure 1. Placenta from 18-week fetal demise, mother with APL, no therapy: Chorionic villi are shrunken and fibrotic with small caliber capillaries (large arrows), with a nucleated erythrocyte, reduced capillary number, and markedly increased trophoblast knotting (small arrows), representing severe and chronic ischemic villous damage. Hematoxylin and eosin stain (102 original magnification).

tent of villous hydrops in addition to the histologic lesions described above.

Given the lack of uniformity of tissue sampling in materials reviewed from referral hospitals, this study was conceived primarily as a descriptive presentation of APL-associated placental histopathology throughout gestation and in relation to therapy for APL syndrome. Statistical comparisons were included as appropriate. Mann–Whitney *U* tests and Fisher's exact tests compared medians and proportions in groups, respectively, with $p < 0.05$ considered significant. All analyses were two-tailed.

RESULTS

Prospectively Ascertained and Treated Pregnancies

Twenty-two of the 23 placentas from prospectively ascertained and treated cases were from pregnancies ending in live births. The sole fetal death (at 18 weeks' gestation) occurred in the group of 13 patients with APL syndrome and recurrent pregnancy loss. All other pregnancies delivered at > 26 weeks' gestation. The 13 women with APL syndrome and two or more prior losses delivered significantly earlier than the 10 women with serological APL (35.4 ± 4.0 weeks vs. 38.1 ± 1.2, $p < 0.05$). The placentas of women with APL syndrome were also lighter (427 ± 113 g) than placentas of women with serological APL (572 ± 80 g, $p < 0.05$); this difference was due to the shorter gestational length of patients with APL syndrome. Tables 2 and 3 present the lesions identified in the placentas of the 23 pregnancies.

Treated Pregnancies from Patients with APL Syndrome and Recurrent Pregnancy Losses (Table 2)

The single case of fetal demise showed extensive uteroplacental vascular pathology and chronic villitis (patient 13, Table 2). Six of the 13 (46%) placentas with APL syndrome had uteroplacental vascular pathology and seven of 13 (54%) placentas had coagulation-related lesions. Two (28.5%) placentas had coagulation related lesions in two or more anatomical sites (i.e., maternal circulation, villous surface, and/or placental circulation). Four of the 13 (31%) placentas with APL syndrome had chronic villitis and/or decidual plasma cell infiltrates. Two placentas had no lesions.

Treated Pregnancies from Patients with APL but No History of Recurrent Pregnancy Loss (Table 3)

Of the 10 cases with serological APL, three placentas (30%) had mild villous fibrosis, and none had uteroplacental vascular pathology. No villous infarcts were observed. Six of 10 (60%) placentas had at least one lesion related to coagulation. Four of the 6 had a single lesion only. Chronic villitis and/or decidual vasculitis were seen in 2 of 10 (20%) cases. Two cases had no lesions.

Inspecting Tables 2 and 3, at least two of the three previously defined categories of placental pathology occurred in 6 of 13 (46%) cases of APL syndrome treated with heparin or prednisone and aspirin, compared to 3 of 10 (30%) of the cases with serological APL. Lesions seen in the 10 serological cases also tended to be of milder severity (e.g., vil-

Table 2. Nature and Distribution of Placental Lesions in Patients with APL Detected and Two or More Pregnancy Losses

Patient	*Uteroplacental Vascular Pathology and Related Villous Lesions*	*Coagulation-Related Lesions*	*Chronic Inflammation*
1	None	None	None
2	Villous infarct, moderate villous fibrosis, fibrinoid necrosis/atherosis	Single uteroplacental thrombus	None
3	Absent physiological change, severe villous fibrosis	Single uteroplacental thrombus	None
4	None	None	Chronic villitis
5	None	Excessive perivillous fibrin deposition	None
6	None	Excessive perivillous fibrin deposition	None
7	Uteroplacental fibrinoid necrosis/atherosis	Multiple intervillous thrombi, excessive perivillous fibrin deposition, numerous avascular villi	None
8	None	None	None
9	None	Excessive perivillous fibrin deposition	None
10	Villous infarct, severe villous fibrosis	Excessive perivillous fibrin deposition	None
11	None	Excessive perivillous fibrin deposition, numerous avascular villi	Chronic villitis, decidual plasma cells
12	Villous infarct	Fetal stem vessel thrombi/ numerous avascular villi	Chronic villitis, uteroplacental vasculitis
13	Multiple villous infarcts	Fetal stem vessel thrombi/ numerous avascular villi	Chronic villitis

Table 3. Nature and Distribution of Placental Lesions in Patients with APL Detected and None or One Pregnancy Loss

Patient	*Uteroplacental Vascular Pathology and Related Villous Lesions*	*Coagulation-Related Lesions*	*Chronic Inflammation*
1	None	Single intervillous thrombus	None
2	Mild villous fibrosis	None	None
3	Mild villous fibrosis	Single uteroplacental thrombus	None
4	None	Excessive perivillous fibrin deposition	None
5	None	Single intervillous thrombus, single uteroplacental thrombus, numerous avascular villi	None
6	None	None	None
7	Mild villous fibrosis	None	Chronic villitis
8	None	Single uteroplacental thrombus	None
9	None	Single intervillous thrombus, excessive perivillous fibrin deposition	Uteroplacental vasculitis
10	None	None	None

lous fibrosis) or a single lesion (e.g., uteroplacental vascular thrombus), compared to the cases with APL syndrome and recurrent pregnancy loss. Among cases with APL syndrome, no differences in placental features could be identified between APL syndrome patients treated with heparin ($N = 7$) and those receiving prednisone ($N = 6$), or between serological APL patients treated with aspirin or usual care, but sample sizes were small.

Review of Placental Samples from Prior, Untreated Pregnancies

Sixteen pregnancies were lost before 22 weeks gestation to 12 patients subsequently determined to have APL. Eleven of 12 had APL and recurrent pregnancy loss (APL syndrome). Eleven of the 16 miscarriages aborted before 18 weeks. Six of the 11 (55%) early miscarriages had histologic evidence of embryo death by 8 weeks' gestation, up to 4 weeks before the clinical miscarriage. The one prior miscarriage of a woman with serological APL demonstrated histologic evidence of early embryo failure. Chronic intervillositis was seen in 4 of 11 (36%) miscarriages, but uteroplacental vascular pathology, uteroplacental vascular thrombus, and placental infarct were not seen in any of the 11 early miscarriages. In contrast, 3 of the 5 (60%) miscarriages lost between 18 and 22 weeks' gestation had multiple lesions of uteroplacental vascular thrombus, placental infarct, abruption, or uteroplacental vascular pathology, compared to 6 of 13 (46%) treated placentas with APL syndrome (Table 2) and 0 of 10 (0%) placentas with APL without clinical symptoms (Table 3).

Figures 1 and 2 compare the histologic features from one placenta from an untreated pregnancy loss after 18 weeks and the placenta from a subsequent successful pregnancy from the same mother treated with heparin. In the placenta from the pregnancy loss, uteroplacental vascular thrombi and resultant villous damage were widespread (Fig. 1). In the treated pregnancy, uteroplacental vascular

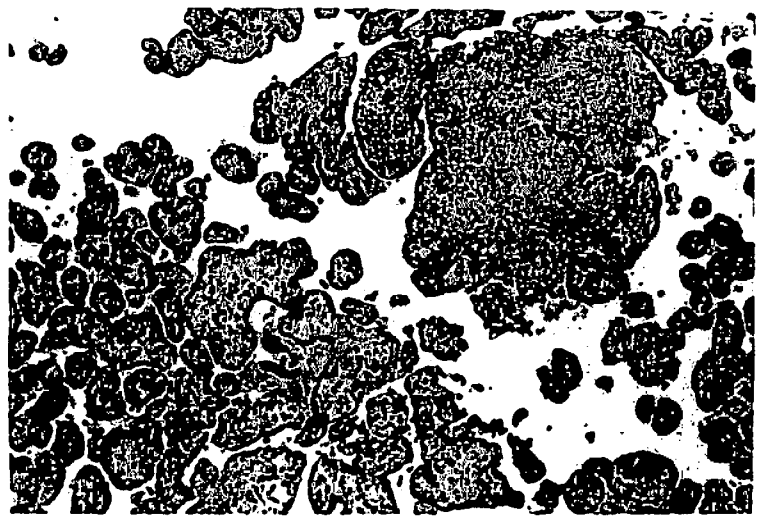

Figure 2. Placenta from 35 delivery of AGA infant, same mother as Figure 1, APL treated with heparin and aspirin: Chorionic villi are well-vascularized and numerous (small arrows). Trophoblast knots are occasional. A focus of chronic villitis (large arrows) with chronic intervillositis (broad arrow) is present. Hematoxylin and eosin stain (42 original magnification).

thrombi were absent but chronic villitis, extensive perivillous fibrin deposition, fetal stem vessel thrombi, and avascular villi were present (Fig. 2).

DISCUSSION

Placentas delivered of women with treated APL syndrome are not histologically normal but show either lesions that are uncommon in normal term deliveries or more extensive lesions of the types seen in normal term deliveries. Absence of physiological change and fibrinoid necrosis/atherosis are rare in normal term placentas[6,17] but have been reported to occur in cases of APL syndrome with fetal loss[18,19] and in patients with systemic lupus erythematosus in the presence or absence of APL.[18,19] Some perivillous fibrin deposition and occasional avascular villi are not uncommon in term placentas,[6,20] but excessive perivillous fibrin deposition and/or multifocal avascular villi were common in cases of APL syndrome and recurrent pregnancy loss despite anticoagulant treatment. In one patient for which an untreated second-trimester loss and a successfully treated pregnancy could be studied, the treated pregnancy showed no uteroplacental vascular thrombi but prominent chronic inflammatory lesions and extensive perivillous fibrin deposition (a lesion reflecting local activation of the coagulation cascade[21]). Each of the three endothelial or endothelial-like surfaces in the pregnant uterus (the maternal uterine vascular endothelium, the trophoblast lining the intervillous space, and the feto-placental endothelium) are potential targets of APL.[22,23] In successful APL pregnancies, the presence of excessive perivillous and intraplacental fibrin deposition may also reflect the effects of APL damaging the syncytiotrophoblast,[24,25] as a "hallmark of rejecting allografted organs."[26] Finally, an isolated uteroplacental thrombosis is also not uncommon at term.[6] Heparin/prednisone plus aspirin given to patients with APL syndrome did not prevent uteroplacental vascular thrombi, but most cases still delivered viable infants, despite an occasional uteroplacental vascular thrombosis. Approximately 40–60 placental functional units are supplied by more than twice that number of spiral vessels. One uteroplacental vascular thrombus in an otherwise intact uteroplacental circulation may have no villous (and fetal) effects given healthy collateral flow from neighboring uteroplacental vessels.

Of the 16 untreated pregnancies from women with APL, 11 were first-trimester losses with histologic evidence of early embryo failure, a finding consistent with a greater likelihood of aneuploidy of the conceptus.[17] Uteroplacental vascular thrombi and infarcts were rare; sampling error cannot be excluded. However, 4 of 11 (36%) had chronic intervillositis, while in a prior study of nonrecurrent spontaneous pregnancy loss the incidence of chronic intervillositis was 9%.[17] This finding may prove to be a clue to the natural evolution of this disorder. Two caveats must be considered. Testing based on the number of prior losses may identify APL in women whose previous early miscarriages were sporadic and unrelated to APL. Also, the excess of chronic inflammatory lesions we observed could reflect a small sample size. Further studies of consecutive losses in women diagnosed with APL are needed.

This is the largest series of systematically examined placentas from pregnancies of women with APL syndrome or serological APL. However, it is assembled from diverse sources. Therefore, we have restricted the extent of statistical manipulation and only future studies with more uniform pathological exam can determine whether its findings can be generalized. Six of the seven cases that were examined initially by outside institutions were cases of APL syndrome, and thus had fewer tissue samples available for review. Therefore, selection bias exists regarding tissue sampling in this study; it would be toward under-reporting of lesions in the APL syndrome group. When APL was present without a history of thrombosis or repeated pregnancy loss (serological APL), aspirin and usual care were associated with delivery of healthy infants with essentially normal term placentas. In APL syndrome, antithrombotic therapy and improved perinatal outcome may be due to effects on the maternal circulation. Nonthrombotic placental lesions, such as chronic inflammation, trophoblast damage, and intraplacental clotting, may not be affected by therapy and may be more extensive following antithrombotic therapy. These lesions may be the result of other APL-associated mechanisms of placental damage. Early pregnancy losses in patients with APL may reflect patient ascertainment bias, but further studies providing uniformity of tissue sampling and a consensus approach to pathological diagnosis may clarify the role(s) of APL in pregnancy compromise.

REFERENCES

1. Feinstein DI. Lupus anticoagulant, thrombosis, fetal loss. N Engl J Med 1985;21:1348
2. Triplett DA. Antiphospholipid antibodies and recurrent pregnancy loss. Am J Reprod Immunol 1989;20:52–67
3. Abramowsky CR, Vegas ME, Swinehart G, Gyles MT. Decidual vasculopathy of the placenta in lupus erythematosus. N Engl J Med 1980;668–72
4. Labarerre CA, Catoggio LJ, Mullen EG, Aldhabe OH. Placental lesions in maternal autoimmune diseases. Am J Reprod Immunol Microbiol 1986;12:78–86
5. Bernirschke K. A review of the pathologic anatomy of the human placenta. Am J Obstet Gynecol 1962;84:1595–1622
6. Fox H (ed), Bennington JL, (consult ed). Pathology of the placenta. In *Major Problems in Pathology*. Philadelphia: WB Saunders; 1978; pp 95–148
7. Cowchock FS, Reece EA, Balaban D, Branch DW, Plouffe L. Repetitive fetal loss associated with antiphospholipid antibodies: A collaborative randomized trial comparing prednisone with low dose heparin therapy. Am J Obstet Gynecol 1992;166:1318
8. Perrin EVDK, (ed). *Pathology of the Placenta*. New York: Churchill Livingston; 1984

9. Robertson WB, Khong TY, Brosens I, De Wolf F, Sheppard BL, Bonnar J. The placental bed biopsy: Review from three European centers. Am J Obstet Gynecol 1986;155: 401–412
10. Pijnenborg R, Dixon G, Robertson WB, Brosens I. Trophoblastic invasion of human decidua from 8 to 18 weeks of pregnancy. Placenta 1980;1:13–19
11. Brosens I, Renaer M. On the pathogenesis of placental infarcts in pre-eclampsia. J Obstet Gynecol Br Commonwealth 1972;79:794–9
12. Kaplan C, Lowell DM, Salafia CM. College of American Pathologists conference XIX on the examination of the placenta report of the working group. Arch Pathol Lab Med 1991;115:709–16
13. Altshuler G, Russell P. The human placental villitides: A review of chronic intrauterine infection. Curr Top Pathol 1975;60:64–112
14. Redline RW, Abramowsky CR. Clinical and pathological aspects of recurrent placental villitis. Hum Pathol 1985;16:727–31
15. Salafia CM, Maier D, Vogel C, Pezzullo JC, Burns JP, Silberman L. Placental and decidual histology in spontaneous abortion: Detailed description and correlations with chromosome number. Obstet Gynecol 1993;82:295–303
16. Out HJ, Kooijman CD, Bruinse HW, Derksen R. Histopathological findings in placentas from patients with intrauterine fetal death and antiphospholipid antibodies Eur J Obstet Gynecol Reprod Biol 1991;41:179–8
17. Salafia CM, Vintzileos AM, Bantham KF, Vogel CA, Pezzullo J, Silberman L. Placental pathologic findings in preterm birth. Am J Obstet Gynecol 1991;165:934–8
18. DeWolf F, Cerreras LO, Moerman P, Vermyles J, VanAssche A, Renaer M. Decidual vasculopathy and extensive placental infarction in a patient with repeated thromboembolic accidents, recurrent fetal loss, and a lupus anticoagulant. Am J Obstet Gynecol 1982;142:829–34
19. Loizou S, Byron MA, Englert HJ, David J, Hughes GRV, Walport MJ. Association of quantitative anticardiolipin levels with fetal loss and time of loss in systemic loss erythematosus. Q J Med 1988;255:525–31
20. Salafia CM, Vintzileos AM, Silberman L, Bantham KF, Vogel CA. Placental pathology of idiopathic intrauterine growth retardation at term. Am J Perinatol 1992;9:179–84
21. Nelson M, Crouch E, Curran E, Farmer D. Trophoblast interaction with fibrin matrix: Epithelialization of perivillous fibrin deposits as a mechanism for villous repair in the human placenta. Am J Pathol 1990;136:855–65
22. Branch DW, Rodgers GM. Induction of endothelial cell tissue factor activity by sera from patients with antiphospholipid syndrome: a possible mechanism of thrombosis. Am J Obstet Gynecol 1993;168:206–10
23. Silver RK, O'Connell PD, Caplan MS. Acetylsalicylic acid inhibits anticardiolipin antibody-induces platelet-activating factor (PAF) synthesis. Prostaglandins 1993;45: 143–51
24. Hasegawa I, Takakuwa K, Adachi S, Kanazawa K. Cytotoxic antibody against trophoblast and lymphocytes present in pregnancy with intrauterine fetal growth retardation and its relation to anti-phospholipid antibody. J Reprod Immunol 1990;17:127–39
25. McCrae KR, DeMichele AM, Pandhi P, Balsai MJ, Samuels P, Graham C, Lala PK, Cines DB. Detection of antitrophoblast antibodies in the sera of patients with anticardiolipin antibodies and fetal loss. Blood 1993;82:2730–41
26. Faulk WP. Placental fibrin. Am J Reprod Immunol 1989; 19:132–5

Contributions of both authors were supported in part by Grant #R01-21657. We acknowledge the technical support of Danbury Hospital, Danbury CT. Review of statistical methodology was provided by John C. Pezzullo, Ph.D., Informatics Chief, Perinatology Research Facility (NICHD, Intramural Division) Georgetown University, Washington, DC.

Published in final edited form as:
Placenta. 2009 November ; 30(11): 988. doi:10.1016/j.placenta.2009.08.010.

Methodologic issues in the study of the relationship between histologic indicators of intraamniotic infection and clinical outcomes

Carolyn M. Salafia, M.D., M.S.[1,2], **Dawn Misra, Ph.D**[3], and **Jeremy N. V. Miles, Ph.D**[4]

[1] Placental Analytics, LLC, Larchmont, NY

[2] Institute for Basic Research, Staten Island, NY

[3] Department of Family Medicine and Public Health Sciences, Wayne State University School of Medicine, Ann Arbor, MI

[4] Rand Corporation, Santa Monica, CA

Abstract

Goal—To determine the structure of the relationships of the histology scores for acute intraamniotic infection collected in the Collaborative Perinatal Project (CPP).

Materials and Methods—44,427 subjects of the CPP had complete histology scores available for the 9 measures that related to acute intraamniotic infection (i.e., neutrophil infiltrates in umbilical cord, amnion of extraplacental membranes and chorionic plate, decidua, chorionic plate and fetal chorionic vessels). Confirmatory factor analysis was used to determine the relationships among the different markers of maternal inflammatory responses (in amnion, chorion and decidua) and fetal inflammatory responses (in umbilical cord and fetal chorionic vessels).

Results—A single CFA model could not be developed across all CPP sites. A well-fit model was developed from the Boston site (N=10,803) and the factor loadings applied to the histology scores from the other CPP sites. The resultant scores for the latent variables (maternal and fetal inflammatory responses) were compared across sites. There was not only considerable variability in factor loadings, and the signs of factor loadings were also inconsistent across sites.

Conclusion—Histopathology scores of neutrophil infiltrates performed by different observers do not have the same interrelationships and, by extension, the latent variables they are supposed to reflect may not be equivalent. The lack of measurement invariance renders their use as indicators of the underlying processes of maternal and fetal inflammatory responses problematic in analysis with any clinical outcome.

INTRODUCTION

Chorioamnionitis, the presence of intraamniotic microbial organisms triggering maternal and/or fetal inflammatory responses, plays a significant role in reproductive and childhood pathology. Numerous investigators have identified ascending infection as a key pathway in the etiology of preterm birth, particularly early preterm births (less than 35 weeks gestation, as reviewed in 1). Ascending infection has also been proposed as a potential explanatory factor for the substantial racial disparity in risk of preterm birth. 2 Neonates born with funisitis, a

Corresponding Author: Carolyn M. Salafia M.D., M.S., Placental Analytics, LLC, 93 Colonial Avenue, Larchmont NY 10538, Carolyn.salafia@gmail.com.

prime histologic marker of fetal inflammatory response, are at increased risk for neurologic handicap and cerebral palsy. 3 However, it is the minority of infants born from such environments that develop any neurodevelopmental disorder and causal inference remains problematic. 4 Evidence has begun to accumulate that gene-environment interactions determine the likelihood of preterm labor and delivery and, probably, the risk of fetal injury.[5]

Holzman et al 6 recently and elegantly summarized the conflicting literature regarding the role of infection diagnosed histologically in preterm birth. . In their own analysis, the choice of inflammatory cell threshold (the number of infiltrating neutrophils required to make a diagnosis of infection) dramatically influenced disease prevalence; the rates of histologic chorioamnionitis ranged "from 85 percent … to 7 percent [in term] and in PTD from 63 percent … to 4 percent" at different inflammatory cell thresholds. [6] They also documented variability in the specific tissue components included, the number of tissue samples reviewed, and the specific features detailed (location, density, and degeneration), additional factors that would affect the prevalence of diagnosis of histologic chorioamnionitis and by extension complicate our understanding of its gestational effects.

Controversy remains in pathology circles regarding whether a multi-category (0–4 stage and 0–4 grading) histologic chorioamnionitis scoring system, or a more simplified system (with fewer categories or a "present/absent" categorization) is optimal. Inter-rater reliability is optimized with a "present/absent" system [7] but such a system must blur the subtleties of the complex mix of genes, cytokines, specific bacterial and other environmental stressors that is inflammation. How best to analyze the individual histology scores derived from the different tissues is also controversial. Should the scores of inflammation in amnion, chorion, decidua and chorionic plate be summed to reflect an overall "maternal inflammatory response" or should a "threshold" level of "normal neutrophil infiltration" in sites such as subchorionic fibrin be used to determine "intraamniotic infection greater than would be common in normal term births?8

Summing scores does not allow finer distinctions among the relative "value" of the different histology indicators. For example, neutrophil infiltrates in the amnion may be a stronger indicator of histologic chorioamnionitis than, for example, decidual neutrophil infiltrates. (e.g., 8) One can empirically assign weights to different indicator scores, and thus tinker with the sum. Alternatively, factor analysis can be used to derive weights (or factor loadings) that reflect the actual intercorrelations among the indicator variables. Exploratory factor analysis is employed when little is known of the underlying structure. Confirmatory factor analysis can be applied when we have biologically based, and theoretically derived concepts regarding the underlying structure, which we want to test.

Given the richness of the histology data in the National Collaborative Perinatal Project (NCPP) data, and the clinical importance of reliable and reproducible diagnoses of histologic chorioamnionitis estimated from histologic slides, we determined to apply confirmatory factor analysis to the histology scores related to histologic chorioamnionitis in the NCPP. Our goal was to explore the structure of the relationships of histologic measures of the maternal and fetal inflammatory responses, respectively, within and among institutions and observers.

MATERIALS AND METHODS

METHODS

The study and analytic sample—Subjects were a subset of the National Collaborative Perinatal Project. Details of the study have been described elsewhere. [9, 10]. Briefly, from 1959 to 1965, women who attended prenatal care at 12 hospitals were invited to participate in the observational, prospective study. At entry, detailed demographic, socioeconomic and

behavioral information was collected by in-person interview. A medical history, physical examination and blood sample were also obtained. In subsequent prenatal visits, women were repeatedly interviewed and physical findings were recorded. During labor and delivery, placental gross morphology was examined and samples were collected for histologic examination. The children were followed up to seven years of age.

The analytic sample for the present analysis was derived from all delivered infants, live or stillborn infants, irregardless of gestational age, and included both singletons and multifetal pregnancies and these clinical data should not prejudice or bias the scoring of neutrophil infiltrates by pathologists blinded to other clinical data. The sample was restricted to those with complete data on the nine measures of neutrophil infiltrates that were specified by the protocol. [11] Expert pathologists at each of 12 institutions were provided a scoring sheet with a written description of the grading scale for neutrophil infiltrates of amnion, chorion and decidua of the membranes, amnion and chorion of the chorionic plate, umbilical artery, vein and Wharton's jelly, and fetal chorionic vessels (9 separate scores).

Analysis Plan

Our a priori understanding led us to formulate a confirmatory factor analysis with 2 latent variables, one reflecting the maternal inflammatory response (indicated by the scores of amnion, chorion and decidua of the membranes, amnion and chorion of the chorionic plate) and one reflecting fetal inflammatory response (indicated by the umbilical cord and fetal chorionic vascular scores). We fitted confirmatory factor analysis models to the data using Mplus 4.2. [12] The data were treated as ordered categorical (that is we modeled the probability of each response, rather than the mean of the responses). Parameters were estimated using the weighted least squares – mean and variance corrected algorithm, this approach has been shown to work well with categorical data.13 We followed the methods described by Joreskog, 14 first attempting a strictly confirmatory approach and then using a model generation approach to modify the model.

To assess model fit, we used the X^2 statistic, in conjunction with its associated p-value. The X^2 statistic assesses the difference between the model and the data. Larger, and more statistically significant values of X^2 are indicative of worse model fit – worse model fit implying a greater mismatch between the model and the data. However, X^2 suffers from well known problems when fitting models based on large samples – specifically it has a large amount of power to find models which differ from the data in only trivial and inconsequential amount. Because of this, a wide range of other indices have been developed along with X^2 to aid in determining when good model fit has been found. For this analysis, we also used the Root Mean Square Error of Approximation (RMSEA15), the Comparative Fit Index (CFI 16) and the Tucker Lewis Index (TLI, also referred to as the non-normed fit index, NNFI). The RMSEA can be thought of as a correction to X^2, to account for the sample size and model complexity; values below 0.05 are often seen as indicative of adequate fit. The CFI and TLI both compare the X^2 of the fitted model to that of the null model, the null model being the worst model that it would be possible to have, with no relations between any of the variables [17] values above 0.95 are usually considered to show good fit. [18]

Confirmatory factor analysis models can be fitted to single groups, or to multiple groups. In a multiple group model, parameters are estimated for each group, and these parameters can then be tested across groups using Wald tests or X^2 difference tests.

RESULTS

We first examined the percentage endorsement of frequencies of scores for each of the 9 measures at each CPP site (Table 1). Of note, certain sites used in effect a 0–2, rather than the

0–3 scale specified by the protocol [11], and the highest severity score was overall used infrequently when used.

Next, Using Mplus 4.2 [12], and considering the histology scores as ordered categorical variables representing underlying continuous processes, we attempted to fit a multiple group model, with hospital sites defining the groups. This model had convergence problems which we identified as being related to particular sites, where measures either varied inconsistently, or were perfectly correlated. As the Boston cohort (N=10803) was the largest of the 12, we elected to develop a model in this cohort and then test its generalizability to the other cohorts. [12] The close correlation between scores of neutrophil infiltrates in membrane chorion and membrane decidua forced removal of the membrane chorion score from the model; of the two variables, the membrane decidua score provided slightly better fit. Figure 1 shows the final model, which had excellent fit according to established criteria (e.g. CFI, TLI each 0.999, RMSEA 0.033). Of interest, model fit was significantly improved by removing the fetal chorionic vessel score as an indicator of fetal inflammatory response; the covariance of this fetal indicator with maternal inflammation was stronger than with fetal inflammation (0.848 vs. 0.693, Table 1).

We then applied this model to each of the other 11 cohorts, and achieved generally as good a fit as for the Boston cohort. However, the loadings for the different histology scores differed significantly from the Boston cohort (Table 2, Wald tests). In addition, comparing the loadings for the group of indicators of maternal and fetal inflammatory responses showed that there were multivariate significant differences from the Boston cohort. In other words, the latent variables of maternal and fetal inflammation are not indicated by the histology scores uniformly across the cohorts. Further inspection of the data revealed other disturbing patterns. In general, maternal and fetal inflammatory responses tend to coincide; there may be variability in the relative strengths of each response, but they tend to be present together. The extent of covariance of maternal and fetal inflammatory responses was widely different among cohorts, ranging from 0.435 (Providence) to 2.094 (Pennsylvania). Moreover the means of the latent variables not only differed from that of the Boston cohort (indicating different prevalences of the histology scores, which would not be unexpected), but they differed in opposite directions (e.g., Buffalo, New Orleans, NY/Columbia, Virginia, Minnesota, NY/Medical, Oregon, Pennsylvania, Providence and Tennessee). These comparisons are, however, difficult to interpret because the measurements are not directly comparable across the cohorts.

Discussion

These data demonstrate that, in the CPP, individual histology scorings of neutrophil infiltrates, markers of intramniotic infection, demonstrate significant differences in their contributions to more general constructs of maternal inflammation and fetal inflammation. While it is possible that demographic and genetic factors may account for part of these differences, at least some of the variability must be due to inter-observer factors. The lack of measurement invariance means that these scorings cannot be used to represent the same construct (or underlying biological process) in different cohorts. In the psychometric literature this is termed “differential item functioning”, or “DIF” [19], and threatens the validity of the measurement instrument. In psychometrics, items showing DIF are rewritten or removed from the instrument in order to generate measures of the latent constructs that can be generalized across groups.

Despite the measurement invariance we have identified in the graded scores of the CPP, we strongly reject one alternative model, namely, collapsing the multiple category scoring system, as has been suggested, because “these distinctions are of no documented clinical significance”. [7] Generally, information is expensive and difficult to collect, and should not be discarded lightly. Certainly if the diagnostic categories are discarded, there will be no chance to document

clinical significance moving forward. Our goals should instead be to explore methods that allow improved reliability including image segmentation from digitized slides. [20]

A more immediate and concrete criticism to collapsing the scoring system is that the neutrophil infiltrates in amnion, chorion and umbilical cord (for example) are of interest to us only insofar as they reflect aspects of the process of intraamniotic infection, a process we cannot otherwise directly access. Neutrophil infiltrates are indicators of the underlying latent (and not directly observable or measureable) variable in which we are truly interested. In modern pathology practice, we are forced to employ categorical scores as representations of one (or more) underlying continuous variables. However, as the categorical scale is progressively reduced from 0–4 to 0–1, as "absent/present"), the correlation of those scores with the underlying latent variable is also reduced.[22] The simpler scale may be more "reliable" but it is less representative of the latent/unobservable process(es) in which we are truly interested. We may trade an appearance of reliability for a long-term limitation on the explanatory value of histology scorings, and ultimately, their utility in both research and clinical contexts.

The HUGE project data underscore the potential disadvantages of "lumping" vs. "splitting' with regard to such information. The understanding that genetic polymorphisms modify aspects of the maternal and fetal inflammatory responses to a commonly perceived intraamnmiotic infectious stimulus is relatively recent. [23] All histologic scores may not be created equal; some neutrophilic infiltrates may represent an "uphill battle" with gene polymorphisms that would down-regulate inflammatory responses. Other inflammatory responses may have been facilitated by the genetic environments of the mother, the fetus or both. Collapsing a continuous process (recruitment of neutrophils and diapedesis from their site of origin) into, at the extreme, present vs absent [7] precludes ever disentangling the complex interplay between maternal and fetal genetic capacities and the infectious stimulus.

As noted above, chorioamnionitis, defined as the presence of intraamniotic microbial organisms triggering maternal and/or fetal inflammatory responses, plays a significant role in reproductive and childhood pathology. While risk of morbidity rises with severity of inflammation, most infants will not experience adverse outcomes. This suggests that the key exposure is heterogeneous and that the heterogeneity is not reflected in commonly used summary measures of infection. The underlying process of acute intraamniotic infection is physiologically complex, involving cytokines, chemokines, prostanoids, proteases, matrix metallo-proteinases, and almost innumerable other biologically active compounds. Is the categorical quantification of neutrophils the only facet of inflammation that is physiologically relevant to the outcomes that have been associated with acute intraamniotic infection? It is not unreasonable to suggest that the answer to this question may be "No". Rather than collapsed into fewer categories, histology scoring may need to be expanded to cover other features (such as connective tissue characteristics, fibroblast proliferation, neutrophil karyorrhexis) that may mark other facets of the complex pathophysiology of intraamniotic infection.

We propose that perinatal researchers should, to use a worn but appropriate cliché, step outside the box and consider alternative approaches to both measurement of histology slides that would yield adequate reliability to allow cross-institutional analysis of the latent construct (s) involved in intraamniotic infection and ultimately to achieve a fuller understanding of the infection-preterm birth pathway.

REFERENCES

1. Romero R, Espinoza J, Gonçalves LF, Kusanovic JP, Friel LA, Nien JK. Inflammation in preterm and term labour and delivery. Semin Fetal Neonatal Med 2006;11(5):317–26. [PubMed: 16839830]
2. Fiscella K. Race, perinatal outcome, and amniotic infection. Obstet Gynecol Surv 1996;51(1):60–6. [PubMed: 8657398]

3. Yoon BH, Park CW, Chaiworapongsa T. Intrauterine infection and the development of cerebral palsy. BJOG 2003;110 (Suppl 20):124–7. [PubMed: 12763129]
4. Dammann O, Leviton A. Inflammatory brain damage in preterm newborns--dry numbers, wet lab, and causal inferences. Early Hum Dev 2004;79(1):1–15. [PubMed: 15282118]
5. Gibson CS, MacLennan AH, Goldwater PN, Dekker GA. Antenatal causes of cerebral palsy: associations between inherited thrombophilias, viral and bacterial infection, and inherited susceptibility to infection. Obstet Gynecol Surv 2003;58(3):209–20. [PubMed: 12612461]
6. Holzman C, Lin X, Senagore P, Chung H. Histologic chorioamnionitis and preterm delivery. Am J Epidemiol 2007;166(7):786–94. [PubMed: 17625222]
7. Redline RW, Faye-Petersen O, Heller D, Qureshi F, Savell V, Vogler C. Society for Pediatric Pathology, Perinatal Section, Amniotic Fluid Infection Nosology Committee. Amniotic infection syndrome: nosology and reproducibility of placental reaction patterns. Pediatr Dev Pathol 2003;6:435–48. [PubMed: 14708737]
8. Salafia CM, Weigl C, Silberman L. The prevalence and distribution of acute placental inflammation in uncomplicated term pregnancies. Obstet Gynecol 1989;73(3 Pt 1):383–9. [PubMed: 2915862]
9. Niswander, K.; Gordon, M. The Collaborative Perinatal Study of the National Institute of Neurological Diseases and Stroke: The Women and Their Pregnancies. W.B. Saunders; Philadelphia, PA: 1972.
10. Hardy J. The Collaborative Perinatal Project: Lessons and Legacy. Annals of Epidemiology 2003;13 (5):303–311. [PubMed: 12821268]
11. Benirschke, K. Examination of the placenta. 1961. Prepared for the Collaborative Study on Cerebral Palsy, Mental Retardation and other Neurological and Sensory Disorders of Infancy and Childhood, National Institute of Neurological Diseases and Blindness, US Department of Health, Education and Welfare, Public Health Service
12. Muthén, B.; Muthén, L. Mplus 4.2 [Computer program]. Los Angeles: Muthén and Muthén; 2006.
13. Flora DB, Curran PJ. An empirical evaluation of alternative methods of estimation for confirmatory factor analysis with ordinal data. Psychological Methods 2004;9:466–491. [PubMed: 15598100]
14. Jöreskog, KG. Testing structural equation models. Bollen, KA.; Long, JS., editors. Thousand Oaks, CA: Sage; 1993.
15. Steiger, JH.; Lind, J. Statistically Based Tests for the Number of Common Factors. Paper presented at the annual meeting of the Psychometric Society; Iowa City. 1980.
16. Bentler PM, Bonett DG. Significance tests and goodness of fit in the analysis of covariance structures. Psychological Bulletin 1980;88:588–606.
17. Miles JN, Shevlin M, McGhee PC. Gender differences in the reliability of the EPQ? A bootstrapping approach. Br J Psychol 1999 Feb;90(Pt 1):145–54. [PubMed: 10085551]
18. Hu LT, Bentler P. Cutoff criteria for fit indexes in covariance structure analysis: Conventional criteria versus new alternatives. Structural Equation Modeling 1999;6:1–55.
19. Millsap, RE.; Meredith. Factorial invariance: historical perspectives and new problems. In: Cudeck, R.; MacCallum, R., editors. Factor analysis at 100: historical developments and future directions. Hillsdale, NJ: Erlbaum; 2007.
20. Thomas, K.; Salafia, CM.; Buhimschi, I.; Buhimschi, CS.; Zambrano, E.; Sottile, M. Reliability of automated neutrophil quantitation in digitized H&E stained slides: Pilot analysis of correlation with amniotic fluid proteomics score. Abstract accepted for presentation International Federation of Placenta Associations; October 2009;
21. MacCallum RC, Zhang S, Preacher KJ, Rucker DD. On the practice of dichotomization of quantitative variables. Psychological Methods 2002;7:19–40. [PubMed: 11928888]
22. MacCallum RC, Zhang S, Preacher KJ, Rucker DD. On the practice of dichotomization of quantitative variables. Psychological Methods 2002;7:19–40. [PubMed: 11928888]
23. Crider KS, Whitehead N, Buus RM. Genetic variation associated with preterm birth: A HuGE review. Genet Med 2005;7(9):593–604. [PubMed: 16301860]

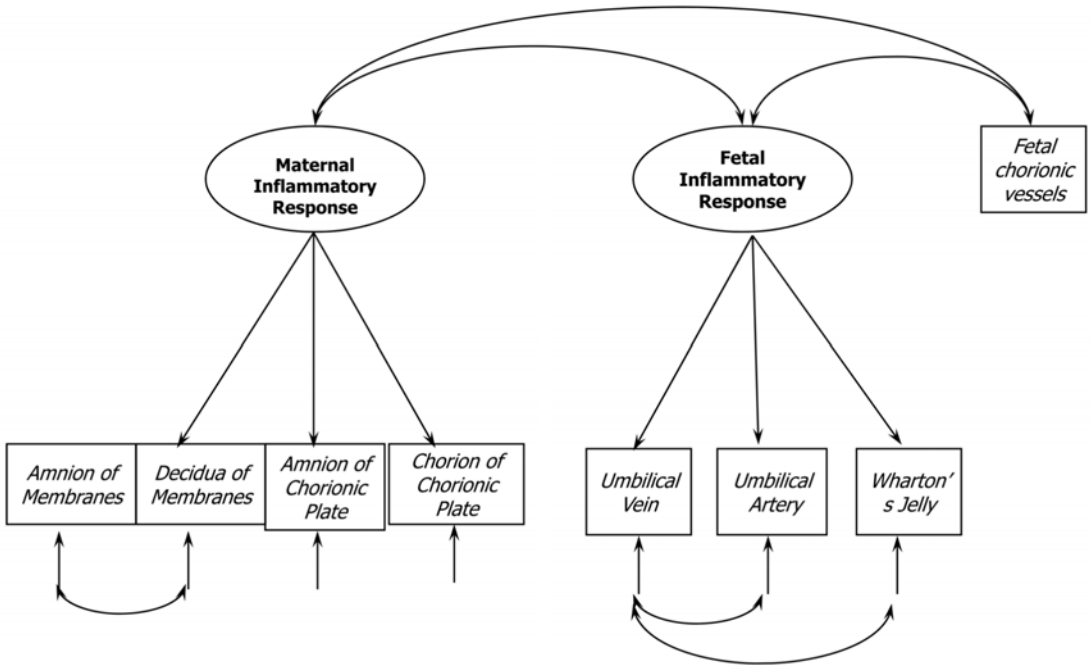

Figure 1.
Path diagram of the best-fit model for the relationships of scores of neutrophil infiltrates in the specified placental tissues, developed in Boston cohort and applied across study sites (see Table 2)

Table 1

Frequencies of histology scores by study site

Sites of neutrophilic infiltrates		Boston		Buffalo		New Orleans		NY/Columbia		Baltimore	
	Sample size	10803		2313		2573		2006		3423	
	Scores	*N*	%	*N*	%	*N*	%	*N*	%	*N*	%
Umbilical artery	0	10531	97.5	2247	97.1	2479	96.3	1881	93.8	3307	96.6
	1	114	1.1	35	1.5	44	1.7	89	4.4	72	2.1
	2	158	1.5	21	0.9	49	1.9	36	1.8	44	1.3
	3	0	0	10	0.4	2	0.1	0	0	0	0
Umbilical vein	0	8610	79.7	1997	86.3	2404	93.4	1794	89.4	3256	95.1
	1	1664	15.4	233	10.1	109	4.2	154	7.7	109	3.2
	2	529	3.8	35	1.5	58	2.3	58	2.9	58	1.7
	3	0	0	48	2.1	2	0.1	0	0	0	0
Umbilical cord substance	0	10281	95.2	2155	93.2	2447	95.1	1855	92.5	3324	97.1
	1	303	2.8	121	5.2	96	3.7	127	6.3	75	2.2
	2	218	2	9	0.4	29	1.1	24	1.2	24	0.7
	3	0	0	28	1.2	2	0.1	0	0	0	0
Amnion of membrane roll	0	9917	92	2066	93.1	2362	95.2	8515	92	3146	96.6
	1	526	4.9	87	3.9	91	3.7	121	6.1	74	2.3
	2	341	3.2	55	2.5	26	1.0	37	1.9	36	1.1
	3	1	0	11	0.5	3	0.1	0	0	0	0
Chorion of membrane roll	0	9650	89.1	2075	89.9	2219	86.3	1740	86	3062	89.1
	1	782	7.2	122	5.3	219	8.5	210	10.4	231	6.7
	2	393		90	3.9	127	4.9	74	3.7	142	4.1
	3	0	0	20	0.9	7	0.3	0	0	2	0.1
Decidua in capsularis	0	9598	88.7	1815	78.8	2002	77.8	1165	57.5	3088	89.8
	1	716	6.6	276	12	366	14.2	720	35.5	251	7.3
	2	504	4.7	150	6.5	188	7.3	141	7	98	2.9
	3	0	0	61	2.6	17	0.7	1	0	0	0
Amnion of placental surface	0	10170	94.4	2147	95.3	2224	96.5	1837	93.6	3190	98.3
	1	341	3.2	49	2.2	56	2.4	91	4.6	38	1.2
	2	259	2.4	50	2.2	23	1.0	35	1.8	17	0.5
	3	1	0	8	0.4	1	0.0	0	0	1	0
Chorion of placental surface	0	9894	91.4	2151	92.9	2293	89.0	1746	86.1	3232	94
	1	613	5.7	92	4	214	8.3	205	10.1	133	3.9
	2	314	2.9	58	2.5	66	2.6	75	3.7	71	2.1
	3	1	0	15	0.6	3	0.1	1	0	1	0
Fetal surface vessels	0	10121	93.6	2167	93.6	2426	94.1	1860	91.8	3283	95.7
	1	406	3.8	75	3.2	127	4.9	116	5.7	102	3
	2	290	2.7	55	1.8	24	0.9	50	2.5	47	1.4
	3	1	0	19	0.8	1	0.0	1	0	0	0

Virginia		Minnesota		NY/Medical		Oregon		Pennsylvania		Providence		Tennessee	
2864		2888		3943		2979		8550		3837		3379	
N	%	*N*	%	*N*	%	*N*	%	*N*	%	*N*	%	*N*	%
2731	95.4	2797	96.8	3822	96.9	2840	95.3	8123	95	3687	96.1	2347	96.1
90	3.1	40	1.4	88	2.2	84	2.8	209	2.4	110	2.9	92	2.7
43	1.5	50	1.7	29	0.7	55	1.8	219	2.6	41	1.1	35	1
0	0	1	0.001	4	0.1	0	0	0	0	0	0	5	0.1
2626	91.7	2516	87.1	3766	95.5	2691	90.3	7972	93.2	3439	89.6	3231	95.6
182	6.4	206	7.1	134	3.4	213	7.2	327	3.8	339	8.8	100	3
56	2	161	5.6	40	1	75	2.5	251	2.9	59	1.5	41	1.2
0	0	5	0.2	3	0.1	0	0	0	0	0	0	7	0.2
2667	93.1	2681	92.9	3847	97.6	2799	94	8072	94.4	3633	94.7	3273	96.9
152	5.3	186	6.4	78	2	140	4	320	3.7	171	4.5	77	2.3
45	1.6	18	0.6	14	0.4	39	1.3	159	1.9	33	0.9	28	0.8
0	0	2	0.1	4	0.1	1	0.001	0	0	0	0	1	0.0001
2198	79.7	2281	90.1	3544	93.4	2549	90.6	7351	95.3	2970	83.6	3127	96.4
446	16.2	236	9.3	198	5.2	206	7.3	362	4.6	524	14.8	85	2.6
111	4	13	0.5	53	1.4	60	2.1	144	1.8	55	1.5	30	0.9
3	0.1	1	0	1	0	0	0	1	0	2	0.1	2	0.1
1935	67.6	2517	87.5	3341	8.557292	2518	84.4	7337	86.2	3064	79.8	3036	89.3
658	23	333	11.6	389	9.9	372	12.5	583	6.9	362	17.8	230	6.8
266	9.3	22	0.8	193	4.9	92	3.1	590	6.9	92	2.4	125	3.7
3	0.1	5	0.2	4	7.827957	1	0	0	0	2	0.1	7	0.2
1696	59.3	1151	40	3027	76.9	1964	65.9	6754	79.4	2926	76.1	2939	86.2
866	30.3	1532	53.2	794	20.2	712	23.9	1167	13.7	618	16.1	336	9.9
293	10.2	133	4.6	112	2.8	302	10.1	583	6.9	301	7.8	133	3.9
6	0.2	61	2.1	4	0.1	1	0	6	0.1	1	0	1	0
2384	88.7	1838	90.1	3586	95.7	2685	95.4	6786	94.2	3189	89.8	3122	96.8
245	9.1	176	8.6	141	3.8	111	3.9	287	4	313	8.8	75	2.3
58	2.2	22	1.1	19	0.5	18	0.6	133	1.8	49	1.4	26	A0 .8
2	0.1	4	0.2	1	0	0	0	1	0	1	0	1	0
2336	81.5	2468	85.5	3576	90.9	2747	92.2	7537	88	3325	86.5	3123	91.6
419	14.6	374	13	312	7.9	210	7	584	6.8	448	11.6	204	6
110	3.8	36	1.2	45	1.1	23	0.8	441	5.2	72	1.9	82	2.4
3	0.1	9	0.3	1	0	1	0	0	0	1	0	2	0.1
2572	89.7	2585	89.8	3753	95.4	2780	93.3	7929	92.6	3534	92	3234	94.8
225	7.8	249	8.6	159	4	166	5.6	379	4.4	247	6.4	130	3.8
67	2.3	34	1.2	22	0.6	35	1.2	256	3	60	1.6	45	1.3
3	0.1	12	0.4	1	0	0	0	0	0	0	0	3	0.1

Table 2

Factor analysis scores, using Boston fitted model, across study sites.

	Boston		Buffalo			New Orleans		NY/Columbia			Baltimore			Virginia		
Sample size	**10,803**		**2313**			**2573**		**2006**			**3423**			**2864**		
Chi-2						**281.798**		**473.704**			**300.567**			**378.709**		
CFI						**0.999**		**0.999**			**0.999**			**0.999**		
TLI						**0.999**		**0.998**			**0.999**			**0.999**		
RMSEA						**0.033**		**0.044**			**0.033**			**0.038**		
MAIR by	Wald test		Wald test		Model test	Model test		Wald test		Model test	Wald test		Model test	Wald test		Model test
AmnMEM	**1**		**1**			**1**		**1**			**1**			**1**		
DecMEM	**0.894**	99.33333	**1.313**	28.54348	<0.0001	**1.286**	0.0000	**1.169**	61.52632	167.856	**0.848**	18.04255	13.806	**1.069**	66.8125	<0.0001
AmnCP	**1.082**	154.5714	**1.065**	38.03571		**1.115**	0.0000	**1.114**	69.625	0	**1.083**	23.54348	0.0032	**1.054**	70.26667	0
ChorCP	**1.064**	177.3333	**1.097**	34.28125		**1.226**	0.0000	**1.135**	70.9375		**1.208**	21.19298		**1.042**	74.42857	
FAIR by							1.0000									
UVEIN	**1**		**1**			**1**	1.0000	**1**	22.81667	<0.0001	**1**			**1**		
UART	**1.15**	57.5	**1.401**	17.2963	0.0009	**1.385**	0.0002	**1.369**	25.76364	0	**1.162**	11.28155	0.124	**1.554**	18.95122	31.313
Wjelly	**1.116**	79.71429	**1.325**	20.07576		**1.296**	0.0001	**1.417**			**1.095**	12.30337	0.9397	**1.441**	21.50746	0
FVCP with							1.0000									
MAIR	**0.848**	106	**0.087**			**0.496**	0.0000	**0.391**	20.57895		**0.682**	13.91837		**0.383**	22.52941	
FAIR	**0.693**	57.75	**0.848**	12.47059		**1.635**	0.0039	**1.501**	9.810458		**2.039**	7.996078		**1.358**	10.05926	
FAIR with							1.0000									
MAIR	**0.684**	62.18182	**0.739**	93.5443		**0.979**	0.0061	**0.6**	8.450704		**1.526**	6.606061		**0.565**	8.828125	
Wjelly with							1.0000									
UVEIN	**0.181**	12.06667	**0.307**	4.873016		**0.003**	0.8754	**0.026**	0.412698		**−0.343**	−1.96		**0.163**	2.397059	
UART with							1.0000									
UVEIN	**0.075**	6.818182	**0.005**			**−0.123**	0.2859	**0.091**	1.516667		**−0.101**	−0.67785		**−0.048**	−0.73846	
DecMEM with							1.0000									
AmnMEM	**0.079**	8.777778	**0.084**	3		**0**	1.0000	**0.025**	6.25		**0.036**	1.2		**0.019**	3.8	
Means							1.0000									
MAIR	**0**		**0.078**	0.069	0.792798	**0.375**		**0.874**	34.96		**−0.067**	−0.77907		**0.968**	40.33333	
FAIR	**0**		**−0.401**	0.097	0.75546	**−2.034**		**−1.063**	−5.26238		**−2.875**	−6.23644		**−1.21**	−5.90244	

Minnesota			NY/Medical			Oregon			Pennsylvania			Providence			Tennessee		
2888			**3943**			**2979**			**8550**			**3837**			**3379**		
505.426			**393.007**			**384.4**			**604.169**			**378.53**			**292.773**		
0.999			**0.999**			**0.999**			**0.999**			**0.999**			**0.999**		
0.998			**0.999**			**0.999**			**0.998**			**0.999**			**0.999**		
0.046			**0.038**			**0.038**			**0.043**			**0.037**			**0.033**		
Wald test		Model test	Wald test		Model test	Wald test		Model test	Wald test		Model test	Wald test		Model test	Wald test		Model test
1			**1**			**1**			**1**			**1**			**1**		
1.157	68.05882	<0.0001	**1.018**	53.57895	49.027	**1.175**	53.40909	<0.0001	**1.168**	53.09091	<0.0001	**0.93**	54.70588	51.89	**1.031**	21.93617	32.996
1.134	87.23077	0	**1.078**	77	0	**1.034**	68.93333	0	**1.111**	69.4375	0	**1.077**	76.92857	0	**1.227**	33.16216	0
1.082	83.23077		**1.048**	65.5		**0.969**	60.5625		**1.22**	64.21053		**1.007**	71.92857		**1.31**	30.46512	
1			**1**			**1**			**1**			**1**			**1**		
1.19	16.76056	0.197	**1.612**	15.9604	20.611	**1.455**	24.66102	28.87	**1.49**	18.86076	18.317	**1.436**	25.19298	44.039	**1.622**	8.27551	6.213
1.129	22.58	0.9063	**1.234**	15.04878	0	**1.329**	28.2766	0	**1.277**	19.34848	0.0001	**1.42**	30.21277	0	**1.225**	6.843575	0.0448
0.25	22.72727		**0.419**	20.95		**0.474**	23.7		**0.667**	25.65385		**0.473**	19.70833		**0.543**	15.97059	
1.604	10.83784		**1.643**	8.557292		**1.677**	9.982143		**2.885**	10.68519		**0.873**	13.22727		**2.612**	6.219048	
0.41	9.534884		**0.728**	7.827957		**0.784**	8.711111		**2.094**	9.475113		**0.435**	10.35714		**1.558**	5.791822	
0.146	1.717647		**0.054**	0.84375		**0.202**	2.589744		**0.071**	0.559055		**0.014**	0.4375		**−0.459**	−1.46178	
0.01	0.135135		**0.013**	0.138298		**−0.006**	−0.11321		**−0.11**	−0.88		**0.026**	0.928571		**−0.368**	−0.84211	
0.006	3		**−0.001**	−0.2		**−0.013**	−2.16667		**0.3**	37.5		**−0.004**	−0.66667		**−0.009**	−0.47368	
1.064	56		**0.733**	22.90625		**0.745**	25.68966		**0.312**	0.821053		**0.802**	25.87097		**0.186**	3.152542	
−1.027	−5.61202		**−2.167**	−6.31778		**−1.511**	−6.21811		**−4.082**	−8.89325		**−0.506**	−5.11111		**−4.647**	−5.42874	

Published in final edited form as:
Placenta. 2010 November ; 31(11): 958–962. doi:10.1016/j.placenta.2010.09.005.

Placental surface shape, function, and effects of maternal and fetal vascular pathology

Carolyn M. Salafia[1,2], **Michael Yampolsky**[3], **Dawn P Misra**[4], **Oleksander Shlakhter**[5], **Danielle Haas**[1], **Barbara Eucker**[6], and **John Thorp**[6]

[1]Placental Analytics, LLC, Larchmont, NY, USA

[2]Department of Obstetrics and Gynecology and Pediatrics, New York Methodist Hospital, Brooklyn, NY

[3]Department of Mathematics, University of Toronto, 40 St. George St, Toronto, Ontario, Canada, M5S2E4

[4]Department of Family Medicine and Public Health Sciences, Wayne State University School of Medicine.101 E. Alexandrine, Room #203, Detroit, MI 48201

[5]Rotman School of Management, University of Toronto, 105 St. George Street, Toronto, ON, M5S 3E6

[6]Department of Obstetrics and Gynecology, University of North Carolina at Chapel Hill, Chapel Hill, NC 27599

Abstract

Goal—In clinical practice, variability of placental surface shape is common. We measure the average placental shape in a birth cohort and the effect deviations from the average have on placental functional efficiency. We test whether altered placental shape improves the specificity of histopathology diagnoses of maternal uteroplacental and feto-placental vascular pathology for clinical outcomes.

Materials and Methods—1225 placentas from a prospective cohort had chorionic plate digital photographs with perimeters marked at 1–2 cm intervals. After exclusions of preterm (n=202) and velamentous cord insertion (n=44), 979 (95.7%) placentas were analyzed. Median shape and mean perimeter were estimated. The relationship of fetal and placental weight was used as an index of placental efficiency termed "β". The principal placental histopathology diagnoses of maternal uteroplacental and fetoplacental vascular pathologies were coded by review of individual lesion scores. Acute fetal inflammation was scored as a"negative control" pathology not expected to affect shape. ANOVA with Bonferroni tests for subgroup comparisons were used.

Results—The mean placental chorionic shape at term was round with a radius estimated at 9.1 cm. Increased variability of the placental shape was associated with lower placental functional efficiency. After stratifying on placental shape, the presence of either maternal uteroplacental or fetoplacental

Corresponding author: Carolyn M Salafia MD MS, Placental Analytics, LLC, 93 Colonial Avenue, Larchmont NY 10538, Carolyn.salafia@gmail.com.

vascular pathology was significantly associated with lower placental efficiency only when shape was abnormal.

Conclusions—Quantifying abnormality of placental shape is a meaningful clinical tool. Abnormal shapes are associated with reduced placental efficiency. We hypothesize that such shapes reflect deformations of placental vascular architecture, and that an abnormal placental shape serves as a marker of maternal uteroplacental and/or fetoplacental vascular pathology of sufficiently long standing to impact placental (and by extension, potentially fetal) development.

Introduction

The chorionic plate of the human placenta is commonly depicted as round, with the umbilical cord inserted roughly at the center [1]. However, in clinical practice, the shape of the chorionic disk is rarely truly circular; its shape commonly varies, from round to oval, bi- or multi- lobate, or otherwise irregular. The shape of the placenta is thought to be influenced by where it is implanted in the uterus, regional variations in the decidua (that may determine areas of atrophy), variations in maternal vascular supply (with placental infarcts resulting in altered shape) and perhaps even the "manner of its original implantation" [1]. Benirschke states that "the mechanism by which [non-round shapes] develop is unclear", although "much supports the notion of a secondary conversion from more normal placentation" [1]. In a recent paper [2], we have related this variability in chorionic plate shape to the structure of the underlying placental vascular tree. We can reliably produce multilobate and regularly irregular shapes by changing a parameter that negatively affected the angiogenesis of the model placental vasculature. Furthermore, our empirical results [2] suggest that the earlier in gestation a placental pathology begins, the more likely it is that the effect on placental vascular branching growth will result in a distortion of the placental shape.

In view of the connection between the shape of the chorionic plate and the structure of the chorionic villous tree, it is particularly important to understand what a normal placental shape is and how to measure deviations from the norm. In this paper we use several different techniques to describe an *average* surface shape for placentas delivered at term. We develop several specific measurements of the deviation from the average which are both practical to implement clinically, and statistically reliable. We further investigate how a deviation from the average placental shape affects the functional efficiency of the placenta, in terms of the birth weight of the baby for a given placental weight.

We then proceed to apply our techniques as a diagnostic tool for the two principal types of vascular pathology that have been described in the placenta, maternal uteroplacental and feto-placental vascular pathology. Placental histopathology diagnoses have been used by clinicians to diagnose these disorders for almost 50 years since the seminal protocol published by Dr. Kurt Benirschke [3]. Refinements have been made, especially in the recognition of a broad range of fetoplacental and uteroplacental vascular lesions e.g. [4], and in attempts to standardize diagnostic criteria [5–7].

Based on the findings of [2], we have hypothesized that either fetoplacental or maternal uteroplacental vascular pathology that is sufficient to alter placental chorionic plate shape will affect placental function. We predict that fetoplacental or maternal uteroplacental vascular pathology features will have a measureable effect on placental function only when placental chorionic surface shape is abnormal. To test this hypothesis, we have compared the effects of maternal-uteroplacental or fetoplacental vascular pathology on placental functional efficiency in cases with round as compared to irregular shaped chorionic plates.

Materials and Methods

Placental Cohort

The *Pregnancy, Infection, and Nutrition Study* is a cohort study of pregnant women recruited at mid pregnancy from an academic health center in central North Carolina. Our study population and recruitment techniques are described in detail elsewhere [11]. Briefly, beginning in March 2002, all women recruited into the *Pregnancy, Infection, and Nutrition Study* were requested to consent to a detailed placental examination. As of October 1, 2004, 94.6 percent of women consented to such examination. Of those women who consented, 87 percent had placentas collected and photographed for image analysis. Of the 1,225 consecutive placentas collected, 202 were delivered pre-term and were excluded. An additional 44 cases were excluded from the present manuscript because the umbilical cord insertion was velamentous; this was not amenable to our mathematical methods which assume that the cord was inserted on the chorionic plate, to be able to center the placenta on the cord insertion point. This left N=979 cases for analysis.

Placental gross examinations, histology review, and image analyses were performed at *EarlyPath Clinical and Research Diagnostics*, a New York State-licensed histopathology facility under the direct supervision of Dr. Salafia. The institutional review board from the University of North Carolina at Chapel Hill approved this protocol.

The fetal surface of the placenta was wiped dry and placed on a clean surface after which the extraplacental membranes and umbilical cord were trimmed from the placenta. The fetal surface was photographed with the Lab ID number and 3 cm. of a plastic ruler in the field of view using a standard high-resolution digital camera (minimum image size 2.3 megapixels). A trained observer (D.H.) captured series of *x*,*y* coordinates that marked the site of the umbilical cord insertion and the perimeter of the fetal surface. The perimeter coordinates were captured at intervals of between 1cm and 2cm, and more coordinates were captured if it appeared essential to accurately capturing the shape of the fetal surface.

Software

Numerical calculations were carried out using *mean-placenta*, a Unix-based, ANSI C, software package developed under the terms of the GNU General Public License as published by Free Software Foundation. For visualizations we have used *PovRay*: a freeware ray tracing program available for a variety of computer platforms; and Maplesoft Maple 9.0 Math & Engineering software.

Placental histopathology diagnoses

Placental disease was characterized by gross and microscopic examination of the placenta and decidua. Histology samples were taken from a minimum of four independent sites in the placental parenchyma; diagnoses were assigned to 1 of 3 categories as outlined by Salafia et al. [12–14].

Fetal inflammatory response in umbilical cord and chorionic plate vessels (as a “negative control) and maternal uteroplacental and/or feto-placental vascular lesions were recorded. For the purposes of this study, a fetal inflammatory response was considered present when there was any fetal inflammatory response (ie, umbilical vasculitis, funisitis, or fetal chorionic vasculitis); these lesions have been shown to be present in <1% of uncomplicated term births. Maternal uteroplacental vascular pathology was diagnosed in cases by 2 routes: (1) all placentas with at least 1 nonmarginal placental infarct (>2 cmfrom the nearest margin) >1cm^3 in volume and (2) cases with summary scores of histologic items of syncytial knotting, syncytial basophilia, villous fibrosis, and excess perivillous fibrin deposition with cytotrophoblast

proliferation (each scored on a 0–4 scale, as previously described [12–15]) greater than the birth cohort median value of 7. Fetoplacental vascular lesions included chorionic and fetal stem vessel mural thrombi, the "hemorrhagic endovasculitis" group of lesions, and avascular villi present in clumps of 50 villi. All placentas were examined by a single expert pathologist (C.M.S.), who was blinded to the patient characteristics when reviewing the placental pathologic findings. For purposes of analysis, the two vascular pathologies and fetal acute inflammatory responses were coded as present vs not present.

Calculating the mean shape of the chorionic plate

A square grid of 500×500 pixels was superimposed on the images of the placentas in the sample, each of which was rescaled to the actual size as reflected by the ruler in the field of view The size of one pixel was chosen to equal 0.1cm, so the total coverage of the grid was a square of 50×50 cm^2. The insertion point of the umbilical cord was placed at the center of the square, and the point on the placental perimeter closest to the rapture of the amniotic sac was placed on the negative vertical axis, for consistency.

For each of the placentas in the dataset, all the pixels inside of the placental perimeter, including those intersecting with the boundary, were marked. Thus, for each placenta, an approximate area covered by it was obtained as the union of the marked pixels. For the n-th placenta in the dataset, we denote S_n the region of the 50×50-square, which is covered by its surface. W_n denotes the union of the marked pixels for this placenta, so that the edge of W_n is no more than the size of one pixel (0.1cm) removed from the edge of S_n. To calculate the mean shape of the chorionic plate, for each pixel $p(x,y)$, $x=1\ldots500$, $y=1\ldots500$ of the grid, we marked the total number $t(x,y)$ of the placentas for which $p(x,y)$ lies in W_n. The central pixels will thus be covered by all of the placentas, that is $t(x,y)\approx N$ (the total number of placentas in the dataset) for $x,y\approx250$, and the peripheral ones will be covered by very few.

We let W_{median} be the union of all pixels $p(x,y)$ with $t(x,y)\geq N/2$.It is thus the *median shape* of the chorionic plate in our sample.

Calculating the mean placental perimeter

To calculate the mean chorionic plate perimeter, the insertion point of the umbilical cord was again placed at the origin, and the point on the perimeter closest to the rupture of the amniotic sac was positioned on the negative vertical axis. The perimeters of the placentas in the dataset were rescaled to the real size. The points in the perimeter were then averaged inside a sector of 18°, thus obtaining 20 radial markers for each placenta (see Figure 2). Each of the markers was then averaged over the whole dataset, thereby giving 20 mean placental radii from the umbilical insertion point spaced at 18° angular intervals. Averaging these 20 mean radii we obtain the *mean placental radius* R_{mean} from which the perimeter is readily calculated.

Measuring the deviation of the placental perimeter from the mean

We have used two measurements of the deviation from the mean placental shape. The first one, which we call sigma, is the mean square deviation of the 20 perimeter radial markers from the mean radius R_{mean}. The second one is based on the difference between the median placental shape W_{median} and the pixellated chorionic plate shape W_n of the *n*-th placenta in our dataset. We add up the area of all the pixels which are covered by one of the shapes W_{median}, W_n but not by both of them at the same time. We call this total area the *symmetric difference* between the placental shape and the mean.

Measuring placental eccentricity

As a measure of placental eccentricity, for each placenta in the dataset we found the farthest and closest of the 20 radial markers, and calculated the ratio of the distances to them from the umbilical insertion point: $E_n = D_{max}/D_{min}$. For a round placenta with centrally inserted umbilical cord, the value of eccentricity is 1.

Placental Functional Efficiency (β)

We have previously shown that placental weight is proportional to birth weight to the ¾ power [8,9]. We suggested that such fractional scaling is due to the fractal structure of the placental vasculature, and introduced a scaling exponent describing placental functional efficiency (in terms of birth weight yielded per gram of placental weight). This scaling exponent, which we termed β, is defined as the ratio of the logs of placental weight and birth weight (β = log PW/ log BW) [8,9]. Thus, as β increases, the placental size is greater relative to birth weight (implying reduced placental functional efficiency), and as β decreases, the birth weight is relatively larger for the given placental weight (indicating greater placental efficiency).

Statistical analysis

Contingency tables compared categorical variables. Sigma, symmetric difference, and *beta* are each normally distributed. ANOVA was used to test for differences between histopathology diagnostic categories and the continuous outcomes. Pearson correlations tested for relationships between continuous variables. Multivariate comparisons were performed using linear regression.

Results

Mean placental shape

The median chorionic plate shape is round, as seen in Figure 1. We calculated the mean radius of a pixel on the boundary of W_{median} from the umbilical insertion point as 9.066 cm (range 8.76– 9.46 cm, mean square deviation 0.181cm, or 2%).We have also calculated the shapes $W_{40\%}$ and $W_{30\%}$ which correspond to the values of $t(x,y)$ greater than $0.4N$ and $0.3N$, respectively. They are also round (Figure 1).

Averaging of the 20 placental radial markers is illustrated in Figure 2. This procedure also yields a round shape with mean average chorionic plate radius R_{mean}=9.01cm. The mean value for each of the 20 marked radii were within 3.3% of the average chorionic plate radius (range 8.71– 9.27cm, and mean square deviation (0.18cm or 1.9%).

We have calculated the average area of the region covered by the chorionic plate shape as the arithmetic mean of chorionic plate area as A_{mean}=285.58cm^2, standard deviation of 60.78cm^2 or 21.2%, range 135.03cm^2 and the maximal value 649.44cm^2. While the standard deviation appears large, recall that for a disk of radius R, the change of radius by ΔR changes the area by approximately $2\pi \cdot \Delta R$. Thus even if our placentas were all round, a 21.2% variance of the area would correspond to less than 3.4% of radial variance. Note that A_{mean} is the area of a disk with radius R_{area}=9.53cm, which can viewed as another measurement of the mean placental radius.

We have calculated the average radius R_n of a chorionic plate in our dataset by averaging the 20 radial markers obtained as described above. The standard deviation of R_n from the mean value R_{mean}=9.01cm is 1.07cm, or 11.8%. Thus both the chorionic plate area, and the outer radius from the umbilical insertion point have tight distributions with narrow standard deviations. The 95% confidence intervals for chorionic plate area and chorionic plate radius are [281.77cm^2, 289.38 cm^2] and [8.94 cm, 9.07 cm] respectively.

Average placental eccentricity

Mean value of placental eccentricity in our birth cohort is $E_{mean} = 1.68$; median value is $E_{median} = 1.49$. This indicates that deviations from the mean round shape are common for placentas in our dataset.

Placental histology features

As noted above in Methods, the principal pathology (most prominent pathology process) was used as the key variable in analysis with the 463 (47% of the total 979 case) cases with any of the histopathology types as defined above. Acute inflammation was considered the "principal" pathology in 83 cases; maternal uteroplacental vascular pathology in 167 cases and fetoplacental vascular pathology in 134 cases Of these 62 had both maternal uteroplacental and fetoplacental vascular pathology.

Histopathology diagnoses and placental shape (deviation measures)

No pathology diagnosis was associated with either sigma or with symmetric difference (all $p>0.10$).

Histopathology diagnoses and placental functional efficiency (β)

Vascular pathology was correlated with increased β ($p<0.0001$), specifically, maternal uteroplacental vascular pathology (absent 0 .748 ± 0.020 v. present 0.754 ± 0.023, $p=0.002$) and fetoplacental vascular pathology (absent 0.748±0 .020 v. present 0.755 ± 0.022, $p=0.001$). The combined presence of both maternal uteroplacental and fetoplacental vascular pathologies did not have a greater effect on β (0.754 + 0.022) than when each pathology was analyzed alone. Acute inflammation was not associated with a difference in β.

Placental shape and placental functional efficiency (β)

Sigma and symmetric difference were both significantly correlated with β, with $\rho = 0.138$ and 0.209 respectively, consistent with previously reported results in which we used an alternative method for analysis of irregularity of placental shape [9,10].

Histopathology diagnosis associations with placental functional efficiency: Modification by placental shape (Table 1)

Stratifying the cohort into those with sigma less or greater than the mean (regular versus more irregular shapes), maternal uteroplacental and fetal fetoplacental vascular pathology were correlated with an increased β only in the cases with greater sigma (more irregular shape, $p=0.006$ and $p=0.004$, respectively). Finally, consistent with the unstratified analyses, acute inflammation was not associated, in either direction, with β regardless of placental shape.

Discussion

In previous work [2], we have shown that the placental chorionic surface shape closely mirrors the pattern of chorionic vascular growth. Burgeoning ultrasonography literature has linked various detectable markers of atypical placental shape to later significant fetal morbidity and/or mortality, making quantification of placental shape imperative.

Our measurements demonstrate that the average placental shape is a disk centered at the umbilical insertion point. This may have been conventionally believed, yet at a closer examination, several aspects of the results are notable. Firstly, very few placentas appear truly round with a centrally inserted umbilical cord. Variability of shape is the norm. This is manifested in our measurements of mean and median placental eccentricity, which are 1.68 and 1.49 respectively, reflecting a typically significant deviation from a round placental shape

with a centrally inserted umbilical cord. Yet, these *deviations are equally likely to happen in every direction*, so they cancel each other in the average. This is confirmed by observing the shapes $W_{40\%}$ and $W_{30\%}$, which average *large* deviations from the mean (Figure 1). To make these observations, it is of a vital importance that placental surface pictures in the dataset have been given a fixed, biologically consistent orientation – and thus no bias has been introduced into the directionality of perturbations of the shape.

The second important point is the impressive agreement of the different methods of measurement which we have used on what the average placental shape is: *a disk centered at the umbilical insertion point with radius of about 9cm*. This, and tight confidence intervals for the measurements, imply that quantifying the abnormality of the placental shape is meaningful in practice, and is little affected by the technique chosen.

We see a significant correlation between large deviations of the placental shape from the mean and reduced placental efficiency, quantified as a larger scaling exponent β (smaller birth weight for the given placental weight). This confirms the hypothesis we developed in [2,8,9]: an abnormal placental shape is associated with an altered placental vascular architecture, which in turn is associated with a reduced functional efficiency.

Turning to the specific diagnostic value of measuring the placental surface shape, we have demonstrated its utility in improving the specificity of placental histology diagnoses for clinical outcomes. In this study, maternal uteroplacental and fetoplacental vasculopathies only affected β (measure of placental functional efficiency) when placental shape was irregular, consistent with perturbation of placental vascular growth at point(s) across gestation [2].

Our results can thus be interpreted as showing that deviations of the placental shape from the mean marks an adverse effect of either maternal uteroplacental vascular pathology or fetoplacental vascular pathology on the fetoplacental development, as measured by placental functional efficiency (β). In combination with our empirical growth model of the placental vasculature [2], these data suggest that the combination of histopathology diagnosis of either maternal uteroplacental or fetoplacental vascular pathology with greater shape deviation represents either a longer standing disease process, a more severe disease process, or both. Adding shape deviation to the clinical diagnostic tool kit should improve diagnostic specificity and clinical understanding.

Acute intraamniotic inflammations were not associated with either abnormal placental efficiency or abnormal shape. These processes are generally believed to arise close to delivery, being analyzed in relation to factors that are counted in minutes or hours [e.g., 16,17]. In agreement with our DLA model of placental vascular growth [2], they appear to be of an insufficiently long duration to have any measurable effect on the placental vascular growth, and hence placental shape.

Limitations of our work are two-fold. The first is computational. We excluded velamentous umbilical cords as the necessary measurements could not be made and therefore we were missing crucial data to compute area and radius. We would speculate that these most asymmetric examples of placental growth would be on the extreme end of the continuum we have analyzed moving from centrally sited cords to more and more peripherally located cords. However, our mathematical methods require centering the placental image on the umbilical cord insertion point. Secondly, histopathology diagnoses remain subjective with problematic interrater reliability. While a single rater performed these assessments blinded to all data except gestational age, we recognize that these diagnoses might not be duplicated by a second reviewer. We maximized potential interrater reliability by dichotomizing the measures as others have done [5–7]. However, the relatively new capacity to digitize an entire histology slide, making it amenable to image analysis techniques, offers the potential for automated,

reliable and more quantitative measures. We have currently demonstrated that such an approach is amenable to diagnoses of acute inflammation [18], and expect that other diagnostic pathologies will follow.

Conclusions

Different mathematical approaches estimated that the mean placental surface shape is a disk centered at the umbilical insertion point with radius of ~ 9cm. The confidence limits provided herein can be useful clinical tools in determining what are the key diagnostic elements of placental pathology, both gross and histologic, that affect placental function.

Combined with a simply calculated measure of abnormal placental shape, the impact of vascular pathology (either maternal uteroplacental or fetoplacental) on placental function depended on placental shape. A burgeoning ultrasonography literature has linked various detectable markers of atypical placental shape to later significant fetal morbidity and/or mortality, thus making a deeper understanding of the genesis of placental shape imperative.

Acknowledgments

This work was partially supported by NSERC Discovery Grant (M. Yampolsky), by NARSAD Young Investigator Award (C. Salafia), by K23 MidCareer Development Award NIMH K23MH06785 (C. Salafia).

References

1. Benirschke, K.; Kaufmann, P.; Baergen, R. Pathology of the Human Placenta. 5th ed.. Vol. Chapter 7. New York, New York: Springer Verlag; 2006. Architecture of Normal Villous Trees; p. 121-159.
2. Yampolsky M, Salafia CM, Shlakhter O, Haas D, Eucker B, Thorp J. Modeling the variability of shapes of a human placenta. Placenta 2008;29:790–797. [PubMed: 18674815]
3. Benirschke K. Examination of the placenta. Prepared for the Collaborative Study on Cerebral Palsy, Mental retardation and other Neurological and Sensory Disorders of Infancy and Childhood, National Institute of Neurological Diseases and Blindness, US Department of Health, Education and Welfare, Public Health Service. 1961
4. Sander CM, Gilliland D, Akers C, McGrath A, Bismar TA, Swart-Hills LA. Livebirths with placental hemorrhagic endovasculitis: interlesional relationships and perinatal outcomes. Arch Pathol Lab Med 2002;126(2):157–164. [PubMed: 11825110]
5. Redline RW, Faye-Petersen O, Heller D, Qureshi F, Savell V, Vogler C. Society for Pediatric Pathology, Perinatal Section, Amniotic Fluid Infection Nosology Committee. Amniotic infection syndrome: nosology and reproducibility of placental reaction patterns. Pediatr Dev Pathol 2003;6(5): 435–448. [PubMed: 14708737]
6. Redline RW, Boyd T, Campbell V, Hyde S, Kaplan C, Khong TY, Prashner HR, Waters BL. Society for Pediatric Pathology, Perinatal Section, Maternal Vascular Perfusion Nosology Committee. Maternal vascular underperfusion: nosology and reproducibility of placental reaction patterns. Pediatr Dev Pathol 2004;7(3):237–249. [PubMed: 15022063]
7. Redline RW, Ariel I, Baergen RN, Desa DJ, Kraus FT, Roberts DJ, Sander CM. Fetal vascular obstructive lesions: nosology and reproducibility of placental reaction patterns. Pediatr Dev Pathol 2004;7(5):443–452. [PubMed: 15547768]
8. Salafia CM, Misra DP, Yampolsky M, Charles AK, Miller RK. Allometric metabolic scaling and fetal and placental weight. Placenta 2009;30(4):355–360. [PubMed: 19264357]
9. Salafia CM, Yampolsky M. Metabolic scaling law for fetus and placenta. Placenta 2009;30(5):468–471. [PubMed: 19285342]
10. Yampolsky M, Salafia CM, Shlakhter O, Haas D, Eucker B, Thorp J. Centrality of the umbilical cord insertion in a human placenta influences the placental efficiency. Placenta 2009;30(12):1058–1064. [PubMed: 19879649]

11. Savitz DA, Dole N, Williams J, et al. Determinants of participation in an epidemiological study of preterm delivery. Paediatr Perinat Epidemiol 1999;13:114–125. [PubMed: 9987790]
12. Salafia CM, Vogel CA, Bantham KF, Vintzileos AM, Pezzullo J, Silberman L. Preterm delivery: Correlations of fetal growth and placental pathology. Am J Perinatol 1992;9:190–193. [PubMed: 1575840]
13. Salafia CM, López-Zeno JA, Sherer DM, Whittington SS, Minior VK, Vintzileos AM. Histologic evidence of old intrauterine bleeding is more frequent in prematurity. Am J Obstet Gynecol 1995;173:1065–1070. [PubMed: 7485294]
14. Salafia CM, Ernst LM, Pezzullo JC, Wolf EJ, Rosenkrantz TS, Vintzileos AM. The very low birthweight infant: Maternal complications leading to preterm birth, placental lesions, and intrauterine growth. Am J Perinatol 1995;12:106–110. [PubMed: 7779189]
15. Baker AM, Braun JM, Salafia CM, Herring AH, Daniels J, Rankins N, Thorp JM. Risk factors for uteroplacental vascular compromise and inflammation. Am J Obstet Gynecol 2008 Sep;199(3) 256.e1-9.
16. Park HS, Romero R, Lee SM, Park CW, Jun JK, Yoon BH. Histologic Chorioamnionitis is More Common after Spontaneous Labor than after Induced Labor at Term. Placenta. 2010 Jul 21; [Epub ahead of print.].
17. Rouse DJ, Weiner SJ, Bloom SL, Varner MW, Spong CY, Ramin SM, Caritis SN, Peaceman AM, Sorokin Y, Sciscione A, Carpenter MW, Mercer BM, Thorp JM Jr, Malone FD, Harper M, Iams JD, Anderson GD. Eunice Kennedy Shriver National Institute of Child Health and Human Development Maternal-Fetal Medicine Units Network. Second-stage labor duration in nulliparous women: relationship to maternal and perinatal outcomes. Am J Obstet Gynecol 2009 Oct;201(4) 357.e1-7.
18. Thomas, KA.; Sottile, MJ.; Salafia, CM. Unsupervised Segmentation for Inflammation Detection in Histopathology Images. In: Elmoataz, A., et al., editors. ICISP 2010, LNCS 6134. 2010. p. 541-549.

Figure 1.
Median placental shape W_{median} (smallest disk) and $W_{40\%}$, $W_{30\%}$ (two larger disks). The position of the insertion point of the umbilical cord is in the center of the picture.

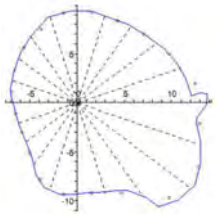

Figure 2.
Calculation of the 20 radial markers for one of the placentas in the dataset. The solid contour marks the perimeter of the placental surface. The 20 radial sectors emanate from the umbilical insertion point. Each marker is indicated with a small circle. It averages the distance from the perimeter curve to the insertion point within the sector.

Figure 3.
The positions of the 20 mean perimeter markers, connected to show the mean placental perimeter. The umbilical insertion point is at the origin.

Table 1

Effect of histopathology diagnoses on placental functional efficiency, stratifying on placental shape

	Mean placental efficiency (95% Confidence Interval)					
SHAPE	**Round (Sigma less than mean)**			**Irregular (Sigma greater than or equal to mean)**		
	Present	**Absent**	**Compare means (ANOVA)**	**Present**	**Absent**	**Compare means (ANOVA)**
Fetal Acute Inflammation (n=118)	0.748, (0.743, 0.754)	0.747, (0.745, 0.749)	P=0.51	0.75, (0.71, 0.84)	0.75, (0.68, 0.84)	P=0.86
Maternal uteroplacental vascular pathology (n=303)	0.750 (0.745, 0.754)	0.746 (0.744, 0.748)	P=0.16	0.758 (0.752, 0.763)	0.750 (0.748, 0.753)	P=0.006
Fetal-placental vascular pathology (n=232)	0.751 (0.747, 0.755)	0.746, 0.744, 0.748)	P=0.08	0.759 (0.753, 0.766)	0.750 (0.748, 0.753)	P=0.004

Sigma = measure of deviation from a circle, see text.

Round defined as ≥ mean sigma; irregular defined as < mean sigma.